MASTERARBEIT / MASTER THESIS

Titel der Masterarbeit / Title of the Master Thesis

„Noise-Receptive Efficient Device-Independent Quantum State Verification of simply-connected Triangle Graph States"

verfasst von / submitted by

Karim-Fabian Osman, BSc

angestrebter akademischer Grad / in partial fulfilment of the requirements for the degree of

Master of Science (MSc)

Wien, 2021 / Vienna, 2021

DEUTSCHSPRACHIGES ABSTRACT

In dieser Arbeit präsentieren wir den ersten Schritt zur Verallgemeinerung von einem neuen geräuschempfindlichen effizienten geräte-unabhängigen Verifizierungsprotokoll für Quantenzustände, das erstmals von Hayata Yamasaki, PhD. präsentiert wurde. Wir demonstrieren seine quadratische Verbesserung bezüglich notwendigerer Testrunden im Vergleich zu zeitgenössischen robusten selbst-testenden Verifizierungsmethoden für eine bestimmte Klasse von Quantenzuständen. Außerdem präsentieren wir Verbesserungen in dessen Anwendung und Skalierbarkeit im Einsatz für eine gewisse Art von Quantencomputer (MBQCs).

Noise-Receptive Efficient Device-Independent Quantum State Verification of simply-connected Triangle Graph States

Within this thesis, we present the first step towards generalization of a novel noise-receptive efficient device-independent quantum state verification protocol introduced by Hayata Yamasaki, PhD. in [52]. We demonstrate its quadratic improvement in necessary rounds K over state-of-the-art robust self-testing protocols for a specific class of quantum graph states. Moreover, we present improvements in applicability and scalability in terms of measurement-based quantum computers and the absence of usual strict restrictions on the statistics of examined quantum states. At the end of this work, we provide insights into possible further improvements, using notions of quantum relative entropy.

CONTENTS

I. INTRODUCTION

Quantum information is one of the most promising research disciplines in the field of modern quantum physics. By using the laws of quantum physics to store and manipulate information in a coherent way, novel possibilities (as compared to classical information processing) emerged, such as quantum computing, quantum meteorology, quantum simulations, and many more, with the promise of having a new technological revolution.

Quantum computation is an example of exploiting the laws of quantum physics to achieve a significant speed-up in solving computational tasks [13, 26, 39]. In the following, we will focus on the verification of *resource states* and measurements being used in *measurement-based quantum computation* (MBQC) [39, 40].

In the paradigm of one-way MBQCs, computation is solely based on local measurements conducted on a highly entangled state (resource state). It is known that MBQCs that use a specific general class of quantum states (general *hypergraph states*) as resource states need to conduct Pauli-X and -Z measurements only to achieve quantum computational universality [46], in contrast to usual MBQC-protocols using ordinary quantum graph states (a trivial subclass of hypergraph states) as resource states [39, 40]. In order for a MBQC-protocol to run expectantly in a laboratory, one needs to assure that the resource state being used in the lab (*experimental state*) is sufficiently close to the state on paper (*theoretical state*). Additionally, for a measurement-based quantum computational protocol, accuracy of the measurements is pivotal. Hence, before starting a computational task, both, the state and the measurements, need to be *verified*

(or *tested*). An example of a contemporary approach concerning this is known as *robust self-testing* [45].

Most of the robust verification protocols for quantum graph states and measurements require measurements in a tilted basis [48, 49]. When using hypergraph states as a resource for a MBQC, this states to be impractical, since an additional measurement basis to Pauli-X and $-Z$ basis would be required to conduct a computational protocol, which is costly with respect to quantum error correction. However, Yamasaki et.al. found out that a specific kind of highly fault-tolerant MBQC-protocol presented in [53] seems to abstain from a tilted basis requirement for verification purposes [52].

In this paper, we will present the idea behind this novel verification protocol for a specific quantum graph state (*triangle graph state*) and demonstrate a possible generalization scheme for a broader class of states.

This work is structured as follows: We start with necessary preliminaries concerning graph states and and self-testing. Then, we introduce an existing efficient verification protocol for graph states presented by Zhu and Hayashi in [56] that refrains from the tilted measurement basis requirement, but is only applicable to a noiseless experimental environment. Subsequently, we introduce Yamasakis novel device-independent verification protocol for a specific kind of graph states [52] that states as an overall improvement of Zhu and Hayashis work. Finally, we try to present a possible first generalization step for his method to a simply-connected two-triangle graph state and discuss further generalization schemes.

II. GRAPH STATES

Quantum graph states (short: graph states) find numerous different applications in quantum information theory [23, 39]. In this chapter, we will give a short overview of their mathematical descriptions and an easy implementable example on how to manipulate them in a fashioned manner.

A. Mathematical Description

Let $G(V, E)$ be a mathematical graph, consisting of n vertices $V = \{v_i\}_{i=1}^n$ that are connected via edges $E = \{e_{ij} \mid i, j \in V\}$ [28]. Let us put one qbit $|+\rangle = \frac{1}{\sqrt{2}}(|0\rangle + |1\rangle)$ on each vertex without letting them interact at first. This results in an initial product state [17] (Fig. 1 as an example for a *triangle graph* with no interaction between the vertices.):

$$|G\rangle_{\text{in}} = \bigotimes_{v_i}^n |+\rangle \equiv |+\rangle^V$$

A pair of qbits interact if their associated vertices are adjacent. In other words, $|+\rangle^i$ and $|+\rangle^j$ may interact if $\exists\, e^{ij} \in E$. It can be shown that, due to constraints that arise from the underlying (simple) graph G, interaction between adjacent qbits can be sufficiently restricted to the case where their interaction
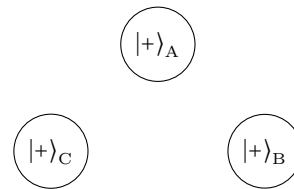
Figure 1. Three non-interacting qbits $|+\rangle^i$ at three vertices $i \in \{A, B, C\}$.

is an *Ising interaction* [17]. Using this, we can define an Ising-like interaction Hamiltonian H_{ij}^{I} [17, 41] as $H_{ij}^{\mathrm{I}} = Z_i Z_j$ and a two-particle unitary interaction operator $U_{ij}^{\mathrm{I}}(\phi_{ij}) := e^{-\phi_{ij} H_{ij}^{\mathrm{I}}}$ where ϕ_{ij} denotes the interaction strength/time between the qbits located at i and j. As argued in [17], in order to reach maximal entanglement within the graph state, we choose $\forall i, j \in V : \phi_{ij} = \pi$.

To avoid unnecessary cluttering of notation, we do not use the Ising- interaction- picture further on, but rather express the interaction between qbits in a quantum graph states by *controlled phase gates*:

$$U_{ij} = e^{-i\pi H_{ij}} \tag{1}$$

with $H_{ij} := |1\rangle^i \langle 1| \otimes |1\rangle^j \langle 1|$. Using

$$P_{(Z;\,m_Z)}^i = \frac{\mathrm{Id}^i + (-1)^{m_Z} Z^i}{2} \tag{2}$$

where $P_{(Z;\,m_Z)}^i$ denotes the projector onto the eigenspace of the Pauli-Z-operator at $|+\rangle^i$, (1) can be rewritten as

$$U_{ij} := P_{(Z;\,0)}^i \otimes \mathrm{Id}^j + P_{(Z;\,1)}^i \otimes Z^j. \tag{3}$$

Equivalently, one may write $U_{ij} = \mathrm{diag}(1, 1, 1, -1)$. One may argue that rewriting the interaction this way corresponds the Ising-interaction-picture only up to possible rotations around the z-axis. Nevertheless, since we are mostly interested in the entanglement properties of states obtained with underlying graphs, we may omit those rotations, as they do not change the physical properties of the quantum states at investigation. Therefore, by establishing the control phase gate U_{ij} as the unitary interaction operator between two adjacent qbits $i, j \in V$ within a simple graph $G(V, E)$ for all practical purposes, we can go on to one possible definition of *graph states* [17, 41]:

Definition II.1 (Graph state in the interaction formalism). A quantum graph state $|G\rangle$ corresponding to an underlying mathematical graph $G(V, E)$ is defined as following:

$$|G\rangle = \prod_{\{i,j\} \in E} U_{ij} |+\rangle^V \tag{4}$$

Note that all U_{ij} within the product of the right hand side of (4) commute. This may intuitively be understood in terms of indistinguishability of the order of interactions between the identical qbits involved in a quantum graph state.

Abuse of notation. Note that one needs to adjust U_{ij} in (3) in order for multiplication over several edges as in (4) to be well defined. This subtle alteration can be done by taking the tensor product of Id^k and U_{ij} for every $k \in V \setminus \{i, j\}$.

Figure 2. Depiction of a graph state $|G\rangle$ on the triangle graph $G(V,E)$ with $V = \{A,B,C\}$ and $E = \{e_{AB}, e_{AC}, e_{BC}\}$.

U_{ij} and Pauli-X and -Z operators fulfill the following commutation relations [41]:

$$U_{ij}(X^i \otimes \mathrm{Id}^j) = (X^i \otimes Z^j)U_{ij}, \qquad (5)$$

$$[U_{ij}, Z^i \otimes \mathrm{Id}^j] = [U_{ij}, \mathrm{Id}^i \otimes Z^j] = 0. \qquad (6)$$

Using (5) and (6), leads to the motivation of an alternative definition of graph states that is independent of a specific interaction picture [41]:
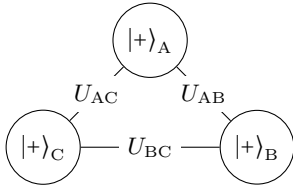
Definition II.2 (Graph state in the stabilizer formalism)**.** Given a mathematical graph $G(V,E)$, the associated *graph state* $|G\rangle$ is the unique simultaneous eigenstate with eigenvalue 1 of every *stabilizer* S^v on each vertex $v \in V$.
A stabilizer S^v on a vertex v is defined as a tensor product of Pauli-X and Pauli-Z operators:

$$S^v := X^v \otimes \bigotimes_{u \in \mathcal{N}(v)} Z^u. \qquad (7)$$

Here $\mathcal{N}(v) := \{v \in V | \exists \{u,v\} \in E\}$ denotes the *neighborhood* of v. I.e., using (7), the following equivalence relation can be obtained:

$$\forall v \in V, \, S^v |G\rangle = |G\rangle \Leftrightarrow |G\rangle \text{ graph state} \qquad (8)$$

This definition will be mostly used further on throughout this work. Interested readers may be referred to (A) for a more detailed derivation of the equivalency of both graph state definitions.

B. Vertex Coloring a Graph

Graph coloring is a merit of graph theory that finds numerous fields of application in quantum physics, one example being quantum graph state verification efficiency [56] that we will shortly present below. One method of graph coloring is known as *vertex coloring*, which is a specific assignment of a color to each vertex $v \in V$ in a mathematical graph $G(V,E)$, such that no adjacent vertices share the same color. The minimum number of colors needed is known as *chromatic number* $\chi(G)$ [12]. A graph that is colored with the minimum number of colors needed k is said to be *k-chromatic*. If the number of used colors might exceed the minimum amount, the graph is called *k-colorable*. For example, the triangular graph in (II A) is 3-chromatic (it is more usual to stick to the term *k-colorable* instead of *k-chromatic* in most of the literature).

C. Changing Graph States by Local Measurements

As shown in [9, 17] f.e., there are many well-known ways to change and manipulate graph states in a precise manner, using certain local Pauli measurements on

singular qbits of the graph state or linear optical devices such as PBSs for fusing different graph states together. As demonstrated there, those manipulations on the quantum state can be easily illustrated with the underlying mathematical graph: Different measurements on the quantum state are demonstrated by different actions on the graph. For the scope of this project, we will demonstrate the effect of a local Pauli-Z measurement on a qbit in a graph state, which can be illustrated as *deletion* of a vertex in the underlying mathematical graph.

1. Local Pauli-Z-Measurement on $|G\rangle$

Let us examine the so-called "deletion property" of Pauli-Z measurements conducted on a quantum graph state having a mathematical graph $G(V,E)$ (depicted in Fig. 3) consisting of two triangle subgraphs, denoted as $\triangle_{ABC}$ and $\triangle_{DEF}$, that are connected via one single edge e^{CD}: Conducting a local Pauli measurement on
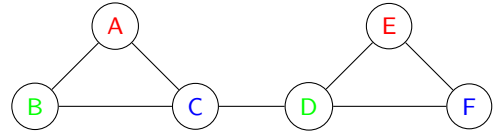
Figure 3. Mathematical graph associated with a six-qbit two-triangle quantum graph state.

a singular vertex $D \in G(V,E)$ on a graph state results in a unitary map original graph state $|G\rangle$ to $|G'\rangle$. For the case of local Pauli-Z-measurements, we find that the newly obtained state $|G'\rangle$ can be deduced from the original $|G\rangle$ by means of deletion of the measured vertex $D \in G(V,E)$ and/or local unitary transformations on the remaining ones. Generally, $|G'\rangle$ can be deduced utilizing the following proposition [17]:

Proposition II.1 (Local Pauli-Z-measurement on $|G\rangle$)**.** *Let $G(V,E)$ be the underlying graph of $|G\rangle$. Let $P^i_{(Z;m_Z)}$, $m_Z \in \{0,1\}$, be a projective Pauli-Z-measurement on the qbit $|+\rangle_i$ associated to the vertex $i \in V$. Then,*

$$P^i_{(Z;m_Z)} |G\rangle = $$
$$= |G'\rangle = \frac{1}{\sqrt{2}}(|m_Z\rangle^i \otimes U^i_{(Z,m_Z)} |G \smallsetminus i\rangle) \qquad (9)$$

with

$$U^i_{(Z;m_Z=0)} = \mathrm{Id}^i \text{ and} \qquad (10)$$

$$U^i_{(Z;m_Z=1)} = Z^{\mathcal{N}(i)}. \qquad (11)$$

For a proof of II.1, the reader may be referred to (A). One may interpret this proposition physically as following: if a single qbit located at $i \in V$ is locally measured with a Pauli-Z measurement, this leads to an isolation of its resulting quantum state with respect to the remaining graph state, hence the subtraction of the measured vertex within $|G \smallsetminus i\rangle$ and the tensor product of $|m_Z\rangle^i$ with the remaining graph state (one can also interpret this as a result of decoherence at the qbit located at $i \in V$). As for the graph state according to the remaining vertices $|G'\rangle$,

it either stays unaffected by that measurement or it undergoes local unitary transformations, depending on the outcome of $P^i_{(Z;\,m_Z)}|G\rangle$. A depiction of a post-measurement underlying graph associated with measurement outcome $m_Z = 0$ can be seen in Fig. 4:
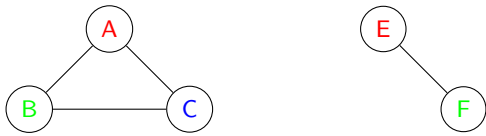
Figure 4. Post-measurement underlying graph corresponding to Pauli-Z-measurement outcome $m_Z = 0$ at $\mathrm{D} \in \triangle_{\mathrm{DEF}} \subset G(V,E)$.

Here, "deletion" of the vertex $\mathrm{D} \in \triangle_{\mathrm{DEF}}$ in a graph $G(V,E)$ consisting of two connected triangles $\triangle_{\mathrm{ABC}}$ and $\triangle_{\mathrm{DEF}}$, can be seen.

The post-measurement underlying graph associated with measurement outcome $m_Z = 1$ can be depicted as: The Z-symbol on the vertices $\{\mathrm{C},\mathrm{E},\mathrm{F}\} \in \mathcal{N}(\mathrm{D})$

Figure 5. Post-measurement underlying graph for Pauli-Z-measurement outcome $m_Z = 1$ at $\mathrm{D} \in \triangle_{\mathrm{DEF}}$, which was connected to $\triangle_{\mathrm{ABC}}$. Z symbolizes the Pauli-Z-measurements on the adjacent vertices $V \in \mathcal{N}(\mathrm{D}) = \{\mathrm{C},\mathrm{E},\mathrm{F}\}$ of D.

symbolize the Pauli-Z-measurements of (11).

III. SELF-TESTING

Self-testing is the experimental verification of a quantum state or quantum measurement in a *device-independent* (DI) scenario [45] where the experimental entity can be prepared in a similar manner for many consecutive times.

The notion of self-testing was firstly introduced by Mayers and Yao in [24]. Since then, it has become synonymous to many approaches of verifying quantum states and/or measurements that need few assumptions.

In this chapter, we will firstly introduce the notion of device-independence, then, we will present a general introduction to self-testing protocols and their underlying assumptions. Within this subsection, we will define the notion of *robust* self-testing as well and lastly, we will present a self-testing protocol for verifying graph states, following the approach of [56].

A. Device-Independent Protocols

The aim of device-independent protocols is to verify quantum physical properties (like entanglement of a quantum system) in a non-abstract fashion by mere examination and evaluation of experimental results without the need to know precisely the physics of how they are achieved. [45]

Imagine Charlie and Dorothy aim to verify entanglement of a quantum state some source prepares. Both are quantum physicists and so, they are familiar with *quantum state tomography*. They know, in order to fulfill their task, first, they need to create a specific *experimental setting*, suitable to verify entanglement. Then, they conduct their experiment, from which they will collect sufficiently enough experimental data (*results*), that they will statistically evaluate at the end, in order to verify entanglement. Their setting consists of two laboratories with the quantum state source in between, both have individual measurement settings and each one of them measures one particle of a bi-partite entangled quantum state (by implementing a beam-splitter f.e.).

Now, imagine Alice and Bob come to visit. They are familiar with the mathematical features of entangled states, but they have no information on with the specific experimental setup Charlie and Dorothy created. The only thing they can do is to evaluate the data the experiment in some unknown setups provides. Nevertheless, both claim to be able to verify entanglement. In order to do so, they need not know anything about the setup, they do not assume the source does provide entangled state, and they even do not need to know the physics behind the experiment. They treat the experimental setup as a black box that gets some *input* (the experimental setting) and provides some *output* (the results). So, Alice visits Charlies laboratory and Dorothy visits Bobs. They ask them to tell if the experimental setups in each round differs in some way, without the need of specifics. They name each input $\mathrm{A}, \mathrm{B}, \dots$ and the respective outcome $a_{\mathrm{A}}, a_{\mathrm{B}}, \dots$. After having collected sufficiently enough data, they can write down *correlations*:

$$p^{\mathrm{AB}}\left(a_{\mathrm{A}}, a_{\mathrm{B}} \,|\, x_{\mathrm{A}}, x_{\mathrm{B}}\right). \tag{12}$$

for each $\mathrm{A}, \mathrm{B}, \dots$. Those correlations are probabilities of measuring $(a_{\mathrm{A}}, a_{\mathrm{B}})$ conditioned on the measurement settings $x_{\mathrm{A}}, x_{\mathrm{B}}$.

The method both choose relies on *Bell non-locality* and *Bells inequality* [6]. J. Bell wrote down inequalities, which use correlation functions of measurement outcomes and their respective measurement settings, in order to proof entanglement of a quantum state. A Bell inequality consists of a function $\mathcal{I}$ on the set of correlations $\left\{p^{\mathrm{AB}}\left(a_{\mathrm{A}}, a_{\mathrm{B}} \,|\, x_{\mathrm{A}}, x_{\mathrm{B}}\right)\right\}_{\mathrm{AB}}$ that is upper bounded by β_C (*classical bound*):

$$\mathcal{I}\left(\left\{p^{\mathrm{AB}}\left(a_{\mathrm{A}}, a_{\mathrm{B}} \,|\, x_{\mathrm{A}}, x_{\mathrm{B}}\right)\right\}_{\mathrm{AB}}\right) \leq \beta_C. \tag{13}$$

(Pure) entangled states violate the Bell inequality. This means, without physical knowledge of any kind, Alice and Bob can verify entangled states. This procedure is known as *device-independent certification of entanglement*. [45].

If Alice and Bob were unsatisfied with the mere verification of entanglement of state, but rather aim to verify a specific quantum state in mind, device-independent scenarios allow for this to be possible as well. It is known that, although entangled state violate Bells inequality, they cannot do so arbitrarily strongly. There exists an upper bound of maximal violation of a Bell inequality, known as the *quantum bound* $\beta_Q > \beta_C$. So,

if Alice and Bob aim to detect a state that maximally violates Bells inequality (a maximally entangled state), they can do so within the described device-independent scenario. One might then say, Alice and Bob conduct a *self-test* on the quantum state.

Nevertheless, although in theory possible, experimental obstacles, such as experimental *noise*, hinder the experimentalists to actually measure data that implies maximal violation of the Bell inequality associated with the respective maximally entangled state they want to verify. In order to take this into account, they need to work within the merits of *robust self-testing*, where upper bounds are respecting realistic experimental scenarios and limits.

After having presented the main idea behind self-testing, let us explore important subtleties and its key points of its mathematical description:

B. Basics of Self-Testing

Self-testing is based on device-independent *Bell tests*. A Bell test is an observation of Bell inequality violations that implies an entangled pure quantum state corresponding to the underlying Bell inequality.

1. POVMs and Bell Operator $\mathcal{B}$

Consider a Bell test on a bipartite quantum system Alice (A) and Bob (B) share. In order for the verification protocol to be device-independent, correlation functions (12) are being examined. According to Borns rule, there should exist some *quantum state* ρ^{AB} and some *positive operator-valued measures* (POVMs)

$$\left\{ M^{A}_{a_A|x_A} \right\}_{a_A}, \left\{ M^{B}_{a_B|x_B} \right\}_{a_B} \tag{14}$$

that represent measurements on Alices and Bobs site with respective measurement settings x_A, x_B and corresponding measurement outcomes a_A, b_B.

Quantum states: Let $\mathcal{P}(\mathcal{H})$ denote the set of positive-semidefinite linear operators on a Hilbert space $\mathcal{H}$. Then, a quantum state may be represented as an element of a subset $S_{\leq}(\mathcal{H}) \subset \mathcal{P}(\mathcal{H})$ (known as the set of *subnormalized states* [47]), which is defined as:

$$S_{\leq}(\mathcal{H}) := \left\{ \rho \in \mathcal{P}(\mathcal{H}) \,|\, 0 < \mathrm{Tr}(\rho) \leq 1 \right\}. \tag{15}$$

Here, the subset of $S_{\leq}(\mathcal{H})$ corresponding to $\mathrm{Tr}(\rho^2) = 1$ represents *pure* quantum states and the subset corresponding to $0 < \mathrm{Tr}(\rho^2) < 1$ represents *mixed* quantum states. In the ongoing of this work, latter will be represented by $\tilde{\rho}$ and former will be represented by ρ. Furthermore, a quantum state $\rho^{AB} \in \mathcal{H}^A \otimes \mathcal{H}^B$ that two parties, Alice (being represented by a Hilbert space $\mathcal{H}^A$) and Bob (being represented by a Hilbert space $\mathcal{H}^B$), share, will be denoted by superscripted letters.

POVM: $M^{A}_{a_A|x_A}, M^{B}_{a_B|x_B}$ of (14) are known as *POVM*

elements and they fulfill the following:

$$\forall x_A, a_A : \sum_{x_A} M^{A}_{a_A|x_A} = \mathbb{1}^A, \ \forall x_A : M^{A}_{a_A|x_A} \geq 0$$
$$\forall x_B, a_B : \sum_{x_B} M^{B}_{a_B|x_B} = \mathbb{1}^B, \ \forall x_B : M^{A}_{a_B|x_B} \geq 0. \tag{16}$$

Using POVM elements, correlations can be rewritten according to Borns rule as:

$$p^{AB}\left(a_A, a_B \,|\, x_A, x_B\right) = \mathrm{Tr}\left(M^{A}_{a_A|x_A} \otimes M^{B}_{a_B|x_B}\, \rho^{AB} \right). \tag{17}$$

Additionally, according to *Naimarks theorem* [29] [36, 45], we may use an isometry $V^{A/B} : \mathcal{H}^{A/B} \to \left(\mathcal{H}^{A/B}\right)'$ to embed the Hilbert space the POVM elements act on, $\mathcal{H}^A$, $\mathcal{H}^B$, respectively, into larger Hilbert spaces $\mathcal{H}^{A'}$ and $\mathcal{H}^{B'}$, respectively, in which they can be represented by orthogonal projectors $P^{A/B}_{a_{A/B}|x_{A/B}}$ satisfying

$$\forall x_A : \sum_{a_A} P^{A}_{a_A|x_A} = \mathbb{1}^A \ ; \ \forall x_B : \sum_{a_B} P^{B}_{a_B|x_B} = \mathbb{1}^B$$

as

$$M^{A}_{a_A|x_A} = \left(V^A\right)^{\dagger} P^{A}_{a_A|x_A} V^A,$$
$$M^{B}_{a_B|x_B} = \left(V^B\right)^{\dagger} P^{B}_{a_B|x_B} V^B. \tag{18}$$

Note that those projectors are also known as *Naimark dilated operators*.

Importantly, the probabilities in (17) obtained by using POVMs on Alices and Bobs respective smaller Hilbert space and the probabilities using Naimark dilated operators coincide [45]. Therefore, we may equivalently investigate

$$P^{A}_{a_A|x_A} \equiv M^{A}_{a_A|x_A},$$
$$P^{B}_{a_B|x_B} \equiv M^{B}_{a_B|x_B} \tag{19}$$

further on. Using this, the following orthogonality property can be obtained (equivalently for $M^{B}_{a_B|x_B}$):

$$\forall a, x, x' : M^{A}_{a_A|x_A} M^{A}_{a'_A|x_A} \equiv \delta_{xx'} M^{A}_{a_A|x_A}. \tag{20}$$

Abuse of notation. Note that in the remainder of this work, we will omit equivalency $\equiv$ in our notation and treat (20) as an equality, meaning, we will actually investigate Naimark dilated operators, $P^{A}_{a_A|x_A}$ and $P^{B}_{a_B|x_B}$, rather than the original POVMs, $M^{A}_{a_A|x_A}$ and $M^{B}_{a_B|x_B}$ in (14).

In order to be able to write (17), we need some underlying physical assumptions [45]:

1. **Quantumness**: The experiment can be described via the laws of quantum physics.

2. **Locality**: Alice and Bob are space-like separated, i.e. there can be no signalling between them.

3. **Freedom of choice**: The measurement settings, x_A, x_B, are being chosen at random and independently from one another (there are no correlations in A to B or vice versa).

4. **IID**: Each round of experiment is independent and identical to one another, i.e. the statistics within the correlation functions (12) are *independently identically distributed* (i.i.d.).

Those are the basic physical assumptions in all self-testing scenarios. In order to verify if $\tilde{\rho}^{\mathrm{AB}}$ in (17) corresponds to the unique maximally entangled state that is to be self-tested, we introduce a *Bell operator* $\mathcal{B}_\rho$ dependent on the state ρ that maximally violates the Bell inequality in consideration. A Bell operator is a sum of *observables*. In general, we may expand observables O in their respective spectral decompositions as a sum of orthogonal projection operators P_α associated to the eigenspaces of eigenvalue α, multiplied by the probability p_α of obtaining α in a measurement:

$$O = \sum_\alpha p_\alpha P_\alpha. \qquad (21)$$

In our case, different measurement settings account to different observables. Additionally, recall that (19) holds. Hence, we may bridge a connection between POVMs (Naimark dilated operators) and the spectral decomposition of observables $O_{a_{\mathrm{A,B}}}^{\mathrm{A,B}}$ on Alices and Bobs site as

$$O_{a_{\mathrm{A/B}}}^{\mathrm{A/B}} = \sum_{a_{\mathrm{A/B}}} p\left(a_{\mathrm{A/B}} \mid x_{\mathrm{A/B}}\right) M_{a_{\mathrm{A/B}} \mid x_{\mathrm{A/B}}}^{\mathrm{A/B}} \qquad (22)$$

Using this, a Bell operator corresponding to self-testing a bipartite quantum system with target state ρ^{AB}, can be written as a sum of POVM elements:

$$\mathcal{B}_{\rho^{\mathrm{AB}}} := \sum_{\substack{a_{\mathrm{A}},a_{\mathrm{B}} \\ x_{\mathrm{A}},x_{\mathrm{B}}}} c_{\substack{a_{\mathrm{A}},a_{\mathrm{B}} \\ x_{\mathrm{A}},x_{\mathrm{B}}}}^{\mathrm{AB}} M_{a_{\mathrm{A}} \mid x_{\mathrm{A}}}^{\mathrm{A}} \otimes M_{a_{\mathrm{B}} \mid x_{\mathrm{B}}}^{\mathrm{B}} \qquad (23)$$

with $c_{\substack{a_{\mathrm{A}},a_{\mathrm{B}} \\ x_{\mathrm{A}},x_{\mathrm{B}}}}^{\mathrm{AB}} \in \mathbb{R}$ and $M_{a_{\mathrm{A/B}} \mid x_{\mathrm{A/B}}}^{\mathrm{A/B}}$ corresponding to the measurements conducted on Alice's/Bob's site.

Using (23), (13) can be rewritten as:

$$\mathcal{I}\left(\left\{p\left(a_{\mathrm{A}}, a_{\mathrm{B}} \mid x_{\mathrm{A}}, x_{\mathrm{B}}\right)\right\}_{\mathrm{AB}}\right) = \mathrm{Tr}\left(\mathcal{B}_{\rho^{\mathrm{AB}}} \tilde{\rho}^{\mathrm{AB}}\right) \leq \beta_C, \qquad (24)$$

where $\tilde{\rho}^{\mathrm{AB}}$ denotes the bipartite quantum system a source in a laboratory emits.

Due to unavoidable imperfections in the measurements and state in a laboratory, maximal violation of a Bell inequality can never be observed. In order to address this, Alice and Bob use the method of *robust self-testing*. Instead of demanding maximal violation of a Bell inequality as an indicator for having a maximally entangled state in the laboratory, robust self-testing hinges on a *self-testing statement*. Mathematically this means, instead of trying to obtain

$$\mathrm{Tr}\left(\mathcal{B}_\rho\left(\tilde{\rho} = \rho\right)\right) = \beta_Q, \qquad (25)$$

in an experiment, one tries to estimate a lower bound β on a *Bell violation* β

$$\beta \leq \beta_Q - \mathrm{Tr}\left(\mathcal{B}_\rho \tilde{\rho}\right), \qquad (26)$$

depending on the Bell operator $\mathcal{B}_\rho$ and the quantum system $\tilde{\rho}$ involved.

C. Analytical Estimations of Self-Testing Statements

There are different state-of-the-art approaches on how to obtain β of (26) analytically [3, 20]. One state-of-the-art approach is presented in [20] by Kaniewski.

Here, the author exerts the idea of *extraction maps* Ξ and *extractability violation trade-off functions* $\mathcal{Q}$:

$$\mathcal{Q}_{\mathcal{B}_\rho}(\beta) := \inf_{\tilde{\rho} \in \mathcal{S}_{\mathcal{B}_\rho}(\beta)} \Xi[\tilde{\rho} \to \rho], \qquad (27)$$

$$\Xi[\tilde{\rho} \to \rho] := \max_\Lambda F^2\left(\Lambda(\tilde{\rho}), \rho\right), \qquad (28)$$

where maximization in (28) is done over all quantum channels Λ (completely positive trace-preserving maps), $\tilde{\rho}$ denotes the actual state the source emits in the laboratory that is to be self-tested (*experimental state*), ρ denotes a unique pure quantum state that maximally violates the Bell inequality connected to the respective self-test (*target state*), $\mathcal{S}_{\mathcal{B}_\rho}(\beta)$ denotes the set of all quantum states that violate the Bell inequality under consideration for (at least) some value β:

$$\mathcal{S}_{\mathcal{B}_\rho}(\beta) = \left\{\tilde{\rho} \mid \beta_C \leq \beta \leq \mathrm{Tr}\left(\mathcal{B}_\rho \tilde{\rho}\right) \leq \beta_Q\right\}. $$

Fidelity:

$$F^2(\rho, \sigma) := \left(\mathrm{Tr}\left(\sqrt{\sqrt{\rho}\sigma\sqrt{\rho}}\right)\right)^2 \qquad (29)$$

denotes the (Uhlmann) *fidelity* [27] between the quantum states ρ and σ. Note that fidelity is symmetric and if one of the states $\rho = |\psi\rangle\langle\psi|$ or σ was pure, it may be rewritten as:

$$F^2(\rho, \sigma) = \langle\psi|\sigma|\psi\rangle. \qquad (30)$$

Furthermore, fidelity provides a definition of a *metric* $P(\cdot, \cdot)$ on the set of subnormalized quantum states $S_\leq(\mathcal{H})$ (15) known as *purified distance* (firstly introduced in [47]):

$$P(\rho, \sigma) := \sqrt{1 - F^2(\rho, \sigma)}. \qquad (31)$$

(28) and (27) provide a natural self-testing statement

$$\Xi[\tilde{\rho} \to \rho] \geq \mathcal{Q}_{\mathcal{B}_\rho}(\beta). \qquad (32)$$

Using a different Bell scenarios in [20], Kaniewski demonstrated in (32) that this statement can be further developed to finding the numerical values of $s \in \mathbb{R}$ and $\mu \in \mathbb{R}$ in

$$F^2\left(\Lambda(\tilde{\rho}), \rho\right) \geq \mu + w\beta = 1 + \frac{w}{\mu}\beta \qquad (33)$$

1. Minimum Amount of Tests in Robust Self-Testing Scenarios

Recall that in a self-testing scenario, correlations are estimated by measurement outcomes of K iid states in a laboratory. After having collected a sufficient finite amount of data, a self-testing statement in the form of (26) is being checked. The Bell violation β depends on the number of rounds K indirect proportionally. Mathematically, this can be seen by utilizing *Hoeffding's inequality* to estimate the correlation functions from the measurement outcomes. [52].
Intuitively, a large amount of iid rounds K, each having an identical mixed state that violates the Bell inequality for at least β, leads to a small deviation off the

maximal Bell violation β_Q for the mean state in the order of:

$$\beta = \mathcal{O}\left(\frac{1}{\sqrt{K}}\right). \tag{34}$$

In quantum state verification experiments, one aims to check if an imperfect state some source produces resembled some perfectly known *theoretical state* [30] on paper. One way to do so is to examine their *closeness*. Mathematically, this can be described using *trace distance* (*Schatten 1-norm*) [27, 38]:

Let ρ denote a theoretical state and let $\tilde{\rho}$ denote an experimental state. They are said to be ϵ-*close*, ($\epsilon > 0$), if they obey the following inequality:

$$T(\tilde{\rho}, \rho) := \frac{1}{2}\|\tilde{\rho} - \rho\|_1 = \frac{1}{2}\text{Tr}\left(|\tilde{\rho} - \rho|\right) \leq \epsilon, \tag{35}$$

where ϵ is frequently referred to as *state accuracy* [52], $\|\cdot\|_1$ denotes the Schatten 1-norm [7, 8]:

$$\|A\|_1 := \sum_{i=1}^{n} s_i^{\downarrow}(A) \tag{36}$$

with $s_i^{\downarrow}(A)$ denoting the *singular values* [19] of some finite dimensional matrix A, $(s_i^{\downarrow}(A) > s_j^{\downarrow}(A)$ if $i > j)$, and the absolute value $|\cdot|$ is defined as

$$|\tilde{\rho} - \rho| := \sqrt{(\tilde{\rho} - \rho)(\tilde{\rho} - \rho)^{\dagger}}. \tag{37}$$

In [14], C.A. Fuchs and J. van de Graaf introduced inequalities, connecting the trace distance (*Kolmogorov distance* in [14]) to the square root of the Uhlmann fidelity (*Bhattacharyya coefficient* in [14]):

$$1 - \sqrt{F^2(\tilde{\rho}, \rho)} \leq T(\tilde{\rho}, \rho) \leq \sqrt{1 - F^2(\tilde{\rho}, \rho)}. \tag{38}$$

These established inequalities are well-known in current literature as *Fuchs- van de Graaf-inequalities*. Note that (38) is a (sufficiently) *tight* inequality, meaning, there may exist no analytically obtainable quantity bounding the trace distance $T(\tilde{\rho}, \rho)$ from above or below closer than the lhs and rhs of (38).

Using the upper bound of the Fuchs- van de Graaf inequality, we note ϵ-closeness in a state-of-the-art robust self-testing scenario as in III C requires K rounds in the order of [52] :

$$K = \mathcal{O}\left(\frac{1}{\epsilon^4}\right). \tag{39}$$

IV. EFFICIENT VERIFICATION PROTOCOL FOR GRAPH STATES

As demonstrated above, self-testing relies on a specific Bell operator that is being used for analyzing upper bounds of fidelities. In [56], Zhu and Hayashi proposed an alternative verification method applicable for graph states [31], utilizing a *verification operator* Ω.

A. Verification Operator Ω

Recall the stabilizer definition of graph states (II.2). In [56], Zhu and Hayashi proposed an operator Ω that

tests if the quantum state in the lab is an simultaneous eigenstate of a set of stabilizers, corresponding to some theoretical quantum graph state. They defined a *verification operator* (or *strategy*) for a graph state corresponding to a mathematical graph $G(V, E)$ as:

$$\Omega^G := \sum_{v=1}^{|V|} \mu_v P^v, \tag{40}$$

$$P^v = \frac{\text{Id} + S^v}{2}, \tag{41}$$

where P^v denotes the *test projector* onto the eigenspace corresponding to eigenvalue 1 of the stabilizer S^v on vertex $v \in V$ (7) and μ_v denotes the weight on vertex $v \in V$. A quantum state ρ passes the *test*, if

$$\text{Tr}\left(\Omega^G \rho\right) = 1. \tag{42}$$

Therefore, passing the test implies that for $\rho = |\psi\rangle\langle\psi|$, $|\psi\rangle$ is a simultaneous eigenstate with eigenvalue 1 of all stabilizers S^v corresponding to the theoretical graph state $|G\rangle$. Uniqueness of graph states guarantees that, in that case, $|\psi\rangle = |G\rangle$.

Note that the stabilizer group is a subgroup of the Pauli group that consists of tensor products between a Pauli-X matrix, Pauli-Z matrices and the identity matrix (recall (II.2)) only. Therefore, in contrast to self-testing protocols, local Pauli-X and Pauli-Z measurements are sufficient for verifying graph states using the method in [56].

B. Efficiency

As demonstrated in [56, 57], the following inequality involving fidelity holds:

$$\text{Tr}\left(\Omega^G \tilde{\rho}\right) \leq \nu(\Omega^G) F^2\left(|G\rangle\langle G|, \tilde{\rho}\right) + \beta(\Omega), \tag{43}$$

where $\tilde{\rho}$ denotes some unknown state that is to be tested (similarly as above), $\beta(\Omega^G)$ denotes the second-largest eigenvalue of the verification operator Ω^G and $\nu(\Omega^G) := 1 - \beta(\Omega^G)$ denotes the *spectral gap*. As can be seen by observation, a larger spectral gap indicates a more efficient test strategy. In [56], it has been shown that, for graph states, the spectral gap is closely connected to the chromatic number of the underlying graph. In particular, the authors showed that for k-chromatic graphs $G(V, E)$ (meaning that the minimum amount of colors have been used in vertex coloring (II B)), the spectral gap equals the inverse of the chromatic number:

$$\nu(\Omega^G) = \frac{1}{\chi\left(\Omega^G\right)} \tag{44}$$

Remark: A verification protocol for quantum graph state corresponding to a k-chromatic mathematical graph is known as *coloring protocol*. In a coloring protocol the verification operator in (40) has equal weights $\forall\, v, w \in G(V, E): \mu_v = \mu_w$ [56].

V. METHOD

Most of the state-of-the-art robust self-testing protocols and other quantum state verification protocols

provide either bounds on the fidelity between the experimental and target quantum state, as in (33), but no bounds for the measurements therein, or only on the measurements, without consolidating the fidelity or similar notions as in [21]. There exists protocols that address both, as the norm-inequality method in [45] f.e., nevertheless, they require an impractical amount of tests K. Within this chapter, we aim present a novel method that includes both, a bound corresponding to the states (*state accuracy*) and a bound corresponding to the measurements (*measurement precision*), requiring a significantly lower amount of required test rounds K than existing robust self-testing and other quantum state verification protocols.

Furthermore, note that the verification scheme presented in IV assumes perfect measurements and perfect states. In reality, state and measurement imperfections in the lab are unavoidable. In Yamasakis work in [52], different sources of imperfections, intrinsic and independent *noise* (*noise*) are being taken into account and treated analytically, in order to establish a noise-receptive quantum graph state verification protocol.

A. Jordans Lemma

Recall that in quantum physics, measurements of physical entities are represented by aforementioned observables (III B 1). Similar to III C, within our model, it suffices to use Pauli-X and -Z measurements only. Lets the denote the observable corresponding to a Pauli-X and -Z measurement at Alices site O_X^A and O_Z^A (same for Bob). Using (22) and assuming both measurement outcomes, $+1$ and 0, are obtained equally likely, we may write observables in terms of corresponding POVMs as:

$$O_X^A = \frac{M_{0|x_A=0}^A - M_{1|x_A=0}^A}{2}, \tag{45}$$

$$O_Z^A = \frac{M_{0|x_A=1}^A - M_{1|x_A=1}^A}{2}, \tag{46}$$

where $x_A = 0/1$ accounts to Pauli-X or -Z measurement.

While in theory, the observables and the POVMs therein (III B 1) may be perfectly known, in reality, unavoidable noises account to additional degrees of freedom. Mathematically, this means that the dimension of the matrices associated with the observables might be unknown and much larger than their theoretical counterpart. Different self-testing protocols [4, 20, 45, 50] corresponding to Bell tests consisting of dichotomic measurements accounted this environmental influence utilizing *Jordans lemma* [37, 45]:

Lemma V.1. *(Jordans Lemma) Given two dichotomic Hermitian finite or countably infinite dimensional matrices $\tilde{A}, \tilde{B}$ with eigenvalues ± 1. There exists a choice of basis in which both $\tilde{A}, \tilde{B}$ take a block diagonal form. Within this basis, they may be written as a direct sum of countably infinite or finitely many 2×2 matrices $\tilde{A}_j, \tilde{B}_j$ as:*

$$\tilde{A} = \bigoplus_j \tilde{A}_j(\theta_j) = \bigoplus_j \cos(\theta_j)X + \sin(\theta_j)Z,$$
$$\tilde{B} = \bigoplus_j \tilde{B}_j(\theta_j) = \bigoplus_j \cos(\theta_j)X - \sin(\theta_j)Z \tag{47}$$

where X denotes Pauli-X matrix, Z denotes Pauli-Z matrix and θ_j denotes the angle between the projectors onto the jth and $j^{\text{th}}+1$ eigenspace in with $\tilde{A}_j$ and $\tilde{A}_{j+1}$ are block diagonal, respectively.

A more detailed layout and a proof of Jordans lemma can be found in [42].

Utilizing V.1 enables us to address ambiguous noise in our measurement apparatus in the lab corresponding to an dichotomic observable in theory. In the ongoing of this work, the basis vectors of the vector spaces in which $\tilde{A}_j(\theta_j)$ are block diagonal will be represented by $\{|j\rangle\}_j$ and they represent the additional statistical mixture the theoretical perfect measurements get (additional degrees of freedom) when implemented in the laboratory, due to intrinsic imperfections. Furthermore, we will refer to summands $\tilde{A}_j(\theta_j)$ in V.1 as *Jordan measurements*. Note that covering all possible angles θ_j in (47) accounts to covering all possible realizations of the corresponding observables, which means, all means of apparatus internal noise in the lab is covered within this analysis.

Note that there exists a unitary transformation U

$$U = \begin{pmatrix} \cos\frac{\pi}{8} & -\sin\frac{\pi}{8} \\ \sin\frac{\pi}{8} & \cos\frac{\pi}{8} \end{pmatrix}.$$

such that $\forall j : \theta_j = \frac{\pi}{4}$ can be linked to the noiseless case. This can be seen by recognizing that

$$\text{If } \forall j : \theta_j = \frac{\pi}{4} \Rightarrow \tilde{A}_j = U\frac{1}{\sqrt{2}}(X+Z)U^\dagger = X,$$
$$\tilde{B}_j = U\frac{1}{\sqrt{2}}(X-Z)U^\dagger = Z. \tag{48}$$

B. Independent Noise

The lab the verification experiment is conducted in might suffer from independent noise as well, coming from external sources. As before, for demonstrative purposes, let us assume verification of a bipartite quantum state shared by Alice and Bob. Let us denote the effect of these noise sources on $p^{AB}(x_A, x_B \,|\, a_A, a_B)_{(k)}$ as completely positive unital matrices $(\mathcal{E}_k^A)^\dagger$ and $(\mathcal{E}_k^B)^\dagger$ [52]. Then, the correlation obtained within the kth-round in the protocol may be written as:

$$p^{AB}(x_A, x_B \,|\, a_A, a_B)_{(k)} = \tag{49}$$

$$= \text{Tr}\left((\mathcal{E}_k^A)^\dagger \tilde{M}_{a_A|x_A}^A \otimes (\mathcal{E}_k^B)^\dagger \tilde{M}_{a_B|x_B}^B \tilde{\rho}_k^{AB}\right) = \tag{50}$$

$$= \text{Tr}\left(\left(\tilde{M}_{a_A|x_A}^A \otimes \tilde{M}_{a_B|x_B}^B\right)\left((\mathcal{E}_k^A)^\dagger \otimes (\mathcal{E}_k^B)^\dagger\right)\tilde{\rho}_k^{AB}\right). \tag{51}$$

(51) demonstrates that, within our model, independent noise in the lab can be accounted to occur as additional noise on the state rather than on the measurements, which indicates stability of $\tilde{M}_{a_A|x_A}^A$ and $\tilde{M}_{a_B|x_B}^B$. Note that this allows us to reuse the same measurement devices each round of verification. Stability of the measurements is crucial for numerous quantum information processing tasks such as verification of large resource states in MBQCs, where implementing a large amount of different measurement devices might not be scalable. With (51), this obstacle might be overcome.

C. Evaluating the Verification Operator

As presented in IV A, our proposed verification operator Ω consists of an addition of stabilizers as well. However, we improve the method presented in [56] by accounting to imperfections in Ω using Jordans lemma (V.1) on the stabilizers. The verification operator consisting of a sum of tensor products of imperfect observables is denoted as $\tilde{\Omega}$.

Apart from generalizing the verification protocol of [56] to be noise-receptive, we use McKague's result on quantum graph states containing odd (induced) cycles in their underlying mathematical (sub)graph [25] (Recall that an odd cycle is a cycle with an odd number of vertices, for example a triangle):

Lemma V.2. *(Odd cycle property) Given a quantum graph state* $|G\rangle$ *with a corresponding mathematical graph* $G(V, E)$ *containing an induced odd cycle subgraph* $G'(V', E')$, *let* $S^{v'}$ *denote the stabilizer on* $v' \in V' \subset G'(V', E')$. *Then:*

$$\prod_{v' \in V'} S^v |G\rangle = - |G\rangle. \tag{52}$$

A proof of this statement can be found in [25].

Interpretation: We aim to provide a verification operator that tests both, the stabilizer property of II.2 and, in our case, the odd-cycle-property of V.2. It is pivotal to recall the physical implementation of a verification operator: please note that Ω should not be misinterpreted as an observable consisting of a superposition of measurements, since this would be impractical and hard to implement in the lab. A verification operator is a sum of test projectors (in short *tests*) that verify if an arbitrary quantum state is a simultaneous eigenstate to all of them with eigenvalue 1. Heuristically, the reader may imagine that more testing possibilities to "check" this property account to a higher efficiency in the verification protocol.

In the case of verifying a single triangular graph state $|G\rangle_\triangle$ as depicted in II A, the according device-independent verification operator $\tilde{\Omega}^{\mathrm{ABC}}$ may be defined as [52]:

$$\tilde{\Omega}^{\mathrm{ABC}} = \frac{1}{4} \left(\frac{\mathrm{Id}^{\mathrm{ABC}} + \tilde{X}^{\mathrm{A}} \otimes \tilde{Z}^{\mathrm{B}} \otimes \tilde{Z}^{\mathrm{C}}}{2} + \frac{\mathrm{Id}^{\mathrm{ABC}} + \tilde{Z}^{\mathrm{A}} \otimes \tilde{X}^{\mathrm{B}} \otimes \tilde{Z}^{\mathrm{C}}}{2} + \right.$$
$$\left. + \frac{\mathrm{Id}^{\mathrm{ABC}} + \tilde{Z}^{\mathrm{A}} \otimes \tilde{Z}^{\mathrm{B}} \otimes \tilde{X}^{\mathrm{C}}}{2} + \frac{\mathrm{Id}^{\mathrm{ABC}} - \tilde{X}^{\mathrm{A}} \otimes \tilde{X}^{\mathrm{B}} \otimes \tilde{X}^{\mathrm{C}}}{2} \right). \tag{53}$$

Utilization of V.2 leads to an improvement of the verification operator presented in (40) by adding the fourth term of 53. This could be also be seen utilizing the inequality of (43).

VI. VERIFICATION PROTOCOL FOR A TRIANGULAR GRAPH STATE

Within this chapter, we will summarize Yamasakis method [52] for verifying a single *triangular graph state* ρ^{ABC} (A triangular quantum graph state is a graph state having a triangle $\triangle_{\mathrm{ABC}}$ with vertex set $V = \{\mathrm{A, B, C}\}$ and non-weighted edges connecting each vertex as an underlying mathematical graph.)

A. Measurement Precision, State Accuracy and Significance Level

Yamasaki bases his protocol on three physical merits: *measurement precision* Δ, *state accuracy* ϵ and the *significance level* δ. Before introducing the mathematical definition and the meaning these notions, we point out one important difference from our method to state-of-the-art self-testing protocols.

1. Non-IID Verification

As listed in III B 1(4), in order to write down a Bell operator for a self-testing scenario, one must assume that the source produces *i.i.d.* states. In our method, such an assumption is not needed. Concerning the statistics the source provides, we only require independence of the states $\tilde{\rho}_k$ and $\tilde{\rho}_{k'}$ for $k \neq k'$ that are produced in the kth and $k^{,\mathrm{th}}$ round/test, meaning that we may write a sequence of states after n rounds as

$$\tilde{\rho}_1 \otimes \tilde{\rho}_2 \otimes \cdots \otimes \tilde{\rho}_n. \tag{54}$$

Using independence, after K rounds, we may define an *average state* as:

$$\tilde{\rho} = \frac{1}{K} \sum_{k=1}^{K} \tilde{\rho}_k. \tag{55}$$

Within the remainder of this paper, K in (55) equals the minimum amount of tests needed for verifying the average state the source produces as precisely as aimed fo. The absence of a subscript in $\tilde{\rho}$ indicates the average state after K rounds and the existence of a subscript $\tilde{\rho}_k$ denotes a specific experimental state the source produces in the kth round.

2. ϵ, Δ and δ

Measurement precision is a lower bound on the total variation distance $\mathfrak{d}(\cdot, \cdot)$ of the probability distributions

of measurement outcomes between Jordan- and perfect measurements:

For $\Delta > 0$:

$$\mathfrak{d}\left(\tilde{p}\left(a_{\mathrm{A}}, a_{\mathrm{B}}, a_{\mathrm{C}} \,|\, x_{\mathrm{A}}, x_{\mathrm{B}}, x_{\mathrm{C}}\right), p\left(a_{\mathrm{A}}, a_{\mathrm{B}}, a_{\mathrm{C}} \,|\, x_{\mathrm{A}}, x_{\mathrm{B}}, x_{\mathrm{C}}\right)\right) :=$$
$$\frac{1}{2}\left\|\mathrm{Tr}\left(\tilde{M}^{\mathrm{A}}_{a_{\mathrm{A}}|x_{\mathrm{A}}}(\boldsymbol{\theta}^{\mathrm{A}}) \otimes \tilde{M}^{\mathrm{B}}_{a_{\mathrm{B}}|x_{\mathrm{B}}}(\boldsymbol{\theta}^{\mathrm{B}}) \otimes \tilde{M}^{\mathrm{C}}_{a_{\mathrm{C}}|x_{\mathrm{C}}}(\boldsymbol{\theta}^{\mathrm{C}})\tilde{\rho}^{\mathrm{ABC}}\right) - \mathrm{Tr}\left(M^{\mathrm{A}}_{a_{\mathrm{A}}|x_{\mathrm{A}}} \otimes M^{\mathrm{B}}_{a_{\mathrm{B}}|x_{\mathrm{B}}} \otimes M^{\mathrm{C}}_{a_{\mathrm{C}}|x_{\mathrm{C}}} \mathcal{D}\left(\rho^{\mathrm{ABC}}\right)\right)\right\|_1 \geq \tag{56}$$
$$\geq \Delta,$$

where $\tilde{p}(\cdot|\cdot)$ denotes the correlation obtained in the lab including noise in the measurements, $p(\cdot|\cdot)$ denotes the correlations assuming perfect measurements, $\mathcal{D}(\cdot)$ denotes a *decoding map* and $\boldsymbol{\theta}^{\mathrm{A/B/C}}$ represents a touple consisting of the angles in the Jordan decomposition (V.1) of $\tilde{M}^{\mathrm{A/B/C}}_{a_{\mathrm{A/B/C}}|x_{\mathrm{A/B/C}}}$. Heuristically, a decoding map is a completely positive trace-preserving linear map (CPTP map) that maps the experimental state $\tilde{\rho}^{\mathrm{ABC}}$ of arbitrary degrees of freedom as closely as possible to the theoretical state (III C 1) ρ^{ABC} of fixed dimensionality.

For a more rigorous interpretation of $\mathcal{D}(\cdot)$, we need the notion of state accuracy:

For $\epsilon > 0$:
$$T\left(\rho^{\mathrm{ABC}}, \mathcal{D}\left(\tilde{\rho}^{\mathrm{ABC}}\right)\right) \geq \epsilon. \tag{57}$$

Here, $T(\cdot)$ denotes the trace distance (35) and ϵ denotes aforementioned *state accuracy* and may be interpreted as the closest possible distance the theoretical state ρ^{ABC} and the decoded experimental state $\mathcal{D}\left(\tilde{\rho}^{\mathrm{ABC}}\right)$ of equal dimensionality share for any choice of $\mathcal{D}(\cdot)$, which is dependent on intrinsic imperfections in the source and external noise in the lab, as argued in, V B.

The theoretical state always passes the test, as demonstrated in (42). Since, in our protocol, we eased the conditions on the experimental state and the measurements to take noise into account, the passing condition may be eased as well. Instead of requiring unity in (42), we use a *significance level* $0 < \delta < 1$ and reformulate the condition after K rounds of all $k \leq K$ states for passing the test as:

For $0 < \delta \leq 1$: $\displaystyle\prod_{k=1}^{K} \mathrm{Tr}\left(\tilde{\Omega}^G \tilde{\rho}_k\right) \leq \delta,$ \hfill (58)

meaning that we assume to have a maximum probability of δ for all $\{\tilde{\rho}_k\}_{k=1}^{K}$ passing the test. Here, $\tilde{\Omega}^G$ denotes an imperfect verification operator associated with a theoretical state $|G\rangle$, which can be obtained by replacing the perfect observables within the theoretical counterpart Ω^G by imperfect observables.

Furthermore, using Jordans lemma (V.1), we may write the test operator as a direct sum of $(2 \times 2)^3$ matrices:

$$\tilde{\Omega}^G = \bigoplus_{j_{\mathrm{A}}} \bigoplus_{j_{\mathrm{B}}} \bigoplus_{j_{\mathrm{C}}} \tilde{\Omega}^G_{j_{\mathrm{A}} j_{\mathrm{B}} j_{\mathrm{C}}}(\theta^{\mathrm{A}}, \theta^{\mathrm{B}}, \theta^{\mathrm{C}}), \tag{59}$$

where the subscripts of j denote the jth block Jordan direct sum decomposition (V.1) of an observable acting on the qbits of the graph state associated with the vertices of the underlying mathematical graph $\triangle_{\mathrm{ABC}}$.

Abuse of notation. In the ongoing of this work, we may omit the angles argument of Jordan measurements and Jordan verification operators if clear from context or irrelevant for explicit calculations. Additionally, we will omit the subscript G, if obvious from context (In this section, we are examining the verification of a triangular graph state, so $G = \triangle_{\mathrm{ABC}}$).

B. Summarizing the Results

Using the notions introduced in VI A, Yamasaki et. al. presented a mathematical layout for a novel verification scheme in [52]. In this chapter, we will summarize the main points of their work. For proofs and deeper investigations, we refer to [52] and further upcoming papers concerning this novel quantum state verification approach.

1. Verifying Measurements

Utilizing the inequality of arithmetic and geometric means, we note that the lhs of (58) is upper-bounded by the passing probability of the average state:

$$\prod_{k=1}^{K} \mathrm{Tr}\left(\tilde{\Omega}\,\tilde{\rho}_k\right) \leq \left(\frac{1}{K}\sum_{k=1}^{K} \mathrm{Tr}\left(\tilde{\Omega}\,\tilde{\rho}_k\right)\right)^K = \tag{60}$$

$$= \left(\mathrm{Tr}\left(\tilde{\Omega}\,\tilde{\rho}\right)\right)^K \leq \delta, \tag{61}$$

hence, it is sufficient to evaluate an upper bound of the passing probability $\mathrm{Tr}\left(\tilde{\Omega}\,\tilde{\rho}\right)$ of the average state $\tilde{\rho}$.

Let $\Pi_{j_{\mathrm{A/B/C}}}$ denote the projector onto the jth eigenspace in which the Jordan measurement in V.1 takes a diagonal form. Then, we may project the state onto the eigenspaces the Jordan measurements act on, resulting in a direct sum:

$$\bigotimes_{j_{\mathrm{A}}} \bigotimes_{j_{\mathrm{B}}} \bigotimes_{j_{\mathrm{C}}} \left(\Pi_{j_{\mathrm{A}}} \otimes \Pi_{j_{\mathrm{B}}} \otimes \Pi_{j_{\mathrm{C}}}\right)\tilde{\rho}\left(\Pi_{j_{\mathrm{A}}} \otimes \Pi_{j_{\mathrm{B}}} \otimes \Pi_{j_{\mathrm{C}}}\right) =$$
$$= \bigotimes_{j_{\mathrm{A}}} \bigotimes_{j_{\mathrm{B}}} \bigotimes_{j_{\mathrm{C}}} p\left(j_{\mathrm{A}}, j_{\mathrm{B}}, j_{\mathrm{C}}\right) \tilde{\rho}_{j_{\mathrm{A}} j_{\mathrm{B}} j_{\mathrm{C}}},$$
$$\tag{62}$$

where the sum over j of $p\left(j_{\mathrm{A}}, j_{\mathrm{B}}, j_{\mathrm{C}}\right)$ comes from

$$\sum_{j_{\mathrm{A}}, j_{\mathrm{B}}, j_{\mathrm{C}}} p\left(j_{\mathrm{A}}, j_{\mathrm{B}}, j_{\mathrm{C}}\right) :=$$
$$:= \mathrm{Tr}\left(\bigotimes_{j_{\mathrm{A}}} \bigotimes_{j_{\mathrm{B}}} \bigotimes_{j_{\mathrm{C}}} \Pi_{j_{\mathrm{A}}} \otimes \Pi_{j_{\mathrm{B}}} \otimes \Pi_{j_{\mathrm{C}}} \tilde{\rho}\right) \tag{63}$$

$p(j_A, j_B, j_C)$ denotes the probability of measuring ("finding") the qbits corresponding to $A, B, C \in \triangle_{ABC}$ quantum state $\tilde{\rho}_{j_A, j_B, j_C}$ in the tensor product space spanned by $\{|j_A\rangle \otimes |j_B\rangle \otimes |j_C\rangle\}_{j_A, j_B, j_C}$.
Using this, we may rewrite (61) as:

$$\text{Tr}\left(\tilde{\Omega}\tilde{\rho}\right) = \sum_{j_A, j_B, j_C} p(j_A, j_B, j_C) \text{Tr}\left(\tilde{\Omega}_{j_A j_B j_C}\tilde{\rho}_{j_A j_B j_C}\right). \tag{64}$$

For any state $\tilde{\rho}_{j_A j_B j_C}$, the maximum passing probability is upper-bounded by the largest eigenvalue $\lambda_{\max}\left(\tilde{\Omega}_{j_A j_B j_C}\right)$ of $\tilde{\Omega}_{j_A j_B j_C}$. This can be seen via decomposing the state in the eigenbasis of the verification operator. Therefore, (64) is upper-bounded by:

$$\text{Tr}\left(\tilde{\Omega}\tilde{\rho}\right) \le \sum_{j_A, j_B, j_C} p(j_A, j_B, j_C) \lambda_{\max}\left(\tilde{\Omega}_{j_A j_B j_C}\right). \tag{65}$$

Before writing down the upper bound of (65), we will sketch another result in [52], connecting the measurement precision in (56) and the Jordan measurements. Yamasaki et. al. showed that the angles magnitude is an indicator for preciseness in measurements and examination of (56) may be surrogated by examination of:

$$\frac{1}{4} \sum_{j_A, j_B, j_C} p(j_A, j_B, j_C)\left(|\theta_{j_A}^A| + |\theta_{j_B}^B| + |\theta_{j_C}^C|\right) \ge \Delta \tag{66}$$

instead. Using the largest eigenvalue of $\tilde{\Omega}_{j_A j_B j_C}$ (we refer to the original work [52] for a full expression of $\lambda_{\max}\left(\tilde{\Omega}_{j_A j_B j_C}\right)$) and (66), Yamasaki et.al. obtained

an upper bound on the passing probability for K states in terms of a given measurement precision Δ as:

$$\prod_{k=1}^{K} \text{Tr}\left(\tilde{\Omega}^{ABC}\tilde{\rho}_k\right) \le \left(\frac{1}{4}\left(2 + \sqrt{1 + 3\cos^2\frac{8}{3}\Delta}\right)\right)^K, \tag{67}$$

which yields a minimum number of tests K in order to reach a significance level δ as:

$$K \ge \frac{\ln \delta}{\ln\left(\frac{1}{4}\left(2 + \sqrt{1 + 3\cos^2\frac{8}{3}\Delta}\right)\right)}. \tag{68}$$

Note that (68) scales quadratically in terms of $\frac{1}{\Delta}$ [52].

2. Verifying the State

For verifying the state, we may assume "sufficiently precise" measurements, meaning, instead of assuming measurement precision as a lower bound as in (56), we may state it as an upper bound:

$$\frac{1}{4} \sum_{j_A, j_B, j_C} p(j_A, j_B, j_C) \overbrace{\left(|\theta_{j_A}^A| + |\theta_{j_B}^A| + |\theta_{j_C}^A|\right)}^{:=\Delta_{\theta_{j_A}^A, \theta_{j_B}^B, \theta_{j_C}^C}} \le \Delta. \tag{69}$$

In his work, Yamasaski chose a particular adequate decoding map:

$$\mathcal{D}(\tilde{\rho}) := \text{Tr}_J\left(V\left(\sum_{j_A, j_B, j_C}\left(\Pi_{j_A}\otimes\Pi_{j_B}\otimes\Pi_{j_C}\right)\tilde{\rho}\left(\Pi_{j_A}\otimes\Pi_{j_B}\otimes\Pi_{j_C}\right)\right)V^\dagger\right) = \sum_{j_A, j_B, j_C} p(j_A, j_B, j_C)\tilde{\rho}_{j_A j_B j_C}, \tag{70}$$

where $\text{Tr}_J(\cdot)$ denotes the partial trace over aforementioned tensor product space $\text{span}\left(\{|j_A\rangle \otimes |j_B\rangle \otimes |j_C\rangle\}_{j_A, j_B, j_C}\right)$ and V denotes a unitary operator changing the basis in such a way that the direct sum of two-dimensional blocks is represented by the tensor product of the space representing the label of the block and the two-dimensional space representing each block [52]. This decoding map can be locally implemented by a tensor product of three CPTP maps acting on each system corresponding to the vertices $V = ABC$.
Using this, (57) can be rewritten as

$$\frac{1}{2}\left\|\sum_{j_A, j_B, j_C} p(j_A, j_B, j_C)\tilde{\rho}_{j_A j_B j_C} - \rho^{ABC}\right\|_1 \ge \epsilon. \tag{71}$$

Lets write the Jordan verification operator in its spectral decomposition:

$$\tilde{\Omega}_{j_A, j_B, j_C} = \sum_{j=1}^{8} \lambda_j |\tilde{\psi}\rangle_j \langle\tilde{\psi}|_j. \tag{72}$$

Using this, we may obtain an upper bound of (64) in terms of the largest $\lambda_1\left(\theta^A, \theta^B, \theta^C\right)$ and second-largest

$\lambda_2\left(\theta^A, \theta^B, \theta^C\right)$ eigenvalue of $\tilde{\Omega}_{j_A, j_B, j_C}\left(\theta^A, \theta^B, \theta^C\right)$ as

$$\text{Tr}\left(\tilde{\Omega}_{j_A j_B j_C}\tilde{\rho}_{j_A j_B j_C}\right) \le \lambda_2 + (1 - \lambda_2)\left\langle\tilde{\psi}_1|\tilde{\rho}_{j_A j_B j_C}|\tilde{\psi}_1\right\rangle. \tag{73}$$

(Note that a similar result exists in [57] and that we omitted the angle argument) Therefore, it suffices to obtain an upper bound of λ_2 and the fidelity between the experimental state and the eigenvector corresponding to the largest eigenvalue λ_1 of the Jordan verification operator $\tilde{\Omega}_{j_A j_B j_C}\left(\theta^A, \theta^B, \theta^C\right)$ (29)

$$F^2\left(|\tilde{\psi}_1\rangle\langle\tilde{\psi}_1|, \tilde{\rho}_{j_A j_B j_C}\right) = \left\langle\tilde{\psi}_1|\tilde{\rho}_{j_A j_B j_C}|\tilde{\psi}_1\right\rangle. \tag{74}$$

Using a similar technique as for upper-bounding the largest eigenvalue in terms of measurement verification, Yamasaki et.al. provides us with an upper bound of $\lambda_2\left(\theta^A, \theta^B, \theta^C\right)$ as:

$$\lambda_2\left(\theta^A, \theta^B, \theta^C\right) \le \frac{1}{4}\left(2 + \frac{2}{3}\Delta_{\theta_{j_A}^A, \theta_{j_B}^B, \theta_{j_C}^C}\right). \tag{75}$$

Note that this upper bound indicates a higher efficiency of this protocol than the existing verification protocol for hypergraph states, which is based on the

chromatic number, in [56] possesses (compare (43)).

For bounding (74), we may analyze the purified distance (31) $P\left(\left|\tilde{\psi}_1\right\rangle\left\langle\tilde{\psi}_1\right|, \tilde{\rho}_{j_A j_B j_C}\right)$. Note that, since purified distance is a metric on $S_{\leq}\left(\mathcal{H}^{\mathrm{ABC}}\right) \ni \left\{\left|\tilde{\psi}_1\right\rangle\left\langle\tilde{\psi}_1\right|, \tilde{\rho}_{j_A j_B j_C}\right\}$, $P(\cdot)$ is symmetric and fulfills the *triangle inequality* on that domain:

$$P\left(\left|\tilde{\psi}_1\right\rangle\left\langle\tilde{\psi}_1\right|, \tilde{\rho}_{j_A j_B j_C}\right) \geq$$
$$\geq P\left(\tilde{\rho}_{j_A j_B j_C}, \rho^{\mathrm{ABC}}\right) - P\left(\rho^{\mathrm{ABC}}, \left|\tilde{\psi}_1\right\rangle\left\langle\tilde{\psi}_1\right|\right). \tag{76}$$

Therefore, the analysis reduces to obtaining a lower bound on

$$P\left(\tilde{\rho}_{j_A j_B j_C}, \rho^{\mathrm{ABC}}\right) \tag{77}$$

and an upper bound on

$$P\left(\rho^{\mathrm{ABC}}, \left|\tilde{\psi}_1\right\rangle\left\langle\tilde{\psi}_1\right|\right). \tag{78}$$

Finding an upper bound on (78) can be achieved by finding a lower bound of:

$$F^2\left(\rho^{\mathrm{ABC}}, \left|\tilde{\psi}_1\right\rangle\left\langle\tilde{\psi}_1\right|\right). \tag{79}$$

Concerning (77), recall the interpretation of the state accuracy definition in (57), associating it with the closest distance two states can be. Following Fuchs- van de Graaf- inequalities (38), this means that the associated purified distance (31) funges as an upper bound on state accuracy as well (considering tightness of the inequality). Henceforth, we are motivated to define the lower bound of (77) in terms of a state accuracy $\epsilon_{j_A j_B j_C}$ which is defined as the trace distance (35) between the target state ρ^{ABC} and the projection of the experimental state onto $\mathrm{span}\left(\left\{|j_A\rangle \otimes |j_B\rangle \otimes |j_C\rangle\right\}\right)$:

$$T\left(\rho^{\mathrm{ABC}}, \tilde{\rho}_{j_A j_B j_C}\right) = \epsilon_{j_A, j_B, j_C}$$
$$\Rightarrow P\left(\rho^{\mathrm{ABC}}, \left|\tilde{\psi}_1\right\rangle\left\langle\tilde{\psi}_1\right|\right) = \epsilon_{j_A, j_B, j_C}. \tag{80}$$

As shown by Yamasaki, $\epsilon_{j_A j_B j_C}$ correlates to the given state accuracy ϵ in (57) as

$$\sum_{j_A, j_B, j_C} p\left(j_A, j_B, j_C\right) \epsilon_{j_A j_B j_C} \geq \epsilon. \tag{81}$$

As for $F^2\left(\rho^{\mathrm{ABC}}, \left|\tilde{\psi}_1\right\rangle\left\langle\tilde{\psi}_1\right|\right)$, Yamasaki obtained a lower bound by means of numerical analysis as:

$$\text{For } C := 0.281\cdots: \tag{82}$$
$$F^2\left(\rho^{\mathrm{ABC}}, \left|\tilde{\psi}_1\right\rangle\left\langle\tilde{\psi}_1\right|\right) \geq 1 - \left(\frac{C}{\sqrt{3}}\Delta_{\theta^A_{j_A}, \theta^B_{j_B}, \theta^C_{j_C}}\right). \tag{83}$$

For a reminder of $\Delta_{\theta^A_{j_A}, \theta^B_{j_B}, \theta^C_{j_C}}$, the reader may recall (69).

Combining both results and recalling (31) yields an upper bound on (74) as

$$F^2\left(\left|\tilde{\psi}_1\right\rangle\left\langle\tilde{\psi}_1\right|, \tilde{\rho}_{j_A j_B j_C}\right) \leq$$
$$\leq 1 - \left(\epsilon_{j_A j_B j_C} - \frac{C}{\sqrt{3}}\Delta_{\theta^A_{j_A}, \theta^B_{j_B}, \theta^C_{j_C}}\right)^2 \tag{84}$$

Using (84), (75) and (81), Yamasaki et.al. showed that the number of required tests concerning state accuray may be lower bounded as

$$K \geq \frac{\ln \delta}{\ln\left(1 - \frac{1}{2}\left(\epsilon - \left(\frac{C}{\sqrt{3}} + \frac{4}{6}\right)\Delta\right)^2 + \frac{8}{36}\Delta^2\right)}. \tag{85}$$

Note that (85) scales quadratically with a leading term in the order of $\mathcal{O}(K) = \frac{1}{\epsilon^2 + \Delta^2}$ (for a more detailed demonstration the reader may be referred to the original paper [52]).

As a result, the minimum number of rounds K for verifying a triangular quantum state with state accuracy ϵ and measurements with measurement precision Δ simultaneously, given a significance level δ, the maximization over the number necessary for state verification and the number necessary for measurement verification:

$$K = \max\left\{\left\lceil\frac{\ln \delta}{\ln\left(\frac{1}{4}\left(2 + \sqrt{1 + 3\cos^2\frac{8}{3}\Delta}\right)\right)}\right\rceil, \left\lceil\frac{\ln \delta}{\ln\left(1 - \frac{1}{2}\left(\epsilon - \left(\frac{C}{\sqrt{3}} + \frac{4}{6}\right)\Delta\right)^2 + \frac{8}{36}\Delta^2\right)}\right\rceil\right\}. \tag{86}$$

VII. GENERALIZATION TO TWO SIMPLY CONNECTED TRIANGULAR GRAPH STATES

In this chapter, we present the main ideas behind our method for verifying a quantum graph state corresponding to a mathematical graph consisting of two simply connected triangles $\triangle_{\mathrm{ABC}}$ and $\triangle_{\mathrm{DEF}}$, further on referred to as *six-qbit two triangle graph state*. This work can be seen as a generalization of Yamasaki et.al. work in [52], which was subsequently summarized in

VI.
More precisely, the mathematical graph $G(V, E)$ (which is depicted in II C, Fig. 3 and, as a reminder, again here in Fig. 6) associated with the quantum state in examination consists of two triangle subgraphs, denoted as $\triangle_{\mathrm{ABC}}$ and $\triangle_{\mathrm{DEF}}$, which are connected via one single edge $e^{\mathrm{CD}}_{1,2}$. In other words, if

$$G(V, E) = \bigcup_{i=1}^{n} \triangle_{V_i} \cup e^{\mathrm{lm}}_{i, i+1}. \tag{87}$$

denotes a n- chain of simply connected triangles with V_i being the vertices set of the ith triangle $\triangle_{V_i}$ and $e^{\text{lm}}_{i,i+1}$ denoting the connecting edge between the ith triangle and its adjacent $i^{\text{th}} + 1$ triangle within this chain with $l \in \triangle_{V_i}, m \in \triangle_{V_{i+1}}$ (or vice versa), then the following analysis will deal with the special case of $n = 2$:
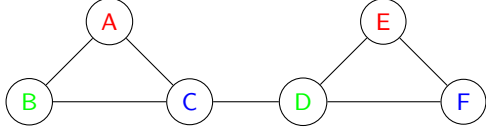

Figure 6. $G = \bigcup\limits_{i=1}^{n=2} \triangle_{V_i} \cup e^{\text{CD}}_{i,i+1}$

A. Verification Operator $\tilde{\Omega}^{\text{ABCDEF}}$

As for a verification operator $\tilde{\Omega}^{\text{ABCDEF}}$, we follow the recipe presented in V C, testing the stabilizer property (II.2) and the odd-cycle-property (V.2) on the subgraph quantum states associated with the subgraphs $\triangle_{\text{ABC}}$, $\triangle_{\text{DEF}}$ simultaneously. Again, our protocol is a coloring protocol (II B), therefore, all terms in the expansion of the verification operator are equally weighted. This leads us to defining $\tilde{\Omega}^{\text{ABCDEF}}$ as:

$$
\begin{aligned}
\tilde{\Omega}^{\text{ABCDEF}} := \frac{1}{5}\Bigg(&\frac{\mathbb{1} + \tilde{X}^{\text{A}} \otimes \tilde{Z}^{\text{B}} \otimes \tilde{Z}^{\text{C}} \otimes \tilde{X}^{\text{D}} \otimes \tilde{Z}^{\text{E}} \otimes \tilde{Z}^{\text{F}}}{2} + \frac{\mathbb{1} + \tilde{Z}^{\text{A}} \otimes \tilde{X}^{\text{B}} \otimes \tilde{Z}^{\text{C}} \otimes \tilde{Z}^{\text{D}} \otimes \tilde{X}^{\text{E}} \otimes \tilde{Z}^{\text{F}}}{2} + \\
&+ \frac{\mathbb{1} + \tilde{Z}^{\text{A}} \otimes \tilde{Z}^{\text{B}} \otimes \tilde{X}^{\text{C}} \otimes \tilde{Z}^{\text{D}} \otimes \tilde{Z}^{\text{E}} \otimes \tilde{X}^{\text{F}}}{2} + \frac{\mathbb{1} - \tilde{X}^{\text{A}} \otimes \tilde{X}^{\text{B}} \otimes \tilde{X}^{\text{C}} \otimes \tilde{Z}^{\text{D}} \otimes \text{Id}^{\text{E}} \otimes \text{Id}^{\text{F}}}{2} + \\
&+ \frac{\mathbb{1} - \text{Id}^{\text{A}} \otimes \text{Id}^{\text{B}} \otimes \tilde{Z}^{\text{C}} \otimes \tilde{X}^{\text{D}} \otimes \tilde{X}^{\text{E}} \otimes \tilde{X}^{\text{F}}}{2}\Bigg).
\end{aligned}
\tag{88}
$$

The (imperfect) Pauli-Z matrices acting on C and D in the fourth and fifth term of (88) account to the connection of the two triangles. They originate from the odd-cycle lemma (V.2). Since $\text{C} \in \triangle_{\text{ABC}}$ and $\text{D} \in \triangle_{\text{DEF}}$ are the connecting vertices of the simply connected two-triangle graph state, respectively, the stabilizers S^{C} and S^{D} with $S^{\text{C}} = \tilde{Z}^{\text{A}} \otimes \tilde{Z}^{\text{B}} \otimes \tilde{X}^{\text{C}} \otimes \tilde{Z}^{\text{D}} \otimes \text{Id}^{\text{E}} \otimes \text{Id}^{\text{F}}$ and $S^{\text{D}} = \text{Id}^{\text{A}} \otimes \text{Id}^{\text{B}} \otimes \tilde{Z}^{\text{C}} \otimes \tilde{X}^{\text{D}} \otimes \tilde{Z}^{\text{E}} \otimes \tilde{Z}^{\text{F}}$, contain terms $\tilde{Z}^{\text{D}}$ and $\tilde{Z}^{\text{C}}$, that account to vertices, which are not element of the respective triangles we aim to verify the odd-cycle property in (V.2) of (they are not element of the induced triangle subgraphs of V.2). Upon multiplication as in (52), they originate naturally and do not influence the examined property as argued in [25].

Using Jordans lemma (V.1), similarly as in (59), we may rewrite (88) as a direct sum of *Jordan verification operators* $\tilde{\Omega}_{j_{\text{A}},j_{\text{B}},j_{\text{C}},j_{\text{D}},j_{\text{E}},j_{\text{F}}}$ as:

$$
\begin{aligned}
\tilde{\Omega}^{\text{ABCDEF}} &= \\
&= \bigoplus_{j_{\text{A}}} \bigoplus_{j_{\text{B}}} \bigoplus_{j_{\text{C}}} \bigoplus_{j_{\text{D}}} \bigoplus_{j_{\text{E}}} \bigoplus_{j_{\text{F}}} \tilde{\Omega}_{j_{\text{A}},j_{\text{B}},j_{\text{C}},j_{\text{D}},j_{\text{E}},j_{\text{F}}},
\end{aligned}
\tag{89}
$$

where we omitted the angle argument in (59), in order to avoid cluttering of notation. The motivation of referring to the summands of (89) as Jordan verification operators is similar to the motivation of naming the summands in V A *Jordan measurements*.

In principle, one may proceed similarly to the protocol of [52] summarized in VI. Nevertheless, computational time and calculations for obtaining bounds as in VI for obtaining a minimum K turn out to be unfeasible in the six-qubit two-triangle case. This motivates the question whether it was possible to use results on aboves single-triangle verification scheme for more general graph states. Within the following chapters, we will present the first step towards a generalization of the verification method of a singular triangle graph state by investigation a chain of two triangles, connected by one edge.

B. Breaking down the Analysis to single Triangle Graph State Verification

Let us recall how local Pauli-Z-measurements $P^i_{(Z;m_Z)}$ (2) act on graph states (II.1): A local Pauli-Z-measurement is dichotomic with measurement outcomes $m_Z = \{0, 1\}$ and accounts to aforementioned *deletion* of a vertex in the associated underlying mathematical graph. For exemplification, let us consider $P^{\text{D}}_{(Z;m_Z)}$ acting on D, which is the connecting vertex in $\triangle_{\text{DEF}}$ to $\triangle_{\text{ABC}}$ via one singular edge $e^{\text{DE}} \in E$ (similar results are true for $P^{\text{C}}_{(Z;m_Z)}$ acting on $\text{C} \in \triangle_{\text{ABC}}$). Now, let us investigate the post-measurement test operator on the triangle subgraph $\triangle_{\text{ABC}}$. Note that two different cases accounting to two different measurement outcomes m_Z of $P^i_{(Z;m_Z)}$ need to be taken into account. This indicates that the post-measurement test operator should be a conditioned on m_Z as $\tilde{\Omega}^{\text{ABC}}|_{m_Z}$:

$$
\begin{aligned}
\tilde{\Omega}^{\text{ABC}}_{|m_Z=0} = \frac{1}{5}\Bigg(&\frac{\text{Id}^{\text{ABC}} + \tilde{X}^{\text{A}} \otimes \tilde{Z}^{\text{B}} \otimes \tilde{Z}^{\text{C}}}{2} + \frac{\text{Id}^{\text{ABC}} + \tilde{Z}^{\text{A}} \otimes \tilde{X}^{\text{B}} \otimes \tilde{Z}^{\text{C}}}{2} + \\
&+ \frac{\text{Id}^{\text{ABC}} + \tilde{Z}^{\text{A}} \otimes \tilde{Z}^{\text{B}} \otimes \tilde{X}^{\text{C}}}{2} + \frac{\text{Id}^{\text{ABC}} - \tilde{X}^{\text{A}} \otimes \tilde{X}^{\text{B}} \otimes \tilde{X}^{\text{C}}}{2} + \frac{\text{Id}^{\text{ABC}} + \text{Id}^{\text{A}} \otimes \text{Id}^{\text{B}} \otimes \text{Id}^{\text{C}}}{2}\Bigg),
\end{aligned}
\tag{90}
$$

$$\tilde{\Omega}^{\mathrm{ABC}}_{|m_Z=1} = \frac{1}{5}\left(\frac{\mathrm{Id}^{\mathrm{ABC}} + \tilde{X}^{\mathrm{A}}\otimes\tilde{Z}^{\mathrm{B}}\otimes\tilde{Z}^{\mathrm{C}}}{2} + \frac{\mathrm{Id}^{\mathrm{ABC}} + \tilde{Z}^{\mathrm{A}}\otimes\tilde{X}^{\mathrm{B}}\otimes\tilde{Z}^{\mathrm{C}}}{2} + \right.$$
$$\left. + \frac{\mathrm{Id}^{\mathrm{ABC}} - \tilde{Z}^{\mathrm{A}}\otimes\tilde{Z}^{\mathrm{B}}\otimes\tilde{X}^{\mathrm{C}}}{2} + \frac{\mathrm{Id}^{\mathrm{ABC}} + \tilde{X}^{\mathrm{A}}\otimes\tilde{X}^{\mathrm{B}}\otimes\tilde{X}^{\mathrm{C}}}{2} + \frac{\mathrm{Id}^{\mathrm{ABC}} + \mathrm{Id}^{\mathrm{A}}\otimes\mathrm{Id}^{\mathrm{B}}\otimes\mathrm{Id}^{\mathrm{C}}}{2}\right). \tag{91}$$

Note that both are connected via a unitary transformation that accounts to flipping the measurement outcomes:

$$O^{\mathrm{C}} : \tilde{\Omega}^{\mathrm{ABC}}_{|m_Z=0} \xrightarrow{\tilde{X}^{\mathrm{C}}\to -\tilde{X}^{\mathrm{C}}} \tilde{\Omega}^{\mathrm{ABC}}_{|m_Z=1}, \tag{92}$$

Using (90) and (91), we propose the following test operators on each triangle subgraph $\triangle_{\mathrm{ABC}}$ and $\triangle_{\mathrm{DEF}}$ respectively:

$$\tilde{\Omega}^{\mathrm{ABC}}_{(6)} := \left(\tilde{\Omega}^{\mathrm{ABC}}_{|m_Z=0}\otimes\tilde{P}^{\mathrm{D}}_{(Z;0)}\otimes\mathrm{Id}^{\mathrm{E}}\otimes\mathrm{Id}^{\mathrm{F}} + \tilde{\Omega}^{\mathrm{ABC}}_{|m_Z=1}\otimes\tilde{P}^{\mathrm{D}}_{(Z;1)}\otimes\mathrm{Id}^{\mathrm{E}}\otimes\mathrm{Id}^{\mathrm{F}}\right), \tag{93}$$

$$\tilde{\Omega}^{\mathrm{DEF}}_{(6)} := \left(\mathrm{Id}^{\mathrm{A}}\otimes\mathrm{Id}^{\mathrm{B}}\otimes\tilde{P}^{\mathrm{C}}_{(Z;0)}\otimes\tilde{\Omega}^{\mathrm{DEF}}_{|m_Z=0} + \mathrm{Id}^{\mathrm{A}}\otimes\mathrm{Id}^{\mathrm{B}}\otimes\tilde{P}^{\mathrm{C}}_{(Z;1)}\otimes\tilde{\Omega}^{\mathrm{DEF}}_{|m_Z=1}\right). \tag{94}$$

Here, the subscript "6" is implemented to avoid confusion with the singular triangle analysis of (VI).

We propose that using (93) and (94) as verification operators for the subgraph states associated with $\triangle_{\mathrm{ABC}}$ and $\triangle_{\mathrm{DEF}}$ is equivalent to using (88) as a verification operator on the original graph state $\tilde{\rho}^{\mathrm{ABCDEF}}$.

1. Generalized Verification Method

Verifying a six-qubit two-triangle quantum graph state may be done by conducing tests on the individual triangle subgraph states associated with $\triangle_{\mathrm{ABC}}$ and $\triangle_{\mathrm{DEF}}$. This may be achieved utilizing the deletion property of (II.1) and, subsequently, using (93) and (94) as verification operators on the post-measurement states, respectively, at random. This method leads to an *alter-native verification operator* $\tilde{\Omega}^{\mathrm{ABC;DEF}}$, defined as:

$$\tilde{\Omega}^{\mathrm{ABC;DEF}} := \frac{1}{2}\left(\tilde{\Omega}^{\mathrm{ABC}}_{(6)} + \tilde{\Omega}^{\mathrm{DEF}}_{(6)}\right). \tag{95}$$

If both triangle subgraph states can be verified that way, using a similar protocol as presented in VI, uniqueness of graph states (II.2) indicates that the praemeasurement initial state $\tilde{\rho}^{\mathrm{ABCDEF}}$ must have fulfilled boundary conditions set by state accuracy $\epsilon_{\mathrm{ABCDEF}}$, measurement precision Δ_{ABCDEF} and significance level δ, similar to VI A 2. Thus, we need to express $\epsilon_{\mathrm{ABCDEF}}$ and Δ_{ABCDEF} in terms of $\epsilon_{\mathrm{ABC/DEF}}$ and $\Delta_{\mathrm{ABC/DEF}}$ on $\triangle_{\mathrm{ABC/DEF}}$, respectively, in order to obtain a minimum number K, dependent on δ, similar as demonstrated in VI.

In order to inspect the subgraph triangular states on $\triangle_{\mathrm{ABC/DEF}}$, we use the following CPTP-map $\mathcal{N}_{\theta^{\mathrm{C/D}}_{j_{\mathrm{C/D}}}}(\cdot)$ reducing $\tilde{\rho}^{(6)}_{j_{\mathrm{A}},j_{\mathrm{B}},\dots,j_{\mathrm{F}}}$ (see (62) for a similar definition) to subgraph states $\tilde{\rho}^{(3)}_{j_{\mathrm{A}},j_{\mathrm{B}},j_{\mathrm{C}}}$ or $\tilde{\rho}^{(3)}_{j_{\mathrm{D}},j_{\mathrm{E}},j_{\mathrm{F}}}$, respectively:

$$\mathcal{N}_{\theta^{\mathrm{D}}_{j_{\mathrm{D}}}}\left(\tilde{\rho}^{(6)}_{j_{\mathrm{A}},j_{\mathrm{B}},j_{\mathrm{C}},j_{\mathrm{D}},j_{\mathrm{E}},j_{\mathrm{F}}}\right) :=$$
$$:= \mathrm{Tr}_{\mathrm{DEF}}\left((\mathbb{1}^{\mathrm{ABC}}\otimes\tilde{M}^{\mathrm{D}}_{0|1,j_{\mathrm{D}}}(\theta^{\mathrm{D}}_{j_{\mathrm{D}}})\otimes\mathbb{1}^{\mathrm{EF}})\tilde{\rho}^{(6)}_{j_{\mathrm{A}},j_{\mathrm{B}},j_{\mathrm{C}},j_{\mathrm{D}},j_{\mathrm{E}},j_{\mathrm{F}}}(\mathbb{1}^{\mathrm{ABC}}\otimes\tilde{M}^{\mathrm{D}}_{0|1,j_{\mathrm{D}}}(\theta^{\mathrm{D}}_{j_{\mathrm{D}}})\otimes\mathbb{1}^{\mathrm{EF}})^{\dagger} + \right.$$
$$\left. + (\mathbb{1}^{\mathrm{AB}}\otimes O^{\mathrm{C}}_{j_{\mathrm{C}}}\otimes\tilde{M}^{\mathrm{D}}_{1|1,j_{\mathrm{D}}}(\theta^{\mathrm{D}}_{j_{\mathrm{D}}})\otimes\mathbb{1}^{\mathrm{EF}})\tilde{\rho}^{(6)}_{j_{\mathrm{A}},j_{\mathrm{B}},j_{\mathrm{C}},j_{\mathrm{D}},j_{\mathrm{E}},j_{\mathrm{F}}}(\mathbb{1}^{\mathrm{AB}}\otimes O^{\mathrm{C}}_{j_{\mathrm{C}}}\otimes\tilde{M}^{\mathrm{D}}_{1|1,j_{\mathrm{D}}}(\theta^{\mathrm{D}}_{j_{\mathrm{D}}})\otimes\mathbb{1}^{\mathrm{EF}})^{\dagger}\right), \tag{96}$$

$$\mathcal{N}_{\theta^{\mathrm{C}}_{j_{\mathrm{C}}}}\left(\tilde{\rho}^{(6)}_{j_{\mathrm{A}},j_{\mathrm{B}},j_{\mathrm{C}},j_{\mathrm{D}},j_{\mathrm{E}},j_{\mathrm{F}}}\right) :=$$
$$:= \mathrm{Tr}_{\mathrm{ABC}}\left((\mathbb{1}^{\mathrm{AB}}\otimes\tilde{M}^{\mathrm{C}}_{0|1}(\theta^{\mathrm{C}}_{j_{\mathrm{C}}})\otimes\mathbb{1}^{\mathrm{DEF}})\tilde{\rho}^{(6)}_{j_{\mathrm{A}},j_{\mathrm{B}},j_{\mathrm{C}},j_{\mathrm{D}},j_{\mathrm{E}},j_{\mathrm{F}}}(\mathbb{1}^{\mathrm{AB}}\otimes\tilde{M}^{\mathrm{C}}_{0|1}(\theta^{\mathrm{C}}_{j_{\mathrm{C}}})\otimes\mathbb{1}^{\mathrm{DEF}})^{\dagger} + \right.$$
$$\left. + (\mathbb{1}^{\mathrm{AB}}\otimes\tilde{M}^{\mathrm{C}}_{1|1}(\theta^{\mathrm{C}}_{j_{\mathrm{C}}})\otimes O^{\mathrm{D}}_{j_{\mathrm{D}}}\otimes\mathbb{1}^{\mathrm{EF}})\tilde{\rho}^{(6)}_{j_{\mathrm{A}},j_{\mathrm{B}},j_{\mathrm{C}},j_{\mathrm{D}},j_{\mathrm{E}},j_{\mathrm{F}}}(\mathbb{1}^{\mathrm{AB}}\otimes\tilde{M}^{\mathrm{C}}_{1|1}(\theta^{\mathrm{C}}_{j_{\mathrm{C}}})\otimes O^{\mathrm{D}}_{j_{\mathrm{D}}}\otimes\mathbb{1}^{\mathrm{EF}})^{\dagger}\right), \tag{97}$$

where $\{\tilde{M}_{0|1,j},\tilde{M}_{1|1,j}\}$ denotes a Jordan Z- measurement with outcomes $m_Z = 0, 1$, and $O^{\mathrm{C/D}}_j$ denotes the

unitary operator flipping the measurement outcomes in the conditional test operator of (91) as shown in (92).

C. Verifying Measurements on $\tilde{\Omega}_{(6)}^{\text{ABC}}$ and $\tilde{\Omega}_{(6)}^{\text{DEF}}$

Similar to VI B 1, we aim to verify measurements on a six-qbit two-triangle quantum graph state described above. As in (56), we assume:

$$\text{For } \Delta_{\text{ABCDEF}} > 0:$$
$$\mathfrak{d}\left(\tilde{p}\left(a_{\text{A}}, \ldots, a_{\text{F}} \,|\, x_{\text{A}}, \ldots, x_{\text{F}}\right), p\left(a_{\text{A}}, \ldots, a_{\text{F}} \,|\, x_{\text{A}}, \ldots, x_{\text{F}}\right)\right) \geq \Delta_{\text{ABCDEF}} \tag{98}$$

and we wish to find a suitable K for a significance level $0 < \delta \leq 1$, such that

$$\left(\frac{1}{K}\sum_{k=1}^{K}\text{Tr}\left(\tilde{\Omega}^{\text{ABC;DEF}}\tilde{\rho}_{k}^{\text{ABCDEF}}\right)\right)^{K} =$$
$$= \left(\text{Tr}\left(\tilde{\Omega}^{\text{ABC;DEF}}\tilde{\rho}^{\text{ABCDEF}}\right)\right)^{K} \leq \delta \tag{99}$$

is an inequality with a tight lower bound. Here, as in VI B 1, $\tilde{\rho}^{\text{ABCDEF}}$ denotes an average state.

As argued in VI B 1, the maximum passing probability of $\tilde{\rho}^{\text{ABCDEF}}$ is upper-bounded by the largest eigenvalue $\lambda_{\max}$ of the test operator $\tilde{\Omega}_{(6)}^{\text{ABC}}$ and $\tilde{\Omega}_{(6)}^{\text{DEF}}$. Recall that estimating the largest singular value (also known as *spectral radius* $\sigma(\cdot)$) of a finite dimensional Hermitian matrix A is equivalent to estimating its *spectral norm*, which is a special case of a *matrix norm* on a normed vector space $\mathcal{H} \ni v$ such that [19, 22]:

$$\|A\|_{\text{op}} := \max_{\|v\|_2 = 1}\|Av\|_2. \tag{100}$$

Here, $\|\cdot\|_2$ denotes the usual Euclidean vector norm. Using the spectral norm, we may show that the largest eigenvalue $\lambda_{\max}\left(\tilde{\Omega}_{(6)}^{\text{ABC}}\right)$ is upper-bounded by:

$$\lambda_{\max}\left(\tilde{\Omega}_{(6)}^{\text{ABC}}\right) \leq \frac{1}{5}\left(3 + \sqrt{1 + 3\cos^2\frac{8}{6}\Delta_{\text{A...F}}}\right) \tag{101}$$

For a proof of (101), the reader is referred to A. Note that this bound is equivalent for the largest eigenvalue of $\tilde{\Omega}_{(6)}^{\text{DEF}}$.

Thus, similar to (67), we obtain an upper-bound on the passing probability for K experimental states as:

$$\prod_{k=1}^{K}\text{Tr}\left(\tilde{\Omega}^{\text{ABC;DEF}}\tilde{\rho}_{k}^{\text{ABCDEF}}\right) \leq$$
$$\leq \left(\frac{1}{5}\left(3 + \sqrt{1 + 3\cos^2\frac{8}{6}\Delta_{\text{ABCDEF}}}\right)\right)^{K} \leq \delta \tag{102}$$

As a result, for a given significance level δ, a minimum number of tests K:

$$K \geq \frac{\ln\delta}{\ln\left(\frac{1}{5}\left(3 + \sqrt{1 + 3\cos^2\frac{8}{6}\Delta_{\text{ABCDEF}}}\right)\right)} \tag{103}$$

is required for verifying the measurements on a six-qbit two triangle state.

D. Verifying the State with $\tilde{\Omega}_{(6)}^{\text{ABC}}$ and $\tilde{\Omega}_{(6)}^{\text{DEF}}$

As argued in VI B 2, obtaining the minimum number to verify a state up to a given significance level δ may be achieved by analyzing bounds on the second-largest eigenvalue of the verification operator involved and on a fidelity of the form (74). Again, for this task, we will use the alternative verification operator (95) and assume:

$$\text{For } \epsilon_{\text{ABCDEF}}, \Delta_{\text{ABCDEF}} > 0: \tag{104}$$

$$\frac{1}{2}\left\|\sum_{j_{\text{A}},\ldots,j_{\text{F}}}p(j_{\text{A}},\ldots,j_{\text{F}})\tilde{\rho}_{j_{\text{A}},\ldots,j_{\text{F}}}^{(6)} - \rho^{\text{A...F}}\right\|_1 \geq \epsilon_{\text{A...F}}, \tag{105}$$

$$\sum_{j_{\text{A}},\ldots,j_{\text{F}}}p(j_{\text{A}},\ldots,j_{\text{F}})(|\theta_{j_{\text{A}}}^{A}| + \cdots + |\theta_{j_{\text{F}}}^{F}|) \leq \Delta_{\text{ABCDEF}}. \tag{106}$$

To verify the state given these assumptions means to find an upper bound of

$$\text{Tr}\left(\tilde{\Omega}^{\text{ABC;DEF}}\tilde{\rho}^{\text{ABCDEF}}\right) =$$
$$= \frac{1}{2}\sum_{j_{\text{A}},\ldots,j_{\text{F}}}p(j_{\text{A}},\ldots,j_{\text{F}})\left(\text{Tr}\left(\tilde{\Omega}_{(6)}^{\text{ABC}}\mathcal{N}_{\theta_{j_{\text{D}}}^{\text{D}}}\left(\tilde{\rho}_{j_{\text{A}},\ldots,j_{\text{F}}}^{(6)}\right)\right) + \text{Tr}\left(\tilde{\Omega}_{(6)}^{\text{DEF}}\mathcal{N}_{\theta_{j_{\text{C}}}^{\text{C}}}\left(\tilde{\rho}_{j_{\text{A}},\ldots,j_{\text{F}}}^{(6)}\right)\right)\right) \tag{107}$$

which is similar to (64). As argued in VI B 2, the task to find an upper-bound of these summands may be

reduced to finding an upper bound of:

$$\mathrm{Tr}\left(\tilde{\Omega}^{\mathrm{ABC}}_{(6)}\mathcal{N}_{\theta^{\mathrm{D}}_{j_{\mathrm{D}}}}\left(\tilde{\rho}^{(6)}_{j_{\mathrm{A}},j_{\mathrm{B}},j_{\mathrm{C}},j_{\mathrm{D}},j_{\mathrm{E}},j_{\mathrm{F}}}\right)\right)\le\lambda^{\mathrm{ABC}}_2+\left(1-\lambda^{\mathrm{ABC}}_2\right)F^2\left(\left|\tilde{\psi}_1\right\rangle\left\langle\tilde{\psi}_1\right|^{\mathrm{ABC}},\mathcal{N}_{\theta^{\mathrm{D}}_{j_{\mathrm{D}}}}\left(\tilde{\rho}^{(6)}_{j_{\mathrm{A}},\dots,j_{\mathrm{F}}}\right)\right); \tag{108}$$

$$\mathrm{Tr}\left(\tilde{\Omega}^{\mathrm{DEF}}_{(6)}\mathcal{N}_{\theta^{\mathrm{C}}_{j_{\mathrm{C}}}}\left(\tilde{\rho}^{(6)}_{j_{\mathrm{A}},j_{\mathrm{B}},j_{\mathrm{C}},j_{\mathrm{D}},j_{\mathrm{E}},j_{\mathrm{F}}}\right)\right)\le\lambda^{\mathrm{DEF}}_2+\left(1-\lambda^{\mathrm{DEF}}_2\right)F^2\left(\left|\tilde{\psi}_1\right\rangle\left\langle\tilde{\psi}_1\right|^{\mathrm{DEF}},\mathcal{N}_{\theta^{\mathrm{C}}_{j_{\mathrm{C}}}}\left(\tilde{\rho}^{(6)}_{j_{\mathrm{A}},\dots,j_{\mathrm{F}}}\right)\right). \tag{109}$$

where $\lambda^{\mathrm{ABC/DEF}}$ denote the second-largest eigenvalue and $\left|\tilde{\psi}_1\right\rangle^{\mathrm{ABC/DEF}}$ the eigenvector associated with the largest eigenvalue of the Jordan operators $\tilde{\Omega}^{\mathrm{ABC/DEF}}_{(6)}$ in (93) and (94), respectively.

As in VII C, for the following, the analysis on both triangles is equivalent, therefore, we conduct the calculations for either one of them up to our choosing. We decided to inspect $\triangle_{\mathrm{ABC}}$ further on.

Considering the upper bound on the fidelity, equivalently to VI B 2, we may investigate the purified distance (31) instead. Since the purified distance is a metric on the set of subnormalized quantum states, it fulfills the *triangle inequality* (or subadditivity [8, 19]):

$$P\left(\left|\tilde{\psi}_1\right\rangle\left\langle\tilde{\psi}_1\right|^{\mathrm{ABC}},\mathcal{N}_{\theta^{\mathrm{D}}_{j_{\mathrm{D}}}}\left(\tilde{\rho}^{(6)}_{j_{\mathrm{A}},\dots,j_{\mathrm{F}}}\right)\right)\ge \tag{110}$$

$$\ge P\left(\left|G^{\mathrm{ABC}}\right\rangle\left\langle G^{\mathrm{ABC}}\right|,\mathcal{N}_{\theta^{\mathrm{D}}_{j_{\mathrm{D}}}}\left(\tilde{\rho}^{(6)}_{j_{\mathrm{A}},\dots,j_{\mathrm{F}}}\right)\right)- \tag{111}$$

$$- P\left(\left|\tilde{\psi}_1\right\rangle\left\langle\tilde{\psi}_1\right|^{\mathrm{ABC}},\left|G^{\mathrm{ABC}}\right\rangle\left\langle G^{\mathrm{ABC}}\right|\right) \tag{112}$$

Now, importantly, we note that the eigenvectors of the conditional verification operators $\tilde{\Omega}^{\mathrm{ABC}}_{|m_z=0,1}$ of (90) and (91) coincide with the eigenvectors of the singular triangle Jordan verification operator $\tilde{\Omega}_{j_{\mathrm{A}}j_{\mathrm{B}}j_{\mathrm{C}}}$ of (64). Following this, we may use the results of (83) to state an equivalent upper-bound for (112). This leaves us to analysing (111).

For this, may reutilize the triangle inequality:

$$P\left(\mathcal{N}_{\theta^{D}_{j_{\mathrm{D}}}}(\tilde{\rho}^{(6)}_{j_{\mathrm{A}},j_{\mathrm{B}},j_{\mathrm{C}},j_{\mathrm{D}},j_{\mathrm{E}},j_{\mathrm{F}}}),\left|G^{\mathrm{ABC}}\right\rangle\left\langle G^{\mathrm{ABC}}\right|\right)= \tag{113}$$

$$= P\left(\mathcal{N}_{\theta^{D}_{j_{\mathrm{D}}}}(\tilde{\rho}^{(6)}_{j_{\mathrm{A}},j_{\mathrm{B}},j_{\mathrm{C}},j_{\mathrm{D}},j_{\mathrm{E}},j_{\mathrm{F}}}),\mathcal{N}_{\theta^{\mathrm{D}}_{j_{\mathrm{D}}}=0}\left(\left|G^{\mathrm{ABCDEF}}\right\rangle\left\langle G^{\mathrm{ABCDEF}}\right|\right)\right)\ge \tag{114}$$

$$\ge P\left(\mathcal{N}_{\theta^{\mathrm{D}}_{j_{\mathrm{D}}}=0}(\tilde{\rho}^{(6)}_{j_{\mathrm{A}},j_{\mathrm{B}},j_{\mathrm{C}},j_{\mathrm{D}},j_{\mathrm{E}},j_{\mathrm{F}}}),\mathcal{N}_{\theta^{\mathrm{D}}_{j_{\mathrm{D}}}=0}\left(\left|G^{\mathrm{ABCDEF}}\right\rangle\left\langle G^{\mathrm{ABCDEF}}\right|\right)\right)- \tag{115}$$

$$- P\left(\mathcal{N}_{\theta^{D}_{j_{\mathrm{D}}}}\left(\tilde{\rho}^{(6)}_{j_{\mathrm{A}},j_{\mathrm{B}},j_{\mathrm{C}},j_{\mathrm{D}},j_{\mathrm{E}},j_{\mathrm{F}}}\right),\mathcal{N}_{\theta^{\mathrm{D}}_{j_{\mathrm{D}}}=0}\left(\tilde{\rho}^{(6)}_{j_{\mathrm{A}},j_{\mathrm{B}},j_{\mathrm{C}},j_{\mathrm{D}},j_{\mathrm{E}},j_{\mathrm{F}}}\right)\right), \tag{116}$$

where $\mathcal{N}_{\theta^{D}_{j_{\mathrm{D}}}=0}(\,\cdot\,)$ is the reducing map of (96) without imperfections, thus, it maps the (perfect) six-qubit two-triangle graph state precisely to the single triangle graph state analyzed in VI. Similarly, for the subgraph state on $\triangle_{\mathrm{DEF}}$, we have

$$P\left(\mathcal{N}_{\theta^{C}_{j_{\mathrm{C}}}}\left(\tilde{\rho}^{(6)}_{j_{\mathrm{A}},j_{\mathrm{B}},j_{\mathrm{C}},j_{\mathrm{D}},j_{\mathrm{E}},j_{\mathrm{F}}}\right),\left|G^{\mathrm{DEF}}\right\rangle\left\langle G^{\mathrm{DEF}}\right|\right)\ge \tag{117}$$

$$\ge P\left(\mathcal{N}_{\theta^{\mathrm{C}}_{j_{\mathrm{C}}}=0}\left(\tilde{\rho}^{(6)}_{j_{\mathrm{A}},j_{\mathrm{B}},j_{\mathrm{C}},j_{\mathrm{D}},j_{\mathrm{E}},j_{\mathrm{F}}}\right),\mathcal{N}_{\theta^{\mathrm{C}}_{j_{\mathrm{C}}}=0}\left(\left|G^{\mathrm{ABCDEF}}\right\rangle\left\langle G^{\mathrm{ABCDEF}}\right|\right)\right)- \tag{118}$$

$$- P\left(\mathcal{N}_{\theta^{C}_{j_{\mathrm{C}}}}\left(\tilde{\rho}^{(6)}_{j_{\mathrm{A}},j_{\mathrm{B}},j_{\mathrm{C}},j_{\mathrm{D}},j_{\mathrm{E}},j_{\mathrm{F}}}\right),\mathcal{N}_{\theta^{\mathrm{C}}_{j_{\mathrm{C}}}=0}\left(\tilde{\rho}^{(6)}_{j_{\mathrm{A}},j_{\mathrm{B}},j_{\mathrm{C}},j_{\mathrm{D}},j_{\mathrm{E}},j_{\mathrm{F}}}\right)\right), \tag{119}$$

where $\left|G\right\rangle^{\mathrm{ABC}}$ denotes the single triangle graph state analyzed in VI and $\left|G\right\rangle^{\mathrm{ABCDEF}}$ denotes the target six-qubit two triangle graph state.

Similarly to considerations in VI B 2, acknowledging the triangle inequality splits the task into finding two bounds, a lower bound of (115) and a upper bound of (116) (similarly an lower bound of (118) and a upper

bound of (119)) in terms of ϵ_{ABCDEF}.

As for (115) and (118), we found lower-bounds of:

$$\frac{\epsilon_{j_A, j_B, j_C, j_D, j_E, j_F}}{\sqrt{2}} \leq P\left(\mathcal{N}_{\theta^{C/D}_{j_{C/D}}=0}\left(\tilde{\rho}^{(6)}_{j_A, j_B, j_C, j_D, j_E, j_F}\right), \mathcal{N}_{\theta^{C/D}_{j_{C/D}}=0}\left(\left|\rho^{\text{ABCDEF}}\right\rangle\left\langle\rho^{\text{ABCDEF}}\right|\right)\right). \qquad (120)$$

For a proof of (120), the reader may be referred to A.

For an upper bound of the second-largest eigenvalue λ_2^{ABC} of $\tilde{\Omega}_{(6)}^{\text{ABC}}$, we propose:

$$\lambda_2^{\text{ABC}}\left(\theta^A, \theta^B, \theta^C\right) \leq \frac{1}{5}\left(3 + \frac{2}{3}\Delta_{\theta^A_{j_A}, \theta^B_{j_B}, \theta^C_{j_C}}\right). \qquad (121)$$

Here, $\Delta_{\theta^A_{j_A}, \theta^B_{j_B}, \theta^C_{j_C}}$ is similarly defined as in (69), being the sum of absolute value of the angle touples of the at $\triangle_{\text{ABC}}$. For a proof of this upper bound, the interested reader may be referred to A.

As for bounding (116), a numerical analysis may be conducted. Due to a lack of computational resource to directly evaluate a bound, we leave this task to the reader. At this point, we want to draw attention to the difference in CPTP maps in the arguments of the purified distance, but equality in the quantum state the maps are applied to. This indicates that this numerical task may be solved within the realms of *semi-definite programming*, which is a numerical technique being treated in [51] for instance. Within this work, we will leave this constant B open and conjecture that it takes a similar quadratically scaling form as the bound of (83).

As shown in A, the lower bound on the total amount of rounds K to verify state accuracy with significance level δ is given as

$$K \geq \frac{\ln\delta}{\ln\left(1 - \frac{1}{2}\left(\sqrt{\frac{3}{5}}\epsilon - \left(\sqrt{\frac{24}{5}}\left(B + \frac{C}{\sqrt{3}}\right) + \sqrt{\frac{8}{135}}\right)\Delta\right)^2 + \frac{4}{135}\Delta^2\right)}. \qquad (122)$$

As a result, the minimum number of rounds K for verifying a six-qubit two triangle quantum state with state accuracy ϵ and measurements with measurement precision Δ simultaneously, given a significance level δ, is:

$$K = \max\left\{\left\lceil\frac{\ln\delta}{\ln\left(\frac{1}{5}\left(3 + \sqrt{1 + 3\cos^2\frac{8}{6}\Delta}\right)\right)}\right\rceil; \left\lceil\frac{\ln\delta}{\ln\left(1 - \frac{1}{2}\left(\sqrt{\frac{3}{5}}\epsilon - \left(\sqrt{\frac{24}{5}}\left(B + \frac{C}{\sqrt{3}}\right) + \sqrt{\frac{8}{135}}\right)\Delta\right)^2 + \frac{4}{135}\Delta^2\right)}\right\rceil\right\}. \qquad (123)$$

VIII. CONCLUSION

In this work, we have demonstrated how a novel improved method for quantum state and measurement verification, introduced by Yamasaki et.al. in [52], may be generalized from a single triangular quantum state case to the a six-qubit two-triangle quantum state case. We have demonstrated how this method states as an improvement of state-of-the-art robust self-testing protocols in terms of being able to simultaneously verify measurements and the quantum state with a quadratically lower amount of necessary rounds. Furthermore, we pointed out that our method may be applied to more general experimental scenarios, since it does not require i.i.d statistics. Moreover, within this method, measurement devices may be viewed as stable, since external noise can always be accounted to act on the state, which results in a better scalability of a possible implementation into a MBQC.

The research conduced here has opened several interesting questions that we leave for future investigations. It is unknown if this protocol was open to further generalizations, the most promising being a unprecedented noise-receptive quantum state verification protocol for hypergraph states, especially for the resource state of Yamasaki et.al. fault-tolerant MBQC of [53]. We conjecture that there might be a possibility of further improvement of the protocol, using insights of the quantum relative entropic behaviour of quantum graph states under CPTP maps, which we gave an unfinished first idea scheme in A.

Acknowledgement

My best acknowledgement goes to Hayata Yamasaki, PhD., whose patience, time, help and ideas helped me tremendously throughout this thesis. Additionally, I want to express my deepest gratitude to Univ. -Prof. Dr. Mag. Marcus Huber, who gave me the chance to work on this topic and to take the my first step into the world of research. Moreover, I thank my parents, whose constant support made my studies of Physics at the university even possible.

Appendices

Appendix A: Pauli-Z deletion property

Proof of II.1.

$$P^i_{(Z;m_Z)} |G\rangle =$$
$$= P^i_{(Z;m_Z)} \prod_{\{i,j\}\in\mathcal{N}(i)\}\in E} (P^i_{(Z;0)} \otimes \mathrm{Id}^j + P^i_{(Z;1)} \otimes Z^j) |+\rangle^i \otimes$$
$$\otimes |G\smallsetminus i\rangle$$

Now, $|G'\rangle$ depends on m_Z with both results having the same probability $p(m_Z) = \frac{1}{2}$. Using the definition of projectors ${P^i_{(Z;m_Z)}}^2 = P^i_{(Z;m_Z)}$ and orthogonality of projectors onto their respective eigenspaces, $|G'\rangle$ can be written as:

$$|G'\rangle = \begin{cases} \frac{1}{\sqrt{2}}(|0\rangle^i \otimes |G\smallsetminus i\rangle) & \text{if } m_Z = 0 \text{ or} \\ \frac{1}{\sqrt{2}}(|1\rangle^i \otimes Z^{\mathcal{N}(i)}|G\smallsetminus i\rangle) & \text{if } m_Z = 1, \end{cases}$$

which proofs (II.1). $\qquad\square$

Note that a similar proof can be found in [17].

Appendix B: From interaction picture to stabilizer formalism

Consider

$$\prod_{\{a,b\}\in E} U_{ab} X^u \otimes \mathrm{Id} =$$
$$= \prod_{\{u,v\in\mathcal{N}(u)\}\in E} \prod_{E\ni\{e,j\}\smallsetminus\{u,v\in\mathcal{N}(u)\}} U_{ej} U_{uv} X^u \otimes \mathrm{Id}. \quad (124)$$

The tensor product $X^u \otimes \mathrm{Id}$ indicates that one Pauli measurement is being conducted on one singular arbitrary vertex $u \in V$. (To be precise, $\mathrm{Id} \equiv \mathrm{Id}^{V\smallsetminus\{u\}}$, but we will not use this to avoid cluttered notation. In the following, Id will denote the tensor product of the identity operators on the vertices not explicitly written down otherwise.) Using (5), we get

$$\prod_{\{a,b\}\in E} U_{ab} X^u \otimes \mathrm{Id} = \prod_{\{u,v\in\mathcal{N}(u)\}\in E}$$
$$\prod_{E\ni\{e,j\}\smallsetminus\{u,v\in\mathcal{N}(u)\}} U_{ej} X^u \otimes Z^v \otimes \mathrm{Id}\, U_{uv}.$$

Therefore, reusing the commutation relations of (5) for each factor $U_{uv}, v \in \mathcal{N}(u)$ in (124), we can show that

[41]

$$\prod_{\{a,b\}\in E} U_{ab} X^u \otimes \mathrm{Id} = (X^u \otimes \bigotimes_{v\in\mathcal{N}(u)} Z^v) \otimes \mathrm{Id} \prod_{\{a,b\}} U_{ab}, \quad (125)$$

which further on implies that

$$(X^u \otimes \bigotimes_{v\in\mathcal{N}(u)} Z^v) \otimes \mathrm{Id} |G\rangle = \prod_{\{a,b\}} U_{ab} X^u |+\rangle^V =$$
$$= \prod_{\{a,b\}} U_{ab} |+\rangle^V = |G\rangle, \quad (126)$$

where the second equality follows from the fact that $|+\rangle^u$ is an eigenstate of X^u (For the rest of the work, the tensor product of the identity operator above will be avoided to simplify notation).

Appendix C: Measurement precision bound

We want to find an upper bound of

$$\mathrm{Tr}\left(\tilde{\Omega}^{\mathrm{ABC}}_{(6)} \tilde{\rho}_6\right). \quad (127)$$

As argued in VI B 1, finding an upper bound of (127) is equivalent to finding the largest eigenvalue of $\tilde{\Omega}^{\mathrm{ABC}}_{(6)}$. As mentioned in VII C, this may be achieved by obtaining the spectral norm of $\tilde{\Omega}^{\mathrm{ABC}}_{(6)}$.

The spectral norm is a *unitarily invariant matrix norm* [19]. Hence, for any unitary matrix U,

$$\left\| U A U^\dagger \right\|_{\mathrm{op}} = \| A \|_{\mathrm{op}}. \quad (128)$$

Additionally, before going into the evaluation of the largest eigenvalue bound, let us recall that the matrix norm of a Kronecker product of matrices factorizes [19]:

$$\| O_1 \otimes O_2 \otimes O_3 \| = \| O_1 \| \| O_2 \| \| O_3 \|. \quad (129)$$

and that the action of any operator $A \in \mathcal{L}(\mathcal{H})$ is upper-bounded by its largest eigenvalue (see also (73)):

$$\forall v \in \mathcal{H}: Av \le \lambda_{\max}(A)\,\mathbb{1}_{\mathcal{H}} v \Leftrightarrow A \le \lambda_{\max}(A)\,\mathbb{1}_{\mathcal{H}}. \quad (130)$$

Note that (130) indicates that the spectral norm is a monotonically increasing functional, i.e.

$$\| A \|_{\mathrm{op}} \le \| B \|_{\mathrm{op}} \Leftrightarrow A \le B. \quad (131)$$

With (128) and (129) and (130) in mind, we may calculate the largest eigenvalue of the (imperfect) verification operator $\tilde{\Omega}^{\mathrm{ABC}}_{(6)}$ on the subtriangle $\triangle_{\mathrm{ABC}}$ as:

$$\lambda_{\max}\left(\tilde{\Omega}^{\mathrm{ABC}}_{(6)}\right) = \left\| \tilde{\Omega}^{\mathrm{ABC}}_{|m_Z=0} \otimes \tilde{P}^{\mathrm{D}}_{(Z;0)} \otimes \mathrm{Id}^{\mathrm{E}} \otimes \mathrm{Id}^{\mathrm{F}} + \tilde{\Omega}^{\mathrm{ABC}}_{|m_Z=1} \otimes \tilde{P}^{\mathrm{D}}_{(Z;1)} \otimes \mathrm{Id}^{\mathrm{E}} \otimes \mathrm{Id}^{\mathrm{F}} \right\|_{\mathrm{op}} \le \quad (132)$$

$$\le \left\| \lambda_{\max}\left(\tilde{\Omega}^{\mathrm{ABC}}_{|m_Z=0}\right) \mathbb{1}_{\mathcal{H}} \otimes \tilde{P}^{\mathrm{D}}_{(Z;0)} \otimes \mathrm{Id}^{\mathrm{E}} \otimes \mathrm{Id}^{\mathrm{F}} + \lambda_{\max}\left(\tilde{\Omega}^{\mathrm{ABC}}_{|m_Z=1}\right) \mathbb{1}_{\mathcal{H}} \otimes \tilde{P}^{\mathrm{D}}_{(Z;1)} \otimes \mathrm{Id}^{\mathrm{E}} \otimes \mathrm{Id}^{\mathrm{F}} \right\|_{\mathrm{op}} = \quad (133)$$

$$= \left\| \tilde{\Omega}^{\mathrm{ABC}}_{|m_Z=0/1} \right\|_{\mathrm{op}} \left(\left\| \tilde{P}^{\mathrm{D}}_{(Z;0)} + \tilde{P}^{\mathrm{D}}_{(Z;1)} \right\|_{\mathrm{op}} \right) = \left\| \tilde{\Omega}^{\mathrm{ABC}}_{|m_Z=0/1} \right\|_{\mathrm{op}} \le \frac{1}{5}\left(3 + \sqrt{1 + 3\cos^2 \frac{8}{3}\Delta_{\mathrm{ABC}}} \right) \quad (134)$$

Here, the lhs of (134) results from the unitary invariance of the spectral norm and the completeness relation of projection operators, whereas the upper bound

on the rhs may be argued in VII C.

To bound the measurement precision Δ_{ABC} on the subgraph triangle $\triangle_{\mathrm{ABC}}$ given the measurement precision Δ_{ABCDEF} on the the graph state $\tilde{\rho}^{\mathrm{ABCDEF}}$ associated with (6), we may recall (66) in the six-qbit two-triangle case, which reads as:

$$\frac{1}{4} \sum_{j_{\mathrm{A}},\ldots,j_{\mathrm{F}}} p(j_{\mathrm{A}},\ldots,j_{\mathrm{F}})(|\theta_{j_{\mathrm{A}}}^{A}|+\cdots+|\theta_{j_{\mathrm{F}}}^{F}|) \geq \Delta_{\mathrm{A}\ldots\mathrm{F}}. \quad (135)$$

We note that at least one of the following inequalities must hold:

$$\frac{1}{4} \sum_{j_{\mathrm{A}},\ldots,j_{\mathrm{F}}} p(j_{\mathrm{A}},\ldots,j_{\mathrm{F}}) \left(|\theta_{j_{\mathrm{A}}}^{\mathrm{A}}| + |\theta_{j_{\mathrm{B}}}^{\mathrm{B}}| + |\theta_{j_{\mathrm{C}}}^{\mathrm{C}}|\right) \geq \frac{\Delta_{\mathrm{A}\ldots\mathrm{F}}}{2} \quad (136)$$

or

$$\frac{1}{4} \sum_{j_{\mathrm{A}},\ldots,j_{\mathrm{F}}} p(j_{\mathrm{A}},\ldots,j_{\mathrm{F}}) \left(|\theta_{j_{\mathrm{D}}}^{\mathrm{D}}| + |\theta_{j_{\mathrm{E}}}^{\mathrm{E}}| + |\theta_{j_{\mathrm{F}}}^{\mathrm{F}}|\right) \geq \frac{\Delta_{\mathrm{A}\ldots\mathrm{F}}}{2}. \quad (137)$$

As both inequalities may be equally likely assumed, we may reduce the further analysis to investigating only one of them. This may be done without loss of generality, recalling the verification method presented in VII C that states that both subgraph triangle state are tested at random. Therefore, by the means of exemplification, let us investigate the case where (136) is true. The probability distribution $p(j_{\mathrm{A}},\ldots,j_{\mathrm{F}})$ factorizes. This can be seen by recalling the definition of $p(j_{\mathrm{A}},\ldots,j_{\mathrm{F}})$ in (63):

$$p(j_{\mathrm{A}},\ldots,j_{\mathrm{F}}) = \mathrm{Tr}\left(\bigotimes_{j_{\mathrm{A}}}\cdots\bigotimes_{j_{\mathrm{F}}} \Pi_{j_{\mathrm{A}}} \otimes \cdots \otimes \Pi_{j_{\mathrm{F}}} \tilde{\rho}^{\mathrm{ABCDEF}}\right) = \quad (138)$$

$$= \mathrm{Tr}\left(\bigotimes_{j_{\mathrm{A}}}\bigotimes_{j_{\mathrm{B}}}\bigotimes_{j_{\mathrm{C}}} \Pi_{j_{\mathrm{A}}} \otimes \Pi_{j_{\mathrm{B}}} \otimes \Pi_{j_{\mathrm{C}}} \tilde{\rho}^{\mathrm{ABCDEF}}\right) \mathrm{Tr}\left(\bigotimes_{j_{\mathrm{D}}}\bigotimes_{j_{\mathrm{E}}}\bigotimes_{j_{\mathrm{F}}} \Pi_{j_{\mathrm{D}}} \otimes \Pi_{j_{\mathrm{E}}} \otimes \Pi_{j_{\mathrm{F}}} \tilde{\rho}^{\mathrm{ABCDEF}}\right) = \quad (139)$$

$$= \mathrm{Tr}\left(\mathcal{N}_{\theta_{j_{\mathrm{D}}}^{\mathrm{D}}}\left(\bigotimes_{j_{\mathrm{A}}}\bigotimes_{j_{\mathrm{B}}}\bigotimes_{j_{\mathrm{C}}} \Pi_{j_{\mathrm{A}}} \otimes \Pi_{j_{\mathrm{B}}} \otimes \Pi_{j_{\mathrm{C}}} \tilde{\rho}^{\mathrm{A}\ldots\mathrm{F}}\right)\right) \mathrm{Tr}\left(\mathcal{N}_{\theta_{j_{\mathrm{C}}}^{\mathrm{C}}}\left(\bigotimes_{j_{\mathrm{D}}}\bigotimes_{j_{\mathrm{E}}}\bigotimes_{j_{\mathrm{F}}} \Pi_{j_{\mathrm{D}}} \otimes \Pi_{j_{\mathrm{E}}} \otimes \Pi_{j_{\mathrm{F}}} \tilde{\rho}^{\mathrm{A}\ldots\mathrm{F}}\right)\right) = \quad (140)$$

$$= \mathrm{Tr}\left(\bigotimes_{j_{\mathrm{A}}}\bigotimes_{j_{\mathrm{B}}}\bigotimes_{j_{\mathrm{C}}} \Pi_{j_{\mathrm{A}}} \otimes \Pi_{j_{\mathrm{B}}} \otimes \Pi_{j_{\mathrm{C}}} \tilde{\rho}^{\mathrm{ABC}}\right) \mathrm{Tr}\left(\bigotimes_{j_{\mathrm{D}}}\bigotimes_{j_{\mathrm{E}}}\bigotimes_{j_{\mathrm{F}}} \Pi_{j_{\mathrm{D}}} \otimes \Pi_{j_{\mathrm{E}}} \otimes \Pi_{j_{\mathrm{F}}} \tilde{\rho}^{\mathrm{DEF}}\right) = \quad (141)$$

$$= \sum_{j_{\mathrm{A}},j_{\mathrm{B}},j_{\mathrm{C}}} p(j_{\mathrm{A}},j_{\mathrm{B}},j_{\mathrm{C}}) \sum_{j_{\mathrm{D}},j_{\mathrm{E}},j_{\mathrm{F}}} p(j_{\mathrm{D}},j_{\mathrm{E}},j_{\mathrm{F}}), \quad (142)$$

where (139) comes from the trace-factorization-property of Kronecker products and equality in (141)

comes from $\mathcal{N}_{\theta_{j_{\mathrm{C/D}}}^{\mathrm{C/D}}}(\,\cdot\,)$ of (96) and (97) being trace-preserving. As a result, we may rewrite (136) (and similarly (137)) as:

$$\frac{1}{4} \sum_{j_{\mathrm{A}},\ldots,j_{\mathrm{F}}} p(j_{\mathrm{A}},\ldots,j_{\mathrm{F}}) \left(|\theta_{j_{\mathrm{A}}}^{\mathrm{A}}| + |\theta_{j_{\mathrm{B}}}^{\mathrm{B}}| + |\theta_{j_{\mathrm{C}}}^{\mathrm{C}}|\right) =$$

$$= \frac{1}{4} \sum_{j_{\mathrm{A}},j_{\mathrm{B}},j_{\mathrm{C}}} p(j_{\mathrm{A}},j_{\mathrm{B}},j_{\mathrm{C}}) \left(|\theta_{j_{\mathrm{A}}}^{\mathrm{A}}| + |\theta_{j_{\mathrm{B}}}^{\mathrm{B}}| + |\theta_{j_{\mathrm{C}}}^{\mathrm{C}}|\right) \overbrace{\sum_{j_{\mathrm{D}},j_{\mathrm{E}},j_{\mathrm{F}}} p(j_{\mathrm{D}},j_{\mathrm{E}},j_{\mathrm{F}})}^{=1} \geq \Delta_{\mathrm{ABC}} \geq \frac{\Delta_{\mathrm{ABCDEF}}}{2}. \quad (143)$$

As a result, we may express (134) by the means of the given measurement precision Δ_{ABCDEF} as:

$$\lambda_{\max}\left(\tilde{\Omega}_{(6)}^{\mathrm{ABC}}\right) \leq \frac{1}{5}\left(3 + \sqrt{1 + 3\cos^2\frac{8}{6}\Delta_{\mathrm{ABCDEF}}}\right) \quad (144)$$

Appendix D: Lower bound of (115) and (118)

Our goal is to find an lower bound of (115). Reformulating this in terms of fidelity and having in mind that both subtriangle graph states associated with $\triangle_{\mathrm{ABC}}$ and $\triangle_{\mathrm{DEF}}$ are being examined, we may reformulate the task to finding:

$$\max_{\tilde{\rho}_{j_{\mathrm{A}},j_{\mathrm{B}},j_{\mathrm{C}},j_{\mathrm{D}},j_{\mathrm{E}},j_{\mathrm{F}}}^{(6)}} \left[F^2\left(\mathcal{N}_{\theta_{j_{\mathrm{D}}}^{\mathrm{D}}=0}(\tilde{\rho}_{j_{\mathrm{A}},\ldots,j_{\mathrm{F}}}^{(6)}), |G^{\mathrm{ABC}}\rangle\langle G^{\mathrm{ABC}}|\right); F^2\left(\mathcal{N}_{\theta_{j_{\mathrm{C}}}^{\mathrm{C}}=0}(\tilde{\rho}_{j_{\mathrm{A}},\ldots,j_{\mathrm{F}}}^{(6)}), |G^{\mathrm{DEF}}\rangle\langle G^{\mathrm{DEF}}|\right)\right]. \quad (145)$$

Starting from the six-qbit two-triangle graph state with underlying mathematical graph $G(V, E)$ being de-

picted in Fig. 6, we may construct a complete set of

mutually orthonormal basis states consisting of general six-qubit graph states $\{|\psi_{\boldsymbol{k}}\rangle\langle\psi_{\boldsymbol{l}}|\}_{\boldsymbol{k},\boldsymbol{l}}$. Let us consider the inner product of stabilizer states (as discussed in [1] f.e.). Two stabilizer states $|G\rangle$ and $|G'\rangle$ are orthonormal if their set of stabilizer operators consists of the same Pauli operator tensor products, but carry an opposite sign. Furthermore, if a graph state $|G\rangle \in \mathcal{H}$ undergoes a unitary transformation $|G\rangle \mapsto U|G\rangle$ for $U \in \mathcal{L}(\mathcal{H})$ being a unitary operator, the set of stabilizers for the final graph state $|G\rangle' = U|G\rangle$ transforms as:

$$|G\rangle' = U|G\rangle \Rightarrow \left\{S^{v'}\right\}_{v'\in V} = U\left\{S^{v}\right\}_{v\in V}U^{\dagger} \quad (146)$$

Keeping this in mind, consider a graph state $|G\rangle$ consisting of of $|V| = n$ qubits. If we applied a Pauli-Z^v unitary transformation on one of qubits located at $v \in V$ of the underlying mathematical graph, the resulting graph state $|G\rangle' = Z^v|G\rangle$ is orthonormal to $|G\rangle$. This can be seen by recalling the anti-commutation relation between the Pauli-X operator in S^v and the applied Pauli-Z transformation, leading to a difference in the sign within the respective stabilizer groups and, hence, to orthonormality. Alternatively, without having to keep [1] in mind, we may recall the interaction picture defintion of stabilizer states of II.1 and the commutation relation between CZ-gates and Pauli-Z matrices (6):

$$Z^v|G\rangle = Z^v \prod_{\{i,j\}\in E} U_{ij}|+\rangle^V = \prod_{\{i,j\}\in E} U_{ij}Z^v|+\rangle^V.$$

Note that $Z|+\rangle = |-\rangle$. This results in:

$$\left\langle \prod_{\{i,j\}\in E} U_{ij}(+)^V \middle| Z^v \middle| \prod_{\{i,j\}\in E} U_{ij}(+)^V \right\rangle = 0.$$

This can be understood in different ways. On the one side, the expectation value $\langle Z\rangle = 0$, on the other side $|+\rangle$ and $|-\rangle$ are orthonormal, leading to the linear independence of the respective graph states.

Using this fact, we may construct the set of basis states by applying Z^v to each $v \in V$ and forming a set out of the resulting states.

In our case, we may define our basis states as following: For $k_A, k_B, k_C, k_D, k_E, k_F \in \{0,1\}$, define

$$\left|\psi_{k_A,k_B,k_C,k_D,k_E,k_F}\right\rangle :=$$
$$:= \left(Z_A^{k_A} \otimes Z_B^{k_B} \otimes Z_C^{k_C} \otimes Z_D^{k_D} \otimes Z_E^{k_E} \otimes Z_F^{k_F}\right)\left|G^{(6)}\right\rangle, \quad (147)$$

where $\rho^{ABCDEF} = \left|G^{(6)}\right\rangle\left\langle G^{(6)}\right|$ denotes the density matrix associated with our theoretical six-qubit two-triangle graph state, $Z^0 = \mathbb{1}$ and $Z^1 = Z$. With this notation, $\left|\psi_{0,0,0,0,0,0}\right\rangle = \left|G^{(6)}\right\rangle$ equals the theoretical state, and if the subscripts $\boldsymbol{k} := \{k_A, k_B, k_C, k_D, k_E, k_F\}$ of $|\psi_{\boldsymbol{k}}\rangle$ include $k_v = 1$, Z is applied to the qubit associated with $v \in V$. We use a set

$$\left\{\left|\psi_{k_A,k_B,k_C,k_D,k_E,k_F}\right\rangle : k_A,\ldots,k_F \in \{0,1\}\right\} \quad (148)$$

of 64 orthonormal states as a basis for any six-qubit graph state $\tilde{\Psi}^{(6)}$ as:

$$\tilde{\Psi}^{(6)} = \sum_{k_A,\ldots,k_F\in\{0,1\}} \sum_{l_A,\ldots,l_F\in\{0,1\}} \alpha_{k_A,k_B,k_C,k_D,k_E,k_F,l_A,l_B,l_C,l_D,l_E,l_F} \left|\psi_{k_A,k_B,k_C,k_D,k_E,k_F}\right\rangle\left\langle\psi_{l_A,l_B,l_C,l_D,l_E,l_F}\right|, \quad (149)$$

where

$$\alpha_{k_A,k_B,k_C,k_D,k_E,k_F,l_A,l_B,l_C,l_D,l_E,l_F} :=$$
$$:= \left\langle\psi_{k_A,k_B,k_C,k_D,k_E,k_F}\middle|\tilde{\Psi}^{(6)}\middle|\psi_{l_A,l_B,l_C,l_D,l_E,l_F}\right\rangle. \quad (150)$$

Let us decompose $\tilde{\rho}^{(6)}_{j_A,j_B,j_C,j_D,j_E,j_F}$ in a basis of pure six-qubits triangle graph states:

$$\tilde{\rho}^{(6)}_{j_A,j_B,j_C,j_D,j_E,j_F} = \sum_{\boldsymbol{k},\boldsymbol{l}} \alpha_{\boldsymbol{k},\boldsymbol{l}} |\psi_{\boldsymbol{k}}\rangle\langle\psi_{\boldsymbol{l}}|, \quad (151)$$

where $\boldsymbol{k},\boldsymbol{l}$ should be understood as $\boldsymbol{k}\cup\boldsymbol{l}$. Due to similar considerations as in (80), we can deduce the normalizability restriction following from the fidelity of

$$F^2\left(\tilde{\rho}^{(6)}_{j_A,j_B,j_C,j_D,j_E,j_F}, \left|G^{(6)}\right\rangle\left\langle G^{(6)}\right|\right) =$$
$$= \left\langle G^{(6)}\middle|\tilde{\rho}^{(6)}_{j_A,j_B,j_C,j_D,j_E,j_F}\middle|G^{(6)}\right\rangle = \quad (152)$$
$$= 1 - \epsilon^2_{j_A,j_B,j_C,j_D,j_E,j_F}$$

as

$$\alpha_{0,\ldots,0} = 1 - \epsilon^2_{j_A,j_B,j_C,j_D,j_E,j_F}. \quad (153)$$

Note that rewriting the fidelity in form of an inner product in (152) is justified by the purity of $\left|G^{(6)}\right\rangle\left\langle G^{(6)}\right|$

as argued in 30. As a result of (152), due to normalization restriction of density states, this indicates the following:

$$\sum_{\boldsymbol{k},\boldsymbol{l}} \alpha_{\boldsymbol{k},\boldsymbol{l}} - \alpha_{0,\ldots,0} = \epsilon^2_{j_A,j_B,j_C,j_D,j_E,j_F}. \quad (154)$$

Keeping this in mind, let us revisit (77):

$$P\left(\mathcal{N}_{\theta^D_{j_D}=0}\left(\tilde{\rho}^{(6)}_{j_A,j_B,j_C,j_D,j_E,j_F}\right), \left|G^{ABC}\right\rangle\left\langle G^{ABC}\right|\right), \quad (155)$$

where we used the fact that $\mathcal{N}_{\theta^D_{j_D}=0}\left(\left|G^{ABCDEF}\right\rangle\left\langle G^{ABCDEF}\right|\right)$ reduces to the single triangle graph state ρ^{ABC} as argued in VII D.

Using the basis expansion of (151), we may rewrite the fidelity terms of (145) as:

$$\left\langle G^{ABC}\middle|\mathcal{N}_{\theta^D_{j_D}=0}(\tilde{\rho}^{(6)}_{j_A,j_B,j_C,j_D,j_E,j_F})\middle|G^{ABC}\right\rangle =$$
$$= \left\langle G^{ABC}\middle|\mathcal{N}_{\theta^D_{j_D}=0}\left(\sum_{\boldsymbol{k},\boldsymbol{l}} \alpha_{\boldsymbol{k},\boldsymbol{l}} |\psi_{\boldsymbol{k}}\rangle\langle\psi_{\boldsymbol{l}}|\right)^{ABC}\middle|G^{ABC}\right\rangle =$$
$$= \sum_{\boldsymbol{k},\boldsymbol{l}} \alpha_{\boldsymbol{k},\boldsymbol{l}}\left\langle G^{ABC}\middle|\mathcal{N}_{\theta^D_D=0}\left(|\psi_{\boldsymbol{k}}\rangle\langle\psi_{\boldsymbol{l}}|\right)^{ABC}\middle|G^{ABC}\right\rangle \quad (156)$$

$$\left\langle G^{\mathrm{DEF}} \left| \mathcal{N}_{\theta_{j_{\mathrm{C}}}^{\mathrm{C}}=0}(\tilde{\rho}_{j_{\mathrm{A}},j_{\mathrm{B}},j_{\mathrm{C}},j_{\mathrm{D}},j_{\mathrm{E}},j_{\mathrm{F}}}^{(6)}) \right| G^{\mathrm{DEF}} \right\rangle =$$

$$= \left\langle G^{\mathrm{DEF}} \left| \mathcal{N}_{\theta_{j_{\mathrm{D}}}^{\mathrm{D}}=0} \left(\sum_{\boldsymbol{k},\boldsymbol{l}} \alpha_{\boldsymbol{k},\boldsymbol{l}} \left| \psi_{\boldsymbol{k}} \right\rangle \left\langle \psi_{\boldsymbol{l}} \right| \right)^{\mathrm{DEF}} \right| G^{\mathrm{DEF}} \right\rangle =$$

$$= \sum_{\boldsymbol{k},\boldsymbol{l}} \alpha_{\boldsymbol{k},\boldsymbol{l}} \left\langle G^{\mathrm{DEF}} \left| \mathcal{N}_{\theta_{\mathrm{C}}=0} \left(\left| \psi_{\boldsymbol{k}} \right\rangle \left\langle \psi_{\boldsymbol{l}} \right| \right)^{\mathrm{DEF}} \right| G^{\mathrm{DEF}} \right\rangle. \tag{157}$$

As a result, the analysis reduces to bounding:

$$\left\langle G^{\mathrm{ABC}} \left| \mathcal{N}_{\theta_{j_{\mathrm{D}}}^{\mathrm{D}}=0} \left(\left| \psi_{\boldsymbol{k}} \right\rangle \left\langle \psi_{\boldsymbol{l}} \right| \right)^{\mathrm{ABC}} \right| G^{\mathrm{ABC}} \right\rangle, \tag{158}$$

$$\left\langle G^{\mathrm{DEF}} \left| \mathcal{N}_{\theta_{j_{\mathrm{C}}}^{\mathrm{C}}=0} \left(\left| \psi_{\boldsymbol{k}} \right\rangle \left\langle \psi_{\boldsymbol{l}} \right| \right)^{\mathrm{DEF}} \right| G^{\mathrm{DEF}} \right\rangle. \tag{159}$$

In the following, we will present an exemplary analysis of different cases of $\tilde{\rho}_{j_{\mathrm{A}},j_{\mathrm{B}},j_{\mathrm{C}},j_{\mathrm{D}},j_{\mathrm{E}},j_{\mathrm{F}}}^{(6)}$ that represent the entirety of all 64 terms occurring in $\mathcal{N}_{\theta_{\mathrm{D}}^{\mathrm{D}}=0}(\tilde{\rho}_{j_{\mathrm{A}},j_{\mathrm{B}},j_{\mathrm{C}},j_{\mathrm{D}},j_{\mathrm{E}},j_{\mathrm{F}}}^{(6)})$ and $\mathcal{N}_{\theta_{\mathrm{C}}^{\mathrm{C}}=0}(\tilde{\rho}_{j_{\mathrm{A}},j_{\mathrm{B}},j_{\mathrm{C}},j_{\mathrm{D}},j_{\mathrm{E}},j_{\mathrm{F}}}^{(6)})$. We will analyse *off-diagonal terms*, which should be understood as terms where $\boldsymbol{k} \neq \boldsymbol{l}$ and *diagonal terms*, where $\boldsymbol{k} = \boldsymbol{l}$. As always, we will exemplify the analysis of $\mathcal{N}_{\theta_{\mathrm{C}}^{\mathrm{C}}=0} \left(\left| \psi_{\boldsymbol{k}} \right\rangle \left\langle \psi_{\boldsymbol{l}} \right| \right)^{\mathrm{DEF}}$, which corresponds to the subtriangle $\triangle_{\mathrm{DEF}}$, by an equivalent analysis on $\triangle_{\mathrm{ABC}}$.

– **Trivial case** $\tilde{\rho}_{j_{\mathrm{A}},j_{\mathrm{B}},j_{\mathrm{C}},j_{\mathrm{D}},j_{\mathrm{E}},j_{\mathrm{F}}}^{(6)} = \rho^{\mathrm{ABCDEF}}$:

$$\mathcal{N}_{\theta_{j_{\mathrm{D}}}^{\mathrm{D}}=0}(\tilde{\rho}_{j_{\mathrm{A}},j_{\mathrm{B}},j_{\mathrm{C}},j_{\mathrm{D}},j_{\mathrm{E}},j_{\mathrm{F}}}^{(6)}) = \rho^{\mathrm{ABC}}. \tag{160}$$

– **Diagonal terms**, Z acting on $\triangle_{\mathrm{ABC}}$:

$$\mathcal{N}_{\theta_{j_{\mathrm{D}}}^{\mathrm{D}}=0} \left(Z^{\mathrm{A}} \rho_{j_{\mathrm{A}},j_{\mathrm{B}},j_{\mathrm{C}},j_{\mathrm{D}},j_{\mathrm{E}},j_{\mathrm{F}}}^{(6)} Z^{\mathrm{A}} \right) =$$

$$= \mathrm{Tr}_{\mathrm{DEF}} \Big(\left(\mathbb{1}^{\mathrm{ABC}} \otimes \tilde{M}_{0|1,j_{\mathrm{D}}}^{\mathrm{D}}(0) \otimes \mathbb{1}^{\mathrm{EF}} \right) Z^{\mathrm{A}} \rho_{j_{\mathrm{A}},j_{\mathrm{B}},j_{\mathrm{C}},j_{\mathrm{D}},j_{\mathrm{E}},j_{\mathrm{F}}}^{(6)} Z^{\mathrm{A}} \left(\mathbb{1}^{\mathrm{ABC}} \otimes \tilde{M}_{0|1,j_{\mathrm{D}}}^{\mathrm{D}}(0) \otimes \mathbb{1}^{\mathrm{EF}} \right)^{\dagger} +$$

$$+ \left(\mathbb{1}^{\mathrm{AB}} \otimes O_{j_{\mathrm{C}}}^{\mathrm{C}} \otimes \tilde{M}_{1|1,j_{\mathrm{D}}}^{\mathrm{D}}(0) \otimes \mathbb{1}^{\mathrm{EF}} \right) Z^{\mathrm{A}} \rho_{j_{\mathrm{A}},j_{\mathrm{B}},j_{\mathrm{C}},j_{\mathrm{D}},j_{\mathrm{E}},j_{\mathrm{F}}}^{(6)} Z^{\mathrm{A}} \left(\mathbb{1}^{\mathrm{AB}} \otimes O_{j_{\mathrm{C}}}^{\mathrm{C}} \otimes \tilde{M}_{1|1,j_{\mathrm{D}}}^{\mathrm{D}}(0) \otimes \mathbb{1}^{\mathrm{EF}} \right)^{\dagger} \Big) = \tag{161}$$

$$= \mathrm{Tr}_{\mathrm{DEF}} \Bigg(\left(\mathbb{1}^{\mathrm{ABC}} \otimes \mathbb{1}^{\mathrm{D}} \otimes \mathbb{1}^{\mathrm{EF}} \right) Z^{\mathrm{A}} \left(\frac{\rho_{j_{\mathrm{A}},j_{\mathrm{B}},j_{\mathrm{C}|0}}}{2} \otimes \rho_{j_{\mathrm{D}|0}} \otimes \rho_{j_{\mathrm{E}},j_{\mathrm{F}}} \right) Z^{\mathrm{A}} \left(\mathbb{1}^{\mathrm{ABC}} \otimes \mathbb{1}^{\mathrm{D}} \otimes \mathbb{1}^{\mathrm{EF}} \right)^{\dagger} +$$

$$+ \left(\mathbb{1}^{\mathrm{AB}} \otimes O_{j_{\mathrm{C}}}^{\mathrm{C}} \otimes \mathbb{1}^{\mathrm{D}} \otimes \mathbb{1}^{\mathrm{EF}} \right) Z^{\mathrm{A}} \left(\frac{\rho_{j_{\mathrm{A}},j_{\mathrm{B}},j_{\mathrm{C}|1}}}{2} \otimes \rho_{j_{\mathrm{D}|1}} \otimes \rho_{j_{\mathrm{E}},j_{\mathrm{F}}} \right) Z^{\mathrm{A}} \left(\mathbb{1}^{\mathrm{AB}} \otimes O_{j_{\mathrm{C}}}^{\mathrm{C}} \otimes \mathbb{1}^{\mathrm{D}} \otimes \mathbb{1}^{\mathrm{EF}} \right)^{\dagger} \Bigg) = \tag{162}$$

$$= Z^{\mathrm{A}} \frac{\rho_{j_{\mathrm{A}},j_{\mathrm{B}},j_{\mathrm{C}|0}}}{2} Z^{\mathrm{A}} \, \mathrm{Tr} \left(\mathbb{1}^{\mathrm{D}} \otimes \mathbb{1}^{\mathrm{EF}} \rho_{j_{\mathrm{D}|0}} \otimes \rho_{j_{\mathrm{E}},j_{\mathrm{F}}} \mathbb{1}^{\mathrm{D}} \otimes \mathbb{1}^{\mathrm{EF}} \right) +$$

$$+ Z^{\mathrm{A}} \otimes \mathbb{1}^{\mathrm{B}} \otimes O_{j_{\mathrm{C}}}^{\mathrm{C}} \frac{\rho_{j_{\mathrm{A}},j_{\mathrm{B}},j_{\mathrm{C}|1}}}{2} Z^{\mathrm{A}} \otimes \mathbb{1}^{\mathrm{B}} \otimes \left(O_{j_{\mathrm{C}}}^{\mathrm{C}} \right)^{\dagger} \mathrm{Tr} \left(\mathbb{1}^{\mathrm{D}} \otimes \mathbb{1}^{\mathrm{EF}} \rho_{j_{\mathrm{D}|1}} \otimes \rho_{j_{\mathrm{E}},j_{\mathrm{F}}} \mathbb{1}^{\mathrm{D}} \otimes \mathbb{1}^{\mathrm{EF}} \right) =$$

$$= Z^{\mathrm{A}} \rho_{j_{\mathrm{A}},j_{\mathrm{B}},j_{\mathrm{C}}} Z^{\mathrm{A}}. \tag{163}$$

– **Diagonal terms,** Z acting on $\triangle_{\mathrm{DEF}}$:

$$\mathcal{N}_{\theta_{j_{\mathrm{D}}}^{\mathrm{D}}=0} \left(Z^{\mathrm{E}} \rho_{j_{\mathrm{A}},j_{\mathrm{B}},j_{\mathrm{C}},j_{\mathrm{D}},j_{\mathrm{E}},j_{\mathrm{F}}}^{(6)} Z^{\mathrm{E}} \right) =$$

$$= \mathrm{Tr}_{\mathrm{DEF}} \Big(\left(\mathbb{1}^{\mathrm{ABC}} \otimes \tilde{M}_{0|1,j_{\mathrm{D}}}^{\mathrm{D}}(0) \otimes \mathbb{1}^{\mathrm{EF}} \right) Z^{\mathrm{E}} \rho_{j_{\mathrm{A}},j_{\mathrm{B}},j_{\mathrm{C}},j_{\mathrm{D}},j_{\mathrm{E}},j_{\mathrm{F}}}^{(6)} Z^{\mathrm{E}} \left(\mathbb{1}^{\mathrm{ABC}} \otimes \tilde{M}_{0|1,j_{\mathrm{D}}}^{\mathrm{D}}(0) \otimes \mathbb{1}^{\mathrm{EF}} \right)^{\dagger} +$$

$$+ \left(\mathbb{1}^{\mathrm{AB}} \otimes O_{j_{\mathrm{C}}}^{\mathrm{C}} \otimes \tilde{M}_{1|1,j_{\mathrm{D}}}^{\mathrm{D}}(0) \otimes \mathbb{1}^{\mathrm{EF}} \right) Z^{\mathrm{E}} \rho_{j_{\mathrm{A}},j_{\mathrm{B}},j_{\mathrm{C}},j_{\mathrm{D}},j_{\mathrm{E}},j_{\mathrm{F}}}^{(6)} Z^{\mathrm{E}} \left(\mathbb{1}^{\mathrm{AB}} \otimes O_{j_{\mathrm{C}}}^{\mathrm{C}} \otimes \tilde{M}_{1|1,j_{\mathrm{D}}}^{\mathrm{D}}(0) \otimes \mathbb{1}^{\mathrm{EF}} \right)^{\dagger} \Big) = \tag{164}$$

$$= \mathrm{Tr}_{\mathrm{DEF}} \Bigg(Z^{\mathrm{E}} \left(\frac{\rho_{j_{\mathrm{A}},j_{\mathrm{B}},j_{\mathrm{C}|0}}}{2} \otimes \rho_{j_{\mathrm{D}|0}} \otimes \rho_{j_{\mathrm{E}},j_{\mathrm{F}}} \right) Z^{\mathrm{E}} +$$

$$+ \left(\mathbb{1}^{\mathrm{AB}} \otimes O_{j_{\mathrm{C}}}^{\mathrm{C}} \otimes \mathbb{1}^{\mathrm{D}} \otimes Z^{\mathrm{E}} \otimes \mathbb{1}^{\mathrm{F}} \right) \left(\frac{\rho_{j_{\mathrm{A}},j_{\mathrm{B}},j_{\mathrm{C}|1}}}{2} \otimes \rho_{j_{\mathrm{D}|1}} \otimes \rho_{j_{\mathrm{E}},j_{\mathrm{F}}} \right) \left(\mathbb{1}^{\mathrm{AB}} \otimes O_{j_{\mathrm{C}}}^{\mathrm{C}} \otimes \mathbb{1}^{\mathrm{D}} \otimes Z^{\mathrm{E}} \otimes \mathbb{1}^{\mathrm{F}} \right)^{\dagger} \Bigg) = \tag{165}$$

$$= \frac{\rho_{j_{\mathrm{A}},j_{\mathrm{B}},j_{\mathrm{C}|0}}}{2} \mathrm{Tr} \left(\mathbb{1}^{\mathrm{D}} \otimes Z^{\mathrm{E}} \otimes \mathbb{1}^{\mathrm{F}} \rho_{j_{\mathrm{D}|0}} \otimes \rho_{j_{\mathrm{E}},j_{\mathrm{F}}} \mathbb{1}^{\mathrm{D}} \otimes Z^{\mathrm{E}} \otimes \mathbb{1}^{\mathrm{F}} \right) +$$

$$+ \mathbb{1}^{\mathrm{AB}} \otimes O_{j_{\mathrm{C}}}^{\mathrm{C}} \frac{\rho_{j_{\mathrm{A}},j_{\mathrm{B}},j_{\mathrm{C}|1}}}{2} \mathbb{1}^{\mathrm{AB}} \otimes \left(O_{j_{\mathrm{C}}}^{\mathrm{C}} \right)^{\dagger} \mathrm{Tr} \left(\mathbb{1}^{\mathrm{D}} \otimes \mathbb{1}^{\mathrm{EF}} \rho_{j_{\mathrm{D}|1}} \otimes \rho_{j_{\mathrm{E}},j_{\mathrm{F}}} \mathbb{1}^{\mathrm{D}} \otimes \mathbb{1}^{\mathrm{EF}} \right) = \rho_{j_{\mathrm{A}},j_{\mathrm{B}},j_{\mathrm{C}}} \tag{166}$$

– **Off-diagonal terms**, Z **acting on** $\triangle_{\text{ABC}}$:

$$\mathcal{N}_{\theta^{\text{D}}_{j_{\text{D}}}=0}\left(Z^{\text{A}}\rho^{(6)}_{j_{\text{A}},j_{\text{B}},j_{\text{C}},j_{\text{D}},j_{\text{E}},j_{\text{F}}}\right) =$$

$$= \text{Tr}_{\text{DEF}}\left(\left(\mathbb{1}^{\text{ABC}}\otimes\tilde{M}^{\text{D}}_{0|1,j_{\text{D}}}(0)\otimes\mathbb{1}^{\text{EF}}\right)Z^{\text{A}}\rho^{(6)}_{j_{\text{A}},j_{\text{B}},j_{\text{C}},j_{\text{D}},j_{\text{E}},j_{\text{F}}}\left(\mathbb{1}^{\text{ABC}}\otimes\tilde{M}^{\text{D}}_{0|1,j_{\text{D}}}(0)\otimes\mathbb{1}^{\text{EF}}\right)^{\dagger}+$$

$$+\left(\mathbb{1}^{\text{AB}}\otimes O^{\text{C}}_{j_{\text{C}}}\otimes\tilde{M}^{\text{D}}_{1|1,j_{\text{D}}}(0)\otimes\mathbb{1}^{\text{EF}}\right)Z^{\text{A}}\rho^{(6)}_{j_{\text{A}},j_{\text{B}},j_{\text{C}},j_{\text{D}},j_{\text{E}},j_{\text{F}}}\left(\mathbb{1}^{\text{AB}}\otimes O^{\text{C}}_{j_{\text{C}}}\otimes\tilde{M}^{\text{D}}_{1|1,j_{\text{D}}}(0)\otimes\mathbb{1}^{\text{EF}}\right)^{\dagger}\right) = \qquad (167)$$

$$= \text{Tr}_{\text{DEF}}\left(\left(\mathbb{1}^{\text{ABC}}\otimes\mathbb{1}^{\text{D}}\otimes\mathbb{1}^{\text{EF}}\right)Z^{\text{A}}\left(\frac{\rho_{j_{\text{A}},j_{\text{B}},j_{\text{C}|0}}}{2}\otimes\rho_{j_{\text{D}|0}}\otimes\rho_{j_{\text{E}},j_{\text{F}}}\right)\left(\mathbb{1}^{\text{ABC}}\otimes\mathbb{1}^{\text{D}}\otimes\mathbb{1}^{\text{EF}}\right)^{\dagger}+\right.$$

$$\left.+\left(\mathbb{1}^{\text{AB}}\otimes O^{\text{C}}_{j_{\text{C}}}\otimes\mathbb{1}^{\text{D}}\otimes\mathbb{1}^{\text{EF}}\right)Z^{\text{A}}\left(\frac{\rho_{j_{\text{A}},j_{\text{B}},j_{\text{C}|1}}}{2}\otimes\rho_{j_{\text{D}|1}}\otimes\rho_{j_{\text{E}},j_{\text{F}}}\right)\left(\mathbb{1}^{\text{AB}}\otimes O^{\text{C}}_{j_{\text{C}}}\otimes\mathbb{1}^{\text{D}}\otimes\mathbb{1}^{\text{EF}}\right)^{\dagger}\right) = \qquad (168)$$

$$= Z^{\text{A}}\frac{\rho_{j_{\text{A}},j_{\text{B}},j_{\text{C}|0}}}{2}\text{Tr}\left(\mathbb{1}^{\text{D}}\otimes\mathbb{1}^{\text{EF}}\rho_{j_{\text{D}|0}}\otimes\rho_{j_{\text{E}},j_{\text{F}}}\mathbb{1}^{\text{D}}\otimes\mathbb{1}^{\text{EF}}\right)+$$

$$+ Z^{\text{A}}\otimes\mathbb{1}^{\text{B}}\otimes O^{\text{C}}_{j_{\text{C}}}\frac{\rho_{j_{\text{A}},j_{\text{B}},j_{\text{C}|1}}}{2}Z^{\text{A}}\otimes\mathbb{1}^{\text{B}}\otimes\left(O^{\text{C}}_{j_{\text{C}}}\right)^{\dagger}\text{Tr}\left(\mathbb{1}^{\text{D}}\otimes\mathbb{1}^{\text{EF}}\rho_{j_{\text{D}|1}}\otimes\rho_{j_{\text{E}},j_{\text{F}}}\mathbb{1}^{\text{D}}\otimes\mathbb{1}^{\text{EF}}\right) = Z^{\text{A}}\rho_{j_{\text{A}},j_{\text{B}},j_{\text{C}}} \quad (169)$$

– **Off-diagonal terms**, Z **acting on** $\triangle_{\text{DEF}}$:

$$\mathcal{N}_{\theta^{\text{D}}_{j_{\text{D}}}=0}\left(Z^{\text{E}}\rho^{(6)}_{j_{\text{A}},j_{\text{B}},j_{\text{C}},j_{\text{D}},j_{\text{E}},j_{\text{F}}}\right) = \qquad (170)$$

$$= \text{Tr}_{\text{DEF}}\left(\left(\mathbb{1}^{\text{ABC}}\otimes\tilde{M}^{\text{D}}_{0|1,j_{\text{D}}}(0)\otimes\mathbb{1}^{\text{EF}}\right)Z^{\text{E}}\rho^{(6)}_{j_{\text{A}},j_{\text{B}},j_{\text{C}},j_{\text{D}},j_{\text{E}},j_{\text{F}}}\left(\mathbb{1}^{\text{ABC}}\otimes\tilde{M}^{\text{D}}_{0|1,j_{\text{D}}}(0)\otimes\mathbb{1}^{\text{EF}}\right)^{\dagger}+\right.$$

$$\left.+\left(\mathbb{1}^{\text{AB}}\otimes O^{\text{C}}_{j_{\text{C}}}\otimes\tilde{M}^{\text{D}}_{1|1,j_{\text{D}}}(0)\otimes\mathbb{1}^{\text{EF}}\right)Z^{\text{E}}\rho^{(6)}_{j_{\text{A}},j_{\text{B}},j_{\text{C}},j_{\text{D}},j_{\text{E}},j_{\text{F}}}\left(\mathbb{1}^{\text{AB}}\otimes O^{\text{C}}_{j_{\text{C}}}\otimes\tilde{M}^{\text{D}}_{1|1,j_{\text{D}}}(0)\otimes\mathbb{1}^{\text{EF}}\right)^{\dagger}\right) = \qquad (171)$$

$$= \text{Tr}_{\text{DEF}}\left(\left(\mathbb{1}^{\text{ABC}}\otimes\mathbb{1}^{\text{D}}\otimes\mathbb{1}^{\text{EF}}\right)Z^{\text{E}}\left(\frac{\rho_{j_{\text{A}},j_{\text{B}},j_{\text{C}|0}}}{2}\otimes\rho_{j_{\text{D}|0}}\otimes\rho_{j_{\text{E}},j_{\text{F}}}\right)\left(\mathbb{1}^{\text{ABC}}\otimes\mathbb{1}^{\text{D}}\otimes\mathbb{1}^{\text{EF}}\right)^{\dagger}+\right.$$

$$\left.+\left(\mathbb{1}^{\text{AB}}\otimes O^{\text{C}}_{j_{\text{C}}}\otimes\mathbb{1}^{\text{D}}\otimes\mathbb{1}^{\text{EF}}\right)Z^{\text{E}}\left(\frac{\rho_{j_{\text{A}},j_{\text{B}},j_{\text{C}|1}}}{2}\otimes\rho_{j_{\text{D}|1}}\otimes\rho_{j_{\text{E}},j_{\text{F}}}\right)\left(\mathbb{1}^{\text{AB}}\otimes O^{\text{C}}_{j_{\text{C}}}\otimes\mathbb{1}^{\text{D}}\otimes\mathbb{1}^{\text{EF}}\right)^{\dagger}\right) = \qquad (172)$$

$$= \frac{\rho_{j_{\text{A}},j_{\text{B}},j_{\text{C}|0}}}{2}\text{Tr}\left(\mathbb{1}^{\text{D}}\otimes Z^{\text{E}}\otimes\mathbb{1}^{\text{F}}\rho_{j_{\text{D}|0}}\otimes\rho_{j_{\text{E}},j_{\text{F}}}\mathbb{1}^{\text{D}}\otimes\mathbb{1}^{\text{EF}}\right)+$$

$$+ \mathbb{1}^{\text{AB}}\otimes O^{\text{C}}_{j_{\text{C}}}\frac{\rho_{j_{\text{A}},j_{\text{B}},j_{\text{C}|1}}}{2}\mathbb{1}^{\text{AB}}\otimes\left(O^{\text{C}}_{j_{\text{C}}}\right)^{\dagger}\text{Tr}\left(\mathbb{1}^{\text{D}}\otimes Z^{\text{E}}\otimes\mathbb{1}^{\text{F}}\rho_{j_{\text{D}|1}}\otimes\rho_{j_{\text{E}},j_{\text{F}}}\mathbb{1}^{\text{D}}\otimes\mathbb{1}^{\text{EF}}\right) = 0. \qquad (173)$$

(160) corresponds to a case where the experimental state would yield no imperfections and, therefore, would equal the theoretical six-qbit two triangle graph state.

For clarifying the tensor product state of (162) and (164), for example, recall the deletion property of II.1 and its depiction in Fig. (4) and Fig. (5).

Note that this property holds for Jordan measurements and imperfect states as well. This can be justified by acknowledging how imperfections may be modelled:

Imperfections may be interpreted as the result of environmental influences. As stated by Nielsen et.al. in [27], the environment may be modelled in an *operator sum convention*:

$$\tilde{\rho}^{(6)}_{j_{\text{A}},j_{\text{B}},j_{\text{C}},j_{\text{D}},j_{\text{E}},j_{\text{F}}} = \sum_k E_k\rho^{(6)}_{j_{\text{A}},j_{\text{B}},j_{\text{C}},j_{\text{D}},j_{\text{E}},j_{\text{F}}}E_k^{\dagger}; \quad (174)$$

$$\tilde{M}^{\text{D}}_{0/1|1,j_{\text{D}}}(\theta^{\text{D}}_{j_{\text{D}}}) = \sum_i E_i M^{\text{D}}_{0/1|1,j_{\text{D}}}(0)E_i^{\dagger}, \qquad (175)$$

where $E_k = \langle e_k|U|e_k\rangle$ are notions of environmental influence, where U represents a unitary interaction between the environment and the theoretical state/perfect measurement and $\{|e_k\rangle\}_k$ is an orthogonal complete set of basis vectors representing the environment. Let us remark that orthogonality here is not a fictitious restriction, but can always be achieved via Gramm-Schmidt process. Henceforth, $E_k E_j^{\dagger} = \delta_{kj}\mathbb{1}$. Up to a sufficient approximation, let us assume that the state and the measurements experience the same environmental interaction/imperfections. [32] Then,

$$\tilde{M}^{\mathrm{D}}_{0/1|1,j_{\mathrm{D}}}(\theta^{\mathrm{D}}_{j_{\mathrm{D}}})\tilde{\rho}^{(6)}_{j_{\mathrm{A}},j_{\mathrm{B}},j_{\mathrm{C}},j_{\mathrm{D}},j_{\mathrm{E}},j_{\mathrm{F}}}\left(\tilde{M}^{\mathrm{D}}_{0/1|1,j_{\mathrm{D}}}(\theta^{\mathrm{D}}_{j_{\mathrm{D}}})\right)^{\dagger}= \tag{176}$$

$$= \sum_{i,j,k} E_i M^{\mathrm{D}}_{0/1|1,j_{\mathrm{D}}}(0) E_i^{\dagger} E_j \rho^{(6)}_{j_{\mathrm{A}},j_{\mathrm{B}},j_{\mathrm{C}},j_{\mathrm{D}},j_{\mathrm{E}},j_{\mathrm{F}}} E_j^{\dagger}\left(E_k M^{\mathrm{D}}_{0/1|1,j_{\mathrm{D}}}(0) E_k^{\dagger}\right)^{\dagger}= \tag{177}$$

$$= \sum_{i} E_i M^{\mathrm{D}}_{0/1|1,j_{\mathrm{D}}}(0) \rho^{(6)}_{j_{\mathrm{A}},j_{\mathrm{B}},j_{\mathrm{C}},j_{\mathrm{D}},j_{\mathrm{E}},j_{\mathrm{F}}} M^{\mathrm{D}}_{0/1|1,j_{\mathrm{D}}}(0) E_i^{\dagger} = \sum_{i} E_i \left(\frac{\rho_{j_{\mathrm{A}},j_{\mathrm{B}},j_{\mathrm{C}|0/1}}}{2}\otimes\rho_{j_{\mathrm{D}|0/1}}\otimes\rho_{j_{\mathrm{E}},j_{\mathrm{F}}}\right)E_i^{\dagger}= \tag{178}$$

$$= \frac{\tilde{\rho}_{j_{\mathrm{A}},j_{\mathrm{B}},j_{\mathrm{C}|0/1}}}{2}\otimes\tilde{\rho}_{j_{\mathrm{D}|0/1}}\otimes\tilde{\rho}_{j_{\mathrm{E}},j_{\mathrm{F}}}. \tag{179}$$

(173) comes from the tracelessness of Pauli operators. The careful reader might wonder if it were necessary to, additionally, differentiate whether the Pauli-Z transformations that are applied on qbits associated with vertices that may undergo Pauli-Z projections according to the generalized verification protocol (VII B 1), since they may act as special cases. Nevertheless, note the commutation relation $\left[Z^D, M^{\mathrm{D}}_{0/1|1,j_{\mathrm{D}}}(0)\right]=0$. Therefore, aboves analysis applies to these cases as well.

Using this, let us revisit the fidelities (158) and (159). We differentiate between the aforementioned different cases:

- *Trivial case of* (160):
  Here, the experimental state and the theoretical state are equal. Thus, its expansion in the basis of (151) is trivial and the fidelity $F^2\left(\tilde{\rho}^{(6)}_{j_{\mathrm{A}},j_{\mathrm{B}},j_{\mathrm{C}},j_{\mathrm{D}},j_{\mathrm{E}},j_{\mathrm{F}}},\left|G^{(6)}\right\rangle\left\langle G^{(6)}\right|\right)=1\Rightarrow\epsilon_{j_{\mathrm{A}},j_{\mathrm{B}},j_{\mathrm{C}},j_{\mathrm{D}},j_{\mathrm{E}},j_{\mathrm{F}}}=0$. This stands in contradiction to our initial assumption of (104) that restricts $\epsilon_{j_{\mathrm{A}},j_{\mathrm{B}},j_{\mathrm{C}},j_{\mathrm{D}},j_{\mathrm{E}},j_{\mathrm{F}}}$ to be strictly positive. As a result, this case will not be examined any further.

- *Fidelity of diagonal terms* on $\triangle_{\mathrm{ABC}}$ *of* (163):

$$F^2\left(Z^{\mathrm{A}}\rho_{j_{\mathrm{A}},j_{\mathrm{B}},j_{\mathrm{C}}}Z^{\mathrm{A}},\left|G^{\mathrm{ABC}}\right\rangle\left\langle G^{\mathrm{ABC}}\right|\right)= \tag{180}$$

$$= \left\langle G^{\mathrm{ABC}}\left|Z^{\mathrm{A}}\right|G^{\mathrm{ABC}}\right\rangle^2=0. \tag{181}$$

Here, (181) can be seen as a result of aforementioned orthogonality between graph states.

- *Fidelity of diagonal terms* on $\triangle_{\mathrm{DEF}}$ *of* (166):

$$F^2\left(Z^{\mathrm{D}}\rho_{j_{\mathrm{A}},j_{\mathrm{B}},j_{\mathrm{C}}}Z^{\mathrm{D}},\rho^{\mathrm{ABC}}\right)= \tag{182}$$

$$= F^2\left(Z^{\mathrm{D}}\rho_{j_{\mathrm{A}},j_{\mathrm{B}},j_{\mathrm{C}}}\otimes\mathbb{1}^{\mathrm{DEF}}Z^{\mathrm{D}},\rho^{\mathrm{ABC}}\otimes\mathbb{1}^{\mathrm{DEF}}\right)= \tag{183}$$

$$= F^2\left(\rho_{j_{\mathrm{A}},j_{\mathrm{B}},j_{\mathrm{C}}},\rho^{\mathrm{ABC}}\right)=1. \tag{184}$$

Here, we embed ρ^{ABC} in $\mathcal{H}^{\mathrm{ABCDEF}}\ni\rho^{\mathrm{ABCDEF}}$, which does not change any physical properties of the state. Subsequently, we used the involutority of Pauli matrices to obtain the result.

- *Fidelity of off-diagonal terms* on $\triangle_{\mathrm{ABC}}$ of (169):

$$F^2\left(Z^{\mathrm{A}}\rho_{j_{\mathrm{A}},j_{\mathrm{B}},j_{\mathrm{C}}},\left|G^{\mathrm{ABC}}\right\rangle\left\langle G^{\mathrm{ABC}}\right|\right)= \tag{185}$$

$$= \left\langle G^{\mathrm{ABC}}\left|Z^{\mathrm{A}}\right|G^{\mathrm{ABC}}\right\rangle\left\langle G^{\mathrm{ABC}}\left|G^{\mathrm{ABC}}\right.\right\rangle=0 \tag{186}$$

As a result, we notice that the expansion of the fidelity on the rhs of

$$F^2\left(\mathcal{N}_{\theta^{\mathrm{D}}_{j_{\mathrm{D}}}=0}(\tilde{\rho}^{(6)}_{j_{\mathrm{A}},\ldots,j_{\mathrm{F}}}),\left|G^{\mathrm{ABC}}\right\rangle\left\langle G^{\mathrm{ABC}}\right|\right)=$$

$$= \sum_{\boldsymbol{k},\boldsymbol{l}}\alpha_{\boldsymbol{k},\boldsymbol{l}}\left\langle G^{\mathrm{ABC}}\left|\mathcal{N}_{\theta^{\mathrm{D}}_{\mathrm{D}}=0}\left(\left|\psi_{\boldsymbol{k}}\right\rangle\left\langle\psi_{\boldsymbol{l}}\right|\right)^{\mathrm{ABC}}\right|G^{\mathrm{ABC}}\right\rangle=$$

$$= \alpha_{0,\ldots,0}+\sum_{\substack{\boldsymbol{k},\boldsymbol{l}\\\boldsymbol{k}\neq\{0,\ldots,0\}\\\boldsymbol{l}\neq\{0,\ldots,0\}}}\alpha_{\boldsymbol{k},\boldsymbol{l}}$$

$$\tag{187}$$

is non-zero for diagonal terms on $\triangle_{\mathrm{DEF}}$ only. Similar calculations indicate the same for

$$F^2\left(\mathcal{N}_{\theta^{\mathrm{C}}_{j_{\mathrm{C}}}=0}(\tilde{\rho}^{(6)}_{j_{\mathrm{A}},\ldots,j_{\mathrm{F}}}),\left|G^{\mathrm{DEF}}\right\rangle\left\langle G^{\mathrm{DEF}}\right|\right)=$$

$$= \sum_{\boldsymbol{k},\boldsymbol{l}}\alpha_{\boldsymbol{k},\boldsymbol{l}}\left\langle G^{\mathrm{DEF}}\left|\mathcal{N}_{\theta^{\mathrm{C}}_{\mathrm{C}}=0}\left(\left|\psi_{\boldsymbol{k}}\right\rangle\left\langle\psi_{\boldsymbol{l}}\right|\right)^{\mathrm{DEF}}\right|G^{\mathrm{DEF}}\right\rangle, \tag{188}$$

namely, that the expansion terms of the fidelity on $\triangle_{\mathrm{DEF}}$ are non-zero for diagonal terms on $\triangle_{\mathrm{ABC}}$. As a result, the normalization condition of (154) may be rewritten as:

$$\sum_{\boldsymbol{k},\boldsymbol{l}}\alpha_{\boldsymbol{k},\boldsymbol{l}}=\sum_{(\boldsymbol{k},\boldsymbol{l})_{\mathrm{ABC}}}\alpha_{(\boldsymbol{k},\boldsymbol{l})_{\mathrm{ABC}}}+\sum_{(\boldsymbol{k},\boldsymbol{l})_{\mathrm{DEF}}}\alpha_{(\boldsymbol{k},\boldsymbol{l})_{\mathrm{DEF}}}=\epsilon^2_{j_{\mathrm{A}},\ldots,j_{\mathrm{F}}}, \tag{189}$$

where

$$(\boldsymbol{k},\boldsymbol{l})_{\mathrm{ABC}}\coloneqq\left\{\boldsymbol{k},\boldsymbol{l}:i\in\{\mathrm{A},\mathrm{B},\mathrm{C}\}:k_{\mathrm{i}}=l_{\mathrm{i}};i\notin\{\mathrm{A},\mathrm{B},\mathrm{C}\}:k_{\mathrm{i}}=l_{\mathrm{i}}=0\right\}\smallsetminus\left\{\boldsymbol{k}=\boldsymbol{l}=\{0,\ldots,0\}\right\}; \tag{190}$$

$$(\boldsymbol{k},\boldsymbol{l})_{\mathrm{DEF}}\coloneqq\left\{\boldsymbol{k},\boldsymbol{l}:i\in\{\mathrm{D},\mathrm{E},\mathrm{F}\}:k_{\mathrm{i}}=l_{\mathrm{i}};i\notin\{\mathrm{D},\mathrm{E},\mathrm{F}\}:k_{\mathrm{i}}=l_{\mathrm{i}}=0\right\}\smallsetminus\left\{\boldsymbol{k}=\boldsymbol{l}=\{0,\ldots,0\}\right\}. \tag{191}$$

Note that this restriction indicates that both summands in (189), representing the fidelities on the individual subtriangles, are indirectly proportional and upper bounded as:

$$\sum_{(\boldsymbol{k},\boldsymbol{l})_{\mathrm{ABC}}} \alpha_{(\boldsymbol{k},\boldsymbol{l})_{\mathrm{ABC}}} \leq \frac{\epsilon^2_{j_\mathrm{A},j_\mathrm{B},j_\mathrm{C},j_\mathrm{D},j_\mathrm{E},j_\mathrm{F}}}{2}, \tag{192}$$

$$\sum_{(\boldsymbol{k},\boldsymbol{l})_{\mathrm{DEF}}} \alpha_{(\boldsymbol{k},\boldsymbol{l})_{\mathrm{DEF}}} \leq \frac{\epsilon^2_{j_\mathrm{A},j_\mathrm{B},j_\mathrm{C},j_\mathrm{D},j_\mathrm{E},j_\mathrm{F}}}{2}. \tag{193}$$

Using the expansion of (187) (similarly for the fidelity on $\triangle_{\mathrm{DEF}}$), (192) and (193) indicate that (145) reaches its maximum at:

$$\max_{\tilde{\rho}^{(6)}_{j_\mathrm{A},j_\mathrm{B},j_\mathrm{C},j_\mathrm{D},j_\mathrm{E},j_\mathrm{F}}} \left[F^2\left(\mathcal{N}_{\theta^\mathrm{D}_{j_\mathrm{D}}=0}(\tilde{\rho}^{(6)}_{j_\mathrm{A},\dots,j_\mathrm{F}}), \left|G^{\mathrm{ABC}}\right\rangle\left\langle G^{\mathrm{ABC}}\right| \right); F^2\left(\mathcal{N}_{\theta^\mathrm{C}_{j_\mathrm{C}}=0}(\tilde{\rho}^{(6)}_{j_\mathrm{A},\dots,j_\mathrm{F}}), \left|G^{\mathrm{DEF}}\right\rangle\left\langle G^{\mathrm{DEF}}\right| \right) \right] =$$
$$= 1 - \frac{\epsilon^2_{j_\mathrm{A},j_\mathrm{B},j_\mathrm{C},j_\mathrm{D},j_\mathrm{E},j_\mathrm{F}}}{2}. \tag{194}$$

Using (31), the upper bound on the fidelities yields

a lower bound on the purified distance of (115) (and (118)) as:

$$P\left(\mathcal{N}_{\theta^\mathrm{D}_{j_\mathrm{D}}=0}(\tilde{\rho}^{(6)}_{j_\mathrm{A},\dots,j_\mathrm{F}}), \left|G^{\mathrm{ABC}}\right\rangle\left\langle G^{\mathrm{ABC}}\right| \right) \leq \sqrt{1 - \left(1 - \frac{\epsilon^2_{j_\mathrm{A},j_\mathrm{B},j_\mathrm{C},j_\mathrm{D},j_\mathrm{E},j_\mathrm{F}}}{2}\right)} = \frac{\epsilon_{j_\mathrm{A},j_\mathrm{B},j_\mathrm{C},j_\mathrm{D},j_\mathrm{E},j_\mathrm{F}}}{\sqrt{2}},$$

$$P\left(\mathcal{N}_{\theta^\mathrm{C}_{j_\mathrm{C}}=0}(\tilde{\rho}^{(6)}_{j_\mathrm{A},\dots,j_\mathrm{F}}), \left|G^{\mathrm{DEF}}\right\rangle\left\langle G^{\mathrm{DEF}}\right| \right) \leq \sqrt{1 - \left(1 - \frac{\epsilon^2_{j_\mathrm{A},j_\mathrm{B},j_\mathrm{C},j_\mathrm{D},j_\mathrm{E},j_\mathrm{F}}}{2}\right)} = \frac{\epsilon_{j_\mathrm{A},j_\mathrm{B},j_\mathrm{C},j_\mathrm{D},j_\mathrm{E},j_\mathrm{F}}}{\sqrt{2}}. \tag{195}$$

Appendix E: Upper bound of λ_2^{ABC}

Following [57], the second-largest eigenvalue of a verification operator Ω without imperfections can be expressed as:

$$\lambda_2 = \left\|\Omega - P_{\max}\right\|_{\mathrm{op}}. \tag{196}$$

Here $P_{\max}$ is the projector onto the eigenspace associated with the largest eigenvalue of Ω and $\|\cdot\|_{\mathrm{op}}$ denotes the spectral norm of (100).

We propose this property still holds similarly in the case of imperfect verification operators:

$$\lambda_2^{\mathrm{ABC}} = \left\|\tilde{\Omega}^{\mathrm{ABC}}_{(6)} - \lambda_{\max}(\tilde{\Omega}^{\mathrm{ABC}}_{(6)})P_{\max}\right\|_{\mathrm{op}}. \tag{197}$$

Note that the spectrum of both conditional operators, $\tilde{\Omega}^{\mathrm{ABC}}_{|m_Z=0}$ and $\tilde{\Omega}^{\mathrm{ABC}}_{|m_Z=1}$ is equivalent. Then, using (197), we may bound the second-largest eigenvalue as following:

$$\lambda_2^{\mathrm{ABC}} = \left\|\left(\tilde{\Omega}^{\mathrm{ABC}}_{|m_Z=0} \otimes \tilde{P}^{\mathrm{D}}_{(Z;0)} \otimes \mathrm{Id}^\mathrm{E} \otimes \mathrm{Id}^\mathrm{F} + \tilde{\Omega}^{\mathrm{ABC}}_{|m_Z=1} \otimes \tilde{P}^{\mathrm{D}}_{(Z;1)} \otimes \mathrm{Id}^\mathrm{E} \otimes \mathrm{Id}^\mathrm{F}\right) - \lambda_{\max}\left(\tilde{\Omega}^{\mathrm{ABC}}_{(6)}\right) P_{\max}\right\|_{\mathrm{op}} = \tag{198}$$

$$= \left\|\sum_i \lambda_i P_i \otimes \tilde{P}^{\mathrm{D}}_{(Z;0)} \otimes \mathrm{Id}^\mathrm{E} \otimes \mathrm{Id}^\mathrm{F} + \sum_j \lambda_j P_j \otimes \tilde{P}^{\mathrm{D}}_{(Z;1)} \otimes \mathrm{Id}^\mathrm{E} \otimes \mathrm{Id}^\mathrm{F} - \lambda_{\max}\left(\tilde{\Omega}^{\mathrm{ABC}}_{(6)}\right) P_{\max}\right\|_{\mathrm{op}} = \tag{199}$$

$$= \left\|\left(\sum_{i,j} \lambda_i \left(P_i \otimes \tilde{P}^{\mathrm{D}}_{(Z;0)} + P_j \otimes \tilde{P}^{\mathrm{D}}_{(Z;1)}\right) - \lambda_{\max}\left(\tilde{\Omega}^{\mathrm{ABC}}_{(6)}\right) P'_{\max}\right) \otimes \mathrm{Id}^\mathrm{E} \otimes \mathrm{Id}^\mathrm{F}\right\|_{\mathrm{op}} = \tag{200}$$

$$= \left\|\sum_{i,j} \lambda_{i-1} \left(P_{i-1} \otimes \tilde{P}^{\mathrm{D}}_{(Z;0)} + P_{j-1} \otimes \tilde{P}^{\mathrm{D}}_{(Z;1)}\right)\right\|_{\mathrm{op}} = \lambda_2\left(\tilde{\Omega}^{\mathrm{ABC}}_{|m_Z=0,1}\right) \leq \frac{1}{5}\left(3 + \frac{2}{3}\Delta_{\theta^\mathrm{A}_{j_\mathrm{A}},\theta^\mathrm{B}_{j_\mathrm{B}},\theta^\mathrm{C}_{j_\mathrm{C}}}\right). \tag{201}$$

Here, in (199), we expand the respective conditional verification operators in their spectral form, in (200)

we write the tensor product in a compact form, using the aforementioned equivalent spectrum of $\tilde{\Omega}^{\mathrm{ABC}}_{|m_Z=0,1}$

and we introduce $P_{\max} = P'_{\max} \otimes \mathrm{Id}^{\mathrm{E}} \otimes \mathrm{Id}^{\mathrm{F}}$. The lhs of (201) comes from the fact that the tensor of (200) associated with the largest eigenvalue is the same as $P'_{\max}$ and the rhs is a modified verrsion of (75), coming

from the difference of (93) and (53).

Appendix F: Minimum K for State Verification of $\tilde{\rho}^{(6)}$

As a reminder, the task is to find an upper bound of:

$$\mathrm{Tr}\left(\tilde{\Omega}^{\mathrm{ABC}}_{(6)} \mathcal{N}_{\theta^{\mathrm{D}}_{j_{\mathrm{D}}}}\left(\tilde{\rho}^{(6)}_{j_{\mathrm{A}},j_{\mathrm{B}},j_{\mathrm{C}},j_{\mathrm{D}},j_{\mathrm{E}},j_{\mathrm{F}}}\right)\right) \le \lambda^{\mathrm{ABC}}_2 + \left(1-\lambda^{\mathrm{ABC}}_2\right) F^2\left(\left|\tilde{\psi}_1\right\rangle\left\langle\tilde{\psi}_1\right|^{\mathrm{ABC}}, \mathcal{N}_{\theta^{\mathrm{D}}_{j_{\mathrm{D}}}}\left(\tilde{\rho}^{(6)}_{j_{\mathrm{A}},\ldots,j_{\mathrm{F}}}\right)\right) \le \quad (202)$$

$$\le \frac{1}{5}\left(3+\frac{2}{3}\Delta_{\theta^{\mathrm{A}}_{j_{\mathrm{A}}},\theta^{\mathrm{B}}_{j_{\mathrm{B}}},\theta^{\mathrm{C}}_{j_{\mathrm{C}}}}\right) + \left(1-\frac{1}{5}\left(3+\frac{2}{3}\Delta_{\theta^{\mathrm{A}}_{j_{\mathrm{A}}},\theta^{\mathrm{B}}_{j_{\mathrm{B}}},\theta^{\mathrm{C}}_{j_{\mathrm{C}}}}\right)\right) F^2\left(\left|\tilde{\psi}_1\right\rangle\left\langle\tilde{\psi}_1\right|^{\mathrm{ABC}}, \mathcal{N}_{\theta^{\mathrm{D}}_{j_{\mathrm{D}}}}\left(\tilde{\rho}^{(6)}_{j_{\mathrm{A}},\ldots,j_{\mathrm{F}}}\right)\right). \quad (203)$$

As argumented in VII D, the fidelity $F^2\left(\left|\tilde{\psi}_1\right\rangle\left\langle\tilde{\psi}_1\right|^{\mathrm{ABC}}, \mathcal{N}_{\theta^{\mathrm{D}}_{j_{\mathrm{D}}}}\left(\tilde{\rho}^{(6)}_{j_{\mathrm{A}},\ldots,j_{\mathrm{F}}}\right)\right)$ may be bounded as:

$$F^2\left(\left|\tilde{\psi}_1\right\rangle\left\langle\tilde{\psi}_1\right|^{\mathrm{ABC}}, \mathcal{N}_{\theta^{\mathrm{D}}_{j_{\mathrm{D}}}}\left(\tilde{\rho}^{(6)}_{j_{\mathrm{A}},\ldots,j_{\mathrm{F}}}\right)\right) \le$$

$$\le 1 - \left(\frac{\epsilon_{j_{\mathrm{A}},j_{\mathrm{B}},j_{\mathrm{C}},j_{\mathrm{D}},j_{\mathrm{E}},j_{\mathrm{F}}}}{\sqrt{2}} - \left(B+\frac{C}{\sqrt{3}}\right)\Delta_{\theta^{\mathrm{A}}_{j_{\mathrm{A}}},\theta^{\mathrm{B}}_{j_{\mathrm{B}}},\theta^{\mathrm{C}}_{j_{\mathrm{C}}}}\right)^2. \quad (204)$$

As a reminder, B is a conjectured constant that scales quadratically as for the single-triangle case. Using this and the fact, that the analysis is equivalent on both triangles $\triangle_{\mathrm{ABC}}$ and $\triangle_{\mathrm{DEF}}$, we may rewrite the upper bound of (107) as:

$$\mathrm{Tr}\left(\tilde{\Omega}^{\mathrm{ABC;DEF}}\tilde{\rho}^{\mathrm{ABCDEF}}\right) = \sum_{j_{\mathrm{A}},\ldots,j_{\mathrm{F}}} p(j_{\mathrm{A}},\ldots,j_{\mathrm{F}})\left(\mathrm{Tr}\left(\tilde{\Omega}^{\mathrm{ABC}}_{(6)}\mathcal{N}_{\theta^{\mathrm{D}}_{j_{\mathrm{D}}}}\left(\tilde{\rho}^{(6)}_{j_{\mathrm{A}},\ldots,j_{\mathrm{F}}}\right)\right)\right) \le \quad (205)$$

$$\le \sum_{j_{\mathrm{A}},\ldots,j_{\mathrm{F}}} p(j_{\mathrm{A}},\ldots,j_{\mathrm{F}})\frac{1}{5}\left(3+\frac{2}{3}\Delta_{\theta^{\mathrm{A}}_{j_{\mathrm{A}}},\theta^{\mathrm{B}}_{j_{\mathrm{B}}},\theta^{\mathrm{C}}_{j_{\mathrm{C}}}}\right) + \quad (206)$$

$$+ \sum_{j_{\mathrm{A}},\ldots,j_{\mathrm{F}}} p(j_{\mathrm{A}},\ldots,j_{\mathrm{F}})\left(1-\frac{1}{5}\left(3+\frac{2}{3}\Delta_{\theta^{\mathrm{A}}_{j_{\mathrm{A}}},\theta^{\mathrm{B}}_{j_{\mathrm{B}}},\theta^{\mathrm{C}}_{j_{\mathrm{C}}}}\right)\right)\left(1-\left(\frac{\epsilon_{j_{\mathrm{A}},\ldots,j_{\mathrm{F}}}}{\sqrt{2}}-\left(B+\frac{C}{\sqrt{3}}\right)\Delta_{\theta^{\mathrm{A}}_{j_{\mathrm{A}}},\theta^{\mathrm{B}}_{j_{\mathrm{B}}},\theta^{\mathrm{C}}_{j_{\mathrm{C}}}}\right)^2\right) = \quad (207)$$

$$= 1 - \left(\frac{3}{5}\left(\sum_{j_{\mathrm{A}},\ldots,j_{\mathrm{F}}} p(j_{\mathrm{A}},\ldots,j_{\mathrm{F}})\left(\frac{\epsilon_{j_{\mathrm{A}},\ldots,j_{\mathrm{F}}}}{\sqrt{2}}-\left(B+\frac{C}{\sqrt{3}}\right)\Delta_{\theta^{\mathrm{A}}_{j_{\mathrm{A}}},\theta^{\mathrm{B}}_{j_{\mathrm{B}}},\theta^{\mathrm{C}}_{j_{\mathrm{C}}}}\right)^2\right)\right) + \quad (208)$$

$$+ \frac{2}{15}\left(\sum_{j_{\mathrm{A}},\ldots,j_{\mathrm{F}}} p(j_{\mathrm{A}},\ldots,j_{\mathrm{F}})\Delta_{\theta^{\mathrm{A}}_{j_{\mathrm{A}}},\theta^{\mathrm{B}}_{j_{\mathrm{B}}},\theta^{\mathrm{C}}_{j_{\mathrm{C}}}}\left(\frac{\epsilon_{j_{\mathrm{A}},\ldots,j_{\mathrm{F}}}}{\sqrt{2}}-\left(B+\frac{C}{\sqrt{3}}\right)\Delta_{\theta^{\mathrm{A}}_{j_{\mathrm{A}}},\theta^{\mathrm{B}}_{j_{\mathrm{B}}},\theta^{\mathrm{C}}_{j_{\mathrm{C}}}}\right)^2\right) \quad (209)$$

To evaluate (208), we look at:

$$1 - \left(\frac{3}{5}\left(\sum_{j_{\mathrm{A}},\ldots,j_{\mathrm{F}}} p(j_{\mathrm{A}},\ldots,j_{\mathrm{F}})\left(\frac{\epsilon_{j_{\mathrm{A}},\ldots,j_{\mathrm{F}}}}{\sqrt{2}}-\left(B+\frac{C}{\sqrt{3}}\right)\Delta_{\theta^{\mathrm{A}}_{j_{\mathrm{A}}},\theta^{\mathrm{B}}_{j_{\mathrm{B}}},\theta^{\mathrm{C}}_{j_{\mathrm{C}}}}\right)^2\right)\right) \le \quad (210)$$

$$\le 1 - \left(\frac{3}{5}\left(\sum_{j_{\mathrm{A}},\ldots,j_{\mathrm{F}}} p(j_{\mathrm{A}},\ldots,j_{\mathrm{F}})\frac{\epsilon_{j_{\mathrm{A}},\ldots,j_{\mathrm{F}}}}{\sqrt{2}}-2\left(B+\frac{C}{\sqrt{3}}\right)\Delta_{\mathrm{ABCDEF}}\right)^2\right), \quad (211)$$

where we used the condition of (106), and the factor-ization property of A and (143) with opposite direction,

which is in line with (106).

To evaluate (209), we calculate:

$$\frac{2}{15}\left(\sum_{j_{\mathrm{A}},\ldots,j_{\mathrm{F}}} p(j_{\mathrm{A}},\ldots,j_{\mathrm{F}})\Delta_{\theta^{\mathrm{A}}_{j_{\mathrm{A}}},\theta^{\mathrm{B}}_{j_{\mathrm{B}}},\theta^{\mathrm{C}}_{j_{\mathrm{C}}}}\left(\frac{\epsilon_{j_{\mathrm{A}},\ldots,j_{\mathrm{F}}}}{\sqrt{2}} - \left(B + \frac{C}{\sqrt{3}}\right)\Delta_{\theta^{\mathrm{A}}_{j_{\mathrm{A}}},\theta^{\mathrm{B}}_{j_{\mathrm{B}}},\theta^{\mathrm{C}}_{j_{\mathrm{C}}}}\right)^2\right) \leq \tag{212}$$

$$\leq \frac{4}{15}\Delta\left(\sum_{j_{\mathrm{A}},\ldots,j_{\mathrm{F}}} p(j_{\mathrm{A}},\ldots,j_{\mathrm{F}})\left(\frac{\epsilon_{j_{\mathrm{A}},\ldots,j_{\mathrm{F}}}}{\sqrt{2}} - \left(B + \frac{C}{\sqrt{3}}\right)\Delta_{\theta^{\mathrm{A}}_{j_{\mathrm{A}}},\theta^{\mathrm{B}}_{j_{\mathrm{B}}},\theta^{\mathrm{C}}_{j_{\mathrm{C}}}}\right)^2\right) \leq \tag{213}$$

$$\leq \frac{4}{15}\Delta_{\mathrm{ABCDEF}}\left(\sum_{j_{\mathrm{A}},\ldots,j_{\mathrm{F}}} p(j_{\mathrm{A}},\ldots,j_{\mathrm{F}})\left(\frac{\epsilon_{j_{\mathrm{A}},\ldots,j_{\mathrm{F}}}}{\sqrt{2}} - \left(B + \frac{C}{\sqrt{3}}\right)\Delta_{\theta^{\mathrm{A}}_{j_{\mathrm{A}}},\theta^{\mathrm{B}}_{j_{\mathrm{B}}},\theta^{\mathrm{C}}_{j_{\mathrm{C}}}}\right)\right) \leq \tag{214}$$

$$\leq \frac{4}{15}\Delta_{\mathrm{ABCDEF}}\left(\sum_{j_{\mathrm{A}},\ldots,j_{\mathrm{F}}} p(j_{\mathrm{A}},\ldots,j_{\mathrm{F}})\frac{\epsilon_{j_{\mathrm{A}},\ldots,j_{\mathrm{F}}}}{\sqrt{2}} - 2\left(B + \frac{C}{\sqrt{3}}\right)\Delta_{\mathrm{ABCDEF}}\right). \tag{215}$$

Here, we use a similar calculational scheme as in the latter parts of [52], which is based on Cauchy-Schwarz-inequality and, for, (214), we refer to

$$0 \leq \frac{\epsilon_{j_{\mathrm{A}},\ldots,j_{\mathrm{F}}}}{\sqrt{2}} - \left(B + \frac{C}{\sqrt{3}}\right)\Delta_{\theta^{\mathrm{A}}_{j_{\mathrm{A}}},\theta^{\mathrm{B}}_{j_{\mathrm{B}}},\theta^{\mathrm{C}}_{j_{\mathrm{C}}}} \leq 1, \tag{216}$$

which comes from the fact that $\epsilon_{j_{\mathrm{A}},\ldots,j_{\mathrm{F}}} \geq \Delta_{\theta^{\mathrm{A}}_{j_{\mathrm{A}}},\theta^{\mathrm{B}}_{j_{\mathrm{B}}},\theta^{\mathrm{C}}_{j_{\mathrm{C}}}}$, which is proven in [27].
This leads to an upper bound of:

$$\mathrm{Tr}\left(\tilde{\Omega}^{\mathrm{ABC;DEF}}\tilde{\rho}^{\mathrm{ABCDEF}}\right) \leq \tag{217}$$

$$\leq 1 - \left(\frac{3}{5}\left(\sum_{j_{\mathrm{A}},\ldots,j_{\mathrm{F}}} p(j_{\mathrm{A}},\ldots,j_{\mathrm{F}})\frac{\epsilon_{j_{\mathrm{A}},\ldots,j_{\mathrm{F}}}}{\sqrt{2}} - 2\left(B + \frac{C}{\sqrt{3}}\right)\Delta_{\mathrm{ABCDEF}}\right)^2\right) + \tag{218}$$

$$+ \frac{4}{15}\Delta_{\mathrm{ABCDEF}}\left(\sum_{j_{\mathrm{A}},\ldots,j_{\mathrm{F}}} p(j_{\mathrm{A}},\ldots,j_{\mathrm{F}})\frac{\epsilon_{j_{\mathrm{A}},\ldots,j_{\mathrm{F}}}}{\sqrt{2}} - 2\left(B + \frac{C}{\sqrt{3}}\right)\Delta_{\mathrm{ABCDEF}}\right) = \tag{219}$$

$$= 1 - \frac{1}{2}\left(\sqrt{\frac{6}{5}}\left(\sum_{j_{\mathrm{A}},\ldots,j_{\mathrm{F}}} p(j_{\mathrm{A}},\ldots,j_{\mathrm{F}})\frac{\epsilon_{j_{\mathrm{A}},\ldots,j_{\mathrm{F}}}}{\sqrt{2}} - 2\left(B + \frac{C}{\sqrt{3}}\right)\Delta_{\mathrm{ABCDEF}}\right)^2\right) + \tag{220}$$

$$+ \frac{4}{15}\Delta_{\mathrm{ABCDEF}}\left(\sum_{j_{\mathrm{A}},\ldots,j_{\mathrm{F}}} p(j_{\mathrm{A}},\ldots,j_{\mathrm{F}})\frac{\epsilon_{j_{\mathrm{A}},\ldots,j_{\mathrm{F}}}}{\sqrt{2}} - 2\left(B + \frac{C}{\sqrt{3}}\right)\Delta_{\mathrm{ABCDEF}}\right) = \tag{221}$$

$$= 1 - \frac{3}{10}\left(\sum_{j_{\mathrm{A}},\ldots,j_{\mathrm{F}}} p(j_{\mathrm{A}},\ldots,j_{\mathrm{F}})\epsilon_{j_{\mathrm{A}},\ldots,j_{\mathrm{F}}}\right)^2 + \frac{\sqrt{72}}{5}\sum_{j_{\mathrm{A}},\ldots,j_{\mathrm{F}}} p(j_{\mathrm{A}},\ldots,j_{\mathrm{F}})\epsilon_{j_{\mathrm{A}},\ldots,j_{\mathrm{F}}}\left(B + \frac{C}{\sqrt{3}}\right)\Delta_{\mathrm{ABCDEF}} - \tag{222}$$

$$- \frac{12}{5}\left(B + \frac{C}{\sqrt{3}}\right)^2\Delta^2_{\mathrm{ABCDEF}} + \frac{4}{15}\Delta_{\mathrm{ABCDEF}}\sum_{j_{\mathrm{A}},\ldots,j_{\mathrm{F}}} p(j_{\mathrm{A}},\ldots,j_{\mathrm{F}})\frac{\epsilon_{j_{\mathrm{A}},\ldots,j_{\mathrm{F}}}}{\sqrt{2}} - \frac{8}{15}\left(B + \frac{C}{\sqrt{3}}\right)\Delta^2_{\mathrm{ABCDEF}} = \tag{223}$$

$$= 1 - \frac{1}{2}\left(\sqrt{\frac{3}{5}}\sum_{j_{\mathrm{A}},\ldots,j_{\mathrm{F}}} p(j_{\mathrm{A}},\ldots,j_{\mathrm{F}})\epsilon_{j_{\mathrm{A}},\ldots,j_{\mathrm{F}}} - \left(\sqrt{\frac{24}{5}}\left(B + \frac{C}{\sqrt{3}}\right) + \sqrt{\frac{8}{135}}\right)\Delta_{\mathrm{ABCDEF}}\right)^2 + \frac{4}{135}\Delta^2_{\mathrm{ABCDEF}} \leq \tag{224}$$

$$\leq 1 - \frac{1}{2}\left(\sqrt{\frac{3}{5}}\epsilon_{\mathrm{ABCDEF}} - \left(\sqrt{\frac{24}{5}}\left(B + \frac{C}{\sqrt{3}}\right) + \sqrt{\frac{8}{135}}\right)\Delta_{\mathrm{ABCDEF}}\right)^2 + \frac{4}{135}\Delta^2_{\mathrm{ABCDEF}}. \tag{225}$$

Here, in (225), we used the relation of (81). Recalling the inequality for geometric and arithmetic means of

(61), we find a lower bound on necessary rounds K for a significance level δ as

$$\text{Tr}\left(\tilde{\Omega}^{\text{ABC;DEF}} \tilde{\rho}^{\text{ABCDEF}}\right)^K \leq \left(1 - \frac{1}{2}\left(\sqrt{\frac{3}{5}}\epsilon - \left(\sqrt{\frac{24}{5}}\left(B + \frac{C}{\sqrt{3}}\right) + \sqrt{\frac{8}{135}}\right)\Delta\right)^2 + \frac{4}{135}\Delta^2\right)^K \leq \delta,$$

$$\tag{226}$$

$$\Rightarrow K \geq \frac{\ln\delta}{\ln\left(1 - \frac{1}{2}\left(\sqrt{\frac{3}{5}}\epsilon - \left(\sqrt{\frac{24}{5}}\left(B + \frac{C}{\sqrt{3}}\right) + \sqrt{\frac{8}{135}}\right)\Delta\right)^2 + \frac{4}{135}\Delta^2\right)}.$$

Here, we have omitted the ABCDEF-subscripts for Δ and ϵ, since they are clear from context.

Appendix G: Quantum Relative Entropy

Let $S(\rho\|\sigma)$ denote the *quantum relative entropy*:

$$S(\rho\|\sigma) := -\text{Tr}\left(\rho\log\sigma\right) - S(\rho), \tag{227}$$

where $S(\rho)$ denotes *von-Neumann entropy*

$$S(\rho) := -\text{Tr}(\rho\log\rho). \tag{228}$$

What is the motivation of considering quantum relative entropy when thinking quantum state verification? Although it is well known that Fuchs-van-de-Graaf inequalties are tight, it has been shown that more information about the physical properties of the systems involved in the fidelity estimations might lead to tightening the bound. As shown in [11, 55], this additional information should be *maximum quantum relative entropy*. Since, within this work, Fuchs- van de Graaf-inequalities have been used extensively to provide tight bounds, we conjecture that further investigation would lead to tighter bounds and hence to a lower number of necessary rounds K for a significance level δ. Within this chapter, we will present general considerations and observations concerning quantum relative entropy.

We will start by finding a connection between the trace distance of a decoded quantum state, (35), projective trace-preserving measurements and quantum relative entropy in case of positive or negative semi-definite density matrices $\tilde{\rho}$ and ρ_B. Throughout this chapter, ρ_B may thought of an embedding of a pure state ρ into a larger Hilbert space $\mathcal{H} \ni \tilde{\rho}$, where the imperfect state $\tilde{\rho}$ resides with $\mathcal{D} \in \mathcal{L}(\mathcal{H})$(compare (57)). In this case, we note that quantum relative entropy provides a lower bound for state-accuracy ϵ:

$$\frac{1}{2}\left\|\mathcal{D}(\tilde{P}_\theta\tilde{\rho}\tilde{P}_\theta - \tilde{P}_0\rho_B\tilde{P}_0)\right\|_1 \leq \tag{229}$$

$$\leq \frac{1}{2}\text{Tr}\left(|\tilde{P}_\theta\tilde{\rho}\tilde{P}_\theta - \tilde{P}_0\rho_B\tilde{P}_0|\right) = \tag{230}$$

$$= \text{Tr}\left(\Pi\left(\tilde{P}_\theta\tilde{\rho}\tilde{P}_\theta - \tilde{P}_0\rho_B\tilde{P}_0\right)\right) \leq \tag{231}$$

$$\leq \text{Tr}\left(\Pi\left|\tilde{P}_\theta\tilde{\rho}\tilde{P}_\theta - \tilde{P}_0\rho_B\tilde{P}_0\right|\right) \leq \tag{232}$$

$$\leq \sqrt{\text{rk}\,\Pi}\sqrt{\text{Tr}\left(\left(\tilde{P}_\theta\tilde{\rho}\tilde{P}_\theta - \tilde{P}_0\rho_B\tilde{P}_0\right)^2\right)} \leq \tag{233}$$

$$\leq \sqrt{\text{rk}\,\Pi}\sqrt{\text{Tr}\left(\left(\tilde{P}_\theta\tilde{\rho}\tilde{P}_\theta - \tilde{P}_0\rho_B\tilde{P}_0\right)\right)^2} \leq \tag{234}$$

$$\leq \pm\sqrt{\text{rk}\,\Pi}\,\text{Tr}\left(\tilde{P}_\theta\tilde{\rho}\tilde{P}_\theta - \tilde{P}_0\rho_B\tilde{P}_0\right) \leq \tag{235}$$

$$\leq \sqrt{\text{rk}\,\Pi}\,S(\tilde{P}_{0/\theta}\rho_B\tilde{P}_{0/\theta}\|\tilde{P}_{\theta/0}\tilde{\rho}\tilde{P}_{\theta/0}). \tag{236}$$

(232) can be deduced from the identity $\left|\text{Tr}(A)\right| = \text{Tr}|A|$ [5] for any Hermitian matrix A as well as the *Hölder duality of Schatten-norms* [15, 27]:

Proposition A.1 (Hölder duality of Schatten-norms). *Let ρ and σ denote density matrices. Then,*

$$\exists\,\Pi^2 = \Pi : \|\rho - \sigma\|_1 = \text{Tr}\left(\Pi(\rho - \sigma)\right). \tag{237}$$

(233) comes from the Cauchy-Schwarz inequality for Frobenius norms on positive matrices, (234) is true for positive real discriminantes (it can also be seen as an application of [54]) and (236) comes from Klein's inequality [7]:

Proposition A.2 (Klein's inequality). *Let A, B denote density matrices. Then:*

$$\text{Tr}\left(A - B\right) \leq \text{Tr}\left(A\left(\log A - \log B\right)\right) = S(A\|B). \tag{238}$$

Note that a similar result, which is true for indefinite matrices as well, is given in [2, 35]. Here, the authors proved the following inequality (also known as a variant of *Csiszár- Kemperman-Kullback-Pinsker inequality* [44]:

$$S\left(\rho\|\sigma\right) \geq \frac{1}{2}\|\rho - \sigma\|_1^2 \tag{239}$$

As a reminder, an indefinite Hermitian matrix is a matrix with both, positive and negative real eigenvalues. Let us considers the eigenvalues of $\rho - \rho'$, where ρ denotes a pure state and ρ' denotes a mixed state. Recall that a pure states associated density matrix is a singular matrix with only one non-zero eigenvalue $\|\rho\| = \lambda_{\max} = 1$ and that a density matrix associated with a mixed quantum state has more than one non-negative eigenvalues, that are smaller than one. Therefore, we note that $\rho - \rho'$ must be indefinite. This indicates that in the realms of quantum state verification, indefinite matrices are being investigated. It can be shown that no explicit connection between quantum relative entropy and the trace distance can be made in that case:

$$\frac{1}{2}\|\tilde{\rho} - \sigma\|_1 = \frac{1}{2}\text{Tr}\left(|\tilde{\rho} - \sigma|\right) = \tag{240}$$

$$= \frac{1}{2}\text{Tr}\left(Q + S\right) = \text{Tr}\,S; \tag{241}$$

$$\text{Tr}\,S > \text{Tr}\left(S - Q\right) = -\text{Tr}\left(Q - S\right) = \tag{242}$$

$$= -\text{Tr}\left(\rho - \sigma\right) = 0 \geq -S\left(\rho\|\sigma\right) \tag{243}$$

$$\Rightarrow \frac{1}{2}\|\tilde{\rho} - \sigma\|_1 \geq -S\left(\rho\|\sigma\right). \tag{244}$$

In (241), we used the fact that we may rewrite $\tilde{\rho} - \sigma = Q - S$, where Q, S denote positive matrices with respective orthogonal support, a calculational technique

being used in [27, 38] for instance. (Note that due to $\mathrm{Tr}(\rho - \sigma) = 0 = \mathrm{Tr}(Q - S) \Rightarrow \mathrm{Tr}\, Q = \mathrm{Tr}\, S$). Although the result stands in no contradiction due to quantum relative entropic positive semi-definiteness [8, 27], it does not provide a clear connection between quantum relative entropy and the trace distance of indefinite matrices. Hence, for indefinite matrices, we decide to use bounds in the form of (239) by taking the square-root on both sides, for definite matrices though, we are able to bound it further on with as shown above.

In the following, we want to investigate under what circumstances quantum relative entropy might be decreasing under different projective quantum channels in

the respective slots of quantum relative entropy. For this, recall the *Kraus representation* of CPTP projection measurements: Let $\mathcal{K}(\cdot)$ be a CPTP projection measurement. Then, there exists projection operators P, such that $\mathcal{K}(\cdot)$ takes the following form in the Kraus representation [43]:

$$\mathcal{K}(\rho) = P\rho P. \tag{245}$$

In the following, we will assume this form and take the projection operators to be Jordan operators $\tilde{P}_0$ and $\tilde{P}_\theta$, where the subscript indicates the respective angle in the Jordan operator. Additionally, we assume that one of the states, ρ_B is pure.
Investigation yields [33]:

$$S(\tilde{P}_0\rho_B P_0 \| \tilde{P}_\theta \tilde{\rho} P_\theta) \overset{!}{\leq} S(\rho_B \| \tilde{\rho}) \tag{246}$$

$$-\mathrm{Tr}\left(\tilde{P}_0\rho_B\tilde{P}_0 \log\left(\tilde{P}_\theta\tilde{\rho}\tilde{P}_\theta\right)\right) + \mathrm{Tr}\left(\tilde{P}_0\rho_B\tilde{P}_0 \log\left(\tilde{P}_0\rho_B\tilde{P}_0\right)\right) \overset{!}{\leq} -\mathrm{Tr}\left(\rho_B \log\tilde{\rho}\right) - S(\rho_B) \tag{247}$$

$$-\mathrm{Tr}\left(\tilde{P}_0\rho_B\tilde{P}_0 \log\left(\tilde{P}_\theta\tilde{\rho}\tilde{P}_\theta\right)\right) + \mathrm{Tr}\left(\tilde{P}_0\rho_B\tilde{P}_0 \log\left(\tilde{P}_0\rho_B\tilde{P}_0\right)\right) \overset{!}{\leq} -\mathrm{Tr}\left(\rho_B \log\tilde{\rho}\right) \tag{248}$$

$$\mathrm{Tr}\left(\tilde{P}_0\rho_B\tilde{P}_0 \log\left(\tilde{P}_\theta\tilde{\rho}\tilde{P}_\theta\right)\right) - \mathrm{Tr}\left(\tilde{P}_0\rho_B\tilde{P}_0 \log\left(\tilde{P}_0\rho_B\tilde{P}_0\right)\right) \overset{!}{\geq} \mathrm{Tr}\left(\rho_B \log\tilde{\rho}\right) \tag{249}$$

$$\mathrm{Tr}\left(\tilde{P}_\theta\tilde{P}_0\rho_B\tilde{P}_0\tilde{P}_\theta \log\tilde{\rho}\right) \overset{!}{\geq} \mathrm{Tr}\left(\rho_B \log\tilde{\rho}\right) + \mathrm{Tr}\left(\tilde{P}_0\rho_B\tilde{P}_0 \log\left(\tilde{P}_0\rho_B\tilde{P}_0\right)\right) \tag{250}$$

$$\mathrm{Tr}\left(\tilde{P}_\theta\tilde{P}_0\rho_B\tilde{P}_0\tilde{P}_\theta \log\tilde{\rho}\right) - \mathrm{Tr}\left(\rho_B \log\tilde{\rho}\right) \overset{!}{\geq} \mathrm{Tr}\left(\tilde{P}_0\rho_B\tilde{P}_0 \log\left(\tilde{P}_0\rho_B\tilde{P}_0\right)\right); \tag{251}$$

$$\mathrm{Tr}\left(\tilde{P}_0\rho_B\tilde{P}_0 \log\left(\tilde{P}_0\rho_B\tilde{P}_0\right)\right) \geq \mathrm{Tr}\left(\tilde{P}_0\rho_B\tilde{P}_0 \log\rho_B\right) \tag{252}$$

$$\mathrm{Tr}\left(\tilde{P}_0\rho_B\tilde{P}_0 \log\left(\tilde{P}_0\rho_B\tilde{P}_0\right)\right) - \mathrm{Tr}\left(\tilde{P}_0\rho_B\tilde{P}_0 \log\rho_B\right) = S\left(\tilde{P}_0\rho_B\tilde{P}_0 \| \rho_B\right) \tag{253}$$

$$\Rightarrow \mathrm{Tr}\left(\tilde{P}_0\rho_B\tilde{P}_0 \log\rho_B\right) + S\left(\tilde{P}_0\rho_B\tilde{P}_0 \| \rho_B\right) \overset{!}{\leq} \mathrm{Tr}\left(\tilde{P}_\theta\tilde{P}_0\rho_B\tilde{P}_0\tilde{P}_\theta \log\tilde{\rho}\right) - \mathrm{Tr}\left(\rho_B \log\tilde{\rho}\right) \tag{254}$$

$$\mathrm{Tr}\left(\tilde{P}_0\rho_B\tilde{P}_0 \log\rho_B\right) \leq \mathrm{Tr}\left(\tilde{P}_0 \left|\rho_B\tilde{P}_0 \log\rho_B\right|\right) \leq \sqrt{\mathrm{rk}\,\tilde{P}_0}\sqrt{\mathrm{Tr}\left|\rho_B\tilde{P}_0 \log\rho_B\right|^2} \tag{255}$$

$$\sqrt{\mathrm{Tr}\left|\rho_B\tilde{P}_0 \log\rho_B\right|^2} \leq \mathrm{Tr}\left|\rho_B\tilde{P}_0 \log\rho_B\right| = \mathrm{Tr}\left|\tilde{P}_0 \log\rho_B\rho_B\right| \leq \sqrt{\mathrm{rk}\,\tilde{P}_0}\,\mathrm{Tr}\left|\log\rho_B\rho_B\right| = 0 \tag{256}$$

$$\Rightarrow S\left(\tilde{P}_0\rho_B\tilde{P}_0 \| \rho_B\right) \overset{!}{\leq} \mathrm{Tr}\left(\tilde{P}_\theta\tilde{P}_0\rho_B\tilde{P}_0\tilde{P}_\theta \log\tilde{\rho}\right) - \mathrm{Tr}\left(\rho_B \log\tilde{\rho}\right) \tag{257}$$

$$S\left(\tilde{P}_0\rho_B\tilde{P}_0 \| \rho_B\right) + \mathrm{Tr}\left(\rho_B \log\tilde{\rho}\right) \overset{!}{\leq} \mathrm{Tr}\left(\tilde{P}_\theta\tilde{P}_0\rho_B\tilde{P}_0\tilde{P}_\theta \log\tilde{\rho}\right); \tag{258}$$

$$\mathrm{Tr}\left(\tilde{P}_\theta\tilde{P}_0\rho_B\tilde{P}_0\tilde{P}_\theta \log\tilde{\rho}\right) \leq \mathrm{Tr}\left(\tilde{P}_\theta\tilde{P}_0 \left|\rho_B\tilde{P}_0\tilde{P}_\theta \log\tilde{\rho}\right|\right) \leq \mathrm{Tr}\left(\tilde{P}_0\tilde{P}_\theta\right)\mathrm{Tr}\left(\left|\rho_B\tilde{P}_0\tilde{P}_\theta \log\tilde{\rho}\right|\right); \tag{259}$$

$$\mathrm{Tr}\left(\left|\rho_B\tilde{P}_0\tilde{P}_\theta \log\tilde{\rho}\right|\right) := \mathrm{Tr}\left(\left|\tilde{P}_0\tilde{P}_\theta \log\tilde{\rho}\rho_B\right|\right) + r \tag{260}$$

$$\Rightarrow \mathrm{Tr}\left(\tilde{P}_0\tilde{P}_\theta\right)\left(\mathrm{Tr}\left(\left|\tilde{P}_0\tilde{P}_\theta \log\tilde{\rho}\rho_B\right|\right) + r\right) \leq \mathrm{Tr}\left(\tilde{P}_0\tilde{P}_\theta\right)\left(\mathrm{Tr}\left|\tilde{P}_0\tilde{P}_\theta\right|\mathrm{Tr}\left|\log\tilde{\rho}\rho_B\right| + r\right) \tag{261}$$

$$\mathrm{Tr}\left(\tilde{P}_0\tilde{P}_\theta\right)\left(\mathrm{Tr}\left(\tilde{P}_0\tilde{P}_\theta\right)\mathrm{Tr}\left|\log\tilde{\rho}\rho_B\right| + r\right) \leq \mathrm{rk}\,\tilde{P}_0\,\mathrm{rk}\,\tilde{P}_\theta\,\mathrm{sgn}\left(\mathrm{Tr}\left(\rho_B \log\tilde{\rho}\right)\right)\mathrm{Tr}\left(\rho_B \log\tilde{\rho}\right) + \mathrm{Tr}\left(\tilde{P}_0\tilde{P}_\theta\right)r \tag{262}$$

$$\Rightarrow S\left(\tilde{P}_0\rho_B\tilde{P}_0 \| \rho_B\right) + \mathrm{Tr}\left(\rho_B \log\tilde{\rho}\right) \overset{!}{\leq} -\mathrm{rk}\,\tilde{P}_0\,\mathrm{rk}\,\tilde{P}_\theta\,\mathrm{Tr}\left(\rho_B \log\tilde{\rho}\right) + \mathrm{Tr}\left(\tilde{P}_0\tilde{P}_\theta\right)r \tag{263}$$

$$S\left(\tilde{P}_0\rho_B\tilde{P}_0 \| \rho_B\right) \overset{!}{\leq} -\left(\mathrm{rk}\,\tilde{P}_0\,\mathrm{rk}\,\tilde{P}_\theta + 1\right)\mathrm{Tr}\left(\rho_B \log\tilde{\rho}\right) + \mathrm{Tr}\left(\tilde{P}_0\tilde{P}_\theta\right)r \tag{264}$$

$$S\left(\tilde{P}_0\rho_B\tilde{P}_0 \| \rho_B\right) \overset{!}{\leq} \left(\mathrm{rk}\,\tilde{P}_0\,\mathrm{rk}\,\tilde{P}_\theta + 1\right)S\left(\rho_B \| \tilde{\rho}\right) + \mathrm{Tr}\left(\tilde{P}_0\tilde{P}_\theta\right)r. \tag{265}$$

In (248), we used that the entropy of a pure state vanishes. In (250) and (252), we used that principal

matrix logarithm is an operator monotone concave function defined on the matrix vector space of positive

definite Hermitian matrices [10] [34]. As such, utilizing *Hansen-Pedersen-characterization* [16, 18], the following inequality holds:

Proposition A.3 (Hansen-Pedersen-Characterization). *Let P denote a finite-dimensional orthogonal projection operator with $P^2 = P$, $P^\dagger = P$. For $X = X^\dagger > 0$, $\log(X)$ is an operator valued monotone concave function. The following equivalency holds:*

$$\log \text{ concave} \quad \Leftrightarrow \quad \log\left(P\rho P\right) \geq P \log \rho P. \quad (266)$$

This equivalency can also be seen as a Jensen-type inequality [7, 8, 19]. In (253), we evaluated the *Jensen gap*, which is the difference of both sides of a Jensen type inequality and noticed that it equals quantum relative entropy of $S\left(\tilde{P}_0\rho_B\tilde{P}_0\|\rho_B\right)$. (256) and (262) are usage of Cauchy-Schwarz inequalities. As we did before, we noticed that the Cauchy-Schwarz inequality for positive discriminantes can be furhter simplified using that $\sqrt{\text{Tr}(\cdot^2)} \leq \sqrt{\text{Tr}(\cdot)^2}$ [54]. In both cases, we notice that the trace was taken over negative definite matrices and as so, we may extract the sign-function off the trace. For exemplification and demonstrative purposes, assume we take the trace over the absolute value of a negative definite $k \times k$ matrix $(\forall \lambda_k, \lambda_k < 0)$, $\text{Tr}(|\rho \log \rho'|)$:

$$\text{Tr}\left(\left|\rho \log \rho'\right|\right) = \sum_k |\lambda_k| = \sum_k \text{sgn}(\lambda_k)\lambda_k = -\sum_k \lambda_k. \quad (267)$$

(260) comes from the loss of the cyclic property of the trace over the absolute value of a multiplication of matrices. It is this loss that leads to the observation that validity of (265) strongly depends on the sign of r. This can be seen by acknowledging that all terms appearing here are positive semi-definite, apart from r, which may be negative.

As a result, we conjecture that the behaviour of quantum relative entropy under CPTP projective measurements strongly depends on the commutation relation between the quantum states involved and the projective measurements. Note that, if $\rho_B = \tilde{\rho}$, this claim is being strengthened as well, since, for negative r, (265) would indicate that the quantum relative entropy increases under projective measurements. We leave further calculations to the reader.

[1] S. Aaronson and D. Gottesman. Improved simulation of stabilizer circuits. *Physical Review A*, 70(5):052328, 2004.

[2] K. M. Audenaert and J. Eisert. Continuity bounds on the quantum relative entropy—ii. *Journal of Mathematical Physics*, 52(11):112201, 2011.

[3] F. Baccari, R. Augusiak, I. Šupić, J. Tura, and A. Acín. Scalable bell inequalities for qubit graph states and robust self-testing. *Physical review letters*, 124(2):020402, 2020.

[4] C.-E. Bardyn, T. C. Liew, S. Massar, M. McKague, and V. Scarani. Device-independent state estimation based on bell's inequalities. *Physical Review A*, 80(6):062327, 2009.

[5] B. Baumgartner. An inequality for the trace of matrix products, using absolute values. *arXiv preprint arXiv:1106.6189*, 2011.

[6] J. S. Bell. On the einstein podolsky rosen paradox. *Physics Physique Fizika*, 1(3):195, 1964.

[7] R. Bhatia. *Positive definite matrices*. Princeton university press, 2009.

[8] R. Bhatia. *Matrix analysis*, volume 169. Springer Science & Business Media, 2013.

[9] D. E. Browne and T. Rudolph. Resource-efficient linear optical quantum computation. *Physical Review Letters*, 95(1):010501, 2005.

[10] P. Chansangiam. A survey on operator monotonicity, operator convexity, and operator means. *International Journal of Analysis*, 2015, 2015.

[11] N. Datta. Min-and max-relative entropies and a new entanglement monotone. *IEEE Transactions on Information Theory*, 55(6):2816–2826, 2009.

[12] R. Diestel. Colouring. In *Graph Theory*, pages 119–148. Springer, 2017.

[13] E. Farhi, J. Goldstone, S. Gutmann, and M. Sipser. Quantum computation by adiabatic evolution. *arXiv preprint quant-ph/0001106*, 2000.

[14] C. A. Fuchs and J. Van De Graaf. Cryptographic distinguishability measures for quantum-mechanical states. *IEEE Transactions on Information Theory*, 45(4):1216–1227, 1999.

[15] A. Gilchrist, N. K. Langford, and M. A. Nielsen. Distance measures to compare real and ideal quantum processes. *Physical Review A*, 71(6):062310, 2005.

[16] F. Hansen and G. K. Pedersen. Jensen's inequality for operators and löwner's theorem. *Mathematische Annalen*, 258(3):229–241, 1982.

[17] M. Hein, W. Dür, J. Eisert, R. Raussendorf, M. Nest, and H.-J. Briegel. Entanglement in graph states and its applications. *arXiv preprint quant-ph/0602096*, 2006.

[18] F. Hiai. Matrix analysis: matrix monotone functions, matrix means, and majorization. *Interdisciplinary Information Sciences*, 16(2):139–248, 2010.

[19] R. A. Horn and C. R. Johnson. *Matrix analysis*. Cambridge university press, 2012.

[20] J. Kaniewski. Analytic and nearly optimal self-testing bounds for the clauser-horne-shimony-holt and mermin inequalities. *Physical review letters*, 117(7):070402, 2016.

[21] J. Kaniewski. Self-testing of binary observables based on commutation. *Physical Review A*, 95(6):062323, 2017.

[22] P. D. Lax. *Functional analysis*. Pure and applied mathematics. Wiley-Interscience, New York, NY, 2002.

[23] Z.-D. Li, R. Zhang, X.-F. Yin, L.-Z. Liu, Y. Hu, Y.-Q. Fang, Y.-Y. Fei, X. Jiang, J. Zhang, L. Li, et al. Experimental quantum repeater without quantum memory. *Nature Photonics*, 13(9):644–648, 2019.

[24] D. Mayers and A. Yao. Self testing quantum apparatus. *arXiv preprint quant-ph/0307205*, 2003.

[25] M. McKague. Self-testing graph states. In *Conference on Quantum Computation, Communication, and Cryptography*, pages 104–120. Springer, 2011.

[26] C. Nayak, S. H. Simon, A. Stern, M. Freedman, and S. D. Sarma. Non-abelian anyons and topological quantum computation. *Reviews of Modern Physics*, 80(3):1083, 2008.

[27] M. A. Nielsen and I. Chuang. Quantum computation and quantum information, 2002.

[28] We will only consider simple graphs, so $e_{ij} = e_{ji}$.

[29] Also known under *Neumarks theorem*.

[30] The reason why we are not choosing the aforementioned similar expression *target state* is that we defined a target state to be a maximally entangled state uniquely corresponding to a Bell-type inequality a theoretical state need not necessarily be maximally entangled and may be seen as a generalization of target states. In principle, one may check ϵ-*closeness* for any pair of quantum states.

[31] They applied it to hypergraph states, which is a generalization of graph states. Nevertheless, we will not go into details corresponding to this general class of quantum states, since this would overdo the scope of this project.

[32] This assumption may be justified when using similar devices for measurements and state creation. Additionally, note the following applies to intrinsic imperfections, external noise is not accounted here.

[33] Notation: note that we use the convention of the exclamation mark in denoting assertions. The reader might read it as *We assert this was true* and then we investigate, what could be deduced from this.

[34] This particular domain set motivates us to remark at this point that within calculations, we used the convention of $0 \cdot \log 0 = 0$.

[35] M. Ohya and D. Petz. *Quantum entropy and its use*. Springer Science & Business Media, 2004.

[36] A. Peres. *Quantum theory: concepts and methods*, volume 57. Springer Science & Business Media, 2006.

[37] S. Pironio, A. Acin, N. Brunner, N. Gisin, S. Massar, and V. Scarani. Device-independent quantum key distribution secure against collective attacks. *New Journal of Physics*, 11(4):045021, 2009.

[38] A. E. Rastegin. Trace distance from the viewpoint of quantum operation techniques. *Journal of Physics A: Mathematical and Theoretical*, 40(31):9533, 2007.

[39] R. Raussendorf and H. J. Briegel. A one-way quantum computer. *Physical Review Letters*, 86(22):5188, 2001.

[40] R. Raussendorf and T.-C. Wei. Quantum computation by local measurement. *Annu. Rev. Condens. Matter Phys.*, 3(1):239–261, 2012.

[41] R. Raussendorf and T.-C. Wei. Quantum computation by local measurement. *Annu. Rev. Condens. Matter Phys.*, 3(1):239–261, 2012.

[42] O. Regev. Quantum computation (lecture notes), 2006.

[43] T. Sagawa. Second law-like inequalities with quantum relative entropy: An introduction. In *Lectures on quantum computing, thermodynamics and statistical physics*, pages 125–190. World Scientific, 2013.

[44] I. Sason and S. Verdú. Upper bounds on the relative entropy and rényi divergence as a function of total variation distance for finite alphabets. In *2015 IEEE Information Theory Workshop-Fall (ITW)*, pages 214–218. IEEE, 2015.

[45] I. Šupić and J. Bowles. Self-testing of quantum systems: a review. *Quantum*, 4:337, 2020.

[46] Y. Takeuchi, T. Morimae, and M. Hayashi. Quantum computational universality of hypergraph states with pauli-x and z basis measurements. *Scientific reports*, 9(1):1–14, 2019.

[47] M. Tomamichel, R. Colbeck, and R. Renner. Duality between smooth min-and max-entropies. *IEEE Transactions on information theory*, 56(9):4674–4681, 2010.

[48] G. Tóth, O. Gühne, and H. J. Briegel. Two-setting bell inequalities for graph states. *Physical Review A*, 73(2):022303, 2006.

[49] X. Valcarce, J. Zivy, N. Sangouard, and P. Sekatski. Self-testing two-qubit maximally entangled states from generalized chsh tests. *arXiv preprint arXiv:2011.03047*, 2020.

[50] X. Valcarce, J. Zivy, N. Sangouard, and P. Sekatski. Self-testing two-qubit maximally entangled states from generalized chsh tests. *arXiv preprint arXiv:2011.03047*, 2020.

[51] J. Watrous. *The theory of quantum information*. Cambridge University Press, 2018.

[52] H. Yamasaki. Efficient device-independent veri cation of quantum states. 1(1):1–29, 2020.

[53] H. Yamasaki, K. Fukui, Y. Takeuchi, S. Tani, and M. Koashi. Polylog-overhead highly fault-tolerant measurement-based quantum computation: all-gaussian implementation with gottesman-kitaev-preskill code. *arXiv preprint arXiv:2006.05416*, 2020.

[54] X. M. Yang, X. Q. Yang, and K. L. Teo. A matrix trace inequality. *Journal of Mathematical Analysis and Applications*, 263(1):327–331, 2001.

[55] L. Zhang, K. Bu, and J. Wu. A lower bound on the fidelity between two states in terms of their trace-distance and max-relative entropy. *Linear and Multilinear Algebra*, 64(5):801–806, 2016.

[56] H. Zhu and M. Hayashi. Efficient verification of hypergraph states. *Physical Review Applied*, 12(5):054047, 2019.

[57] H. Zhu and M. Hayashi. General framework for verifying pure quantum states in the adversarial scenario. *Physical Review A*, 100(6):062335, 2019.